JAERI 1235

JAERI 1235

EUREKA : A Computer Code for Uranium-Oxide Fueled, Water Cooled Reactor Kinetic Analysis

September 1974

日 本 原 子 力 研 究 所
Japan Atomic Energy Research Institute

JAERI レポート

この報告書は，日本原子力研究所で行なわれた研究および技術の成果を研究成果編集委員会の審査を経て，不定期に刊行しているものです．

入手（資料交換による），複製などのお問わせは，日本原子力研究所技術情報部（〒319-11 茨城県那珂郡東海村）あて，お申しこみください．なお，このほかに財団法人原子力弘済会情報サービス事業部（茨城県那珂郡東海村日本原子力研究所内）で複写による実費頒布をおこなっております．

JAERI Report

Inquiries about the availability of reports and their reproduction should be addressed to the Division of Technical Information, Japan Atomic Energy Research Institute, Tokai-mura, Naka-gun, Ibaraki-ken, Japan.

編集兼発行　日本原子力研究所

印　　刷　三美印刷株式会社

EUREKA : A Computer Code for Uranium-Oxide Fueled, Water Cooled Reactor Kinetic Analysis

Michio ISHIKAWA, Yasushi KUGE*, Nobuaki OHNISHI,
Eiji TAKEUCHI** and Yuichiro KANBAYASHI

Japan Atomic Energy Research Institute

(Received Feburuary 15, 1974)

EUREKA— A computer code for uranium-oxide fueled, water cooled reactor kinetic analysis—has been developed in order to analyze neutronic, thermal and hydrodynamic transient behaviors in light water power reactors.

EUREKA can analyze the transient response of the core against the reactivity change caused by control rod drop (or withdrawal), coolant flow change and/or coolant temperature change. Especially, it can well simulate fast transient behaviors represented by serious reactivity accidents. In this code, coupled neutronic and thermal-hydrodynamic response is calculated for multi-regions in the core although one point neutron kinetics, one-dimensional heat transfer and one-dimensional hydrodynamics model is applied.

SPERT-III E-core experimental results were used to check the adequacy of EUREKA. It has been shown that the calculation results of EUREKA are in excellent agreement with the experimental results with regard to transient power shapes, burst energies, reactivity feedback and others.

The code was written in FORTRAN IV language for CDC-6600, IBM-360/75 and FACOM-230/60. This report presents detailed descriptions of the code, including basic equations, lists of input and output and the evaluation of the test calculations.

* Now with Japan Atomic Power Co. Tokyo.
** Now with Chubu Electric Power Co. Nagoya.

軽水動力炉の動特性解析コードEUREKA

石川迪夫・久家靖史*・大西信秋
竹内栄次**・上林有一郎

1974年2月15日 受理

要旨

本稿は，軽水動力炉の反応度事故時における核・熱水力学的挙動を計算するために開発した点状動特性・多領域熱水力結合の動特性解析コードEUREKAについて詳説したものである．

EUREKAコードでは，制御棒落下（制御棒逸失），冷却材流量変化あるいは冷却材温度変化などによって誘起される反応度変化による原子炉の過渡的応答を計算することができる．とりわけ反応度事故のような苛酷な事故現象を取扱うのに適している．

EUREKAコードの妥当性を検証するためにSPERT-III・E炉心の実験結果を用いて，過渡出力，積分出力などについて計算結果と実験結果の比較を行なったが，種々の原子炉初期条件からの暴走実験に対してEUREKAの計算値は実験値とよく一致した．

本コードはFORTRAN IV言語で記述し，CDC-6600，IBM-360/75およびFACOM-230/60用のバージョンを用意している．

* 日本原子力発電株式会社
** 中部電力株式会社

CONTENTS

目　次

1. Introduction

Importance of moderator feedback effect on controlling fast power transient has been demonstrated by a series of SPERT-III E-core experiments[1)~5)] and analysis[6),7)], and necessity to develop a practical kinetic model including thermal-hydrodynamics has been requested to predict precise transient behaviors for power reactor safety. EUREKA has been developed in accordance with the object of stated above.

The SPERT-III E-core is a small, oxided fueled, pressurized-water reactor (PWR) and general characteristics of the E-core is well simulated to those of currently used pressurized water power reactor. Total of eighty power excursion tests were performed in the E-core under various operating conditions that are cold-startup, hot-startup, hot-standby and power operating conditions.

SPERT analyses were performed by IREKIN and PARET codes for these experiments. IREKIN is typical one point neutron kinetic code in which doppler feedback effect is only taken into account, and which has been generally used for reactor kinetic analysis. PARET is newly developed by SPERT, which is multi-region, coupled nuclear thermal-hydrodynamic kinetic code, but it is not published to use at this moment.

SPERT reports that IREKIN calculates reasonable results to cold-startup tests of E-core, however, it overestimates burst energy by 40 to 60% for hot-startup tests and underestimates it at hot-standby and power operating tests. Against to IREKIN, it is reported that PARET shows reasonable results to all of E-core experiments, and also reported that the reasons are reduced to taking into account of moderator feedback at transient, especially by the prompt moderator feedback effect due to violent burst power.

It is very much comprehensive and carefull work to introduce precise moderator feedback effects into reactor kinetics because all the thermal-hydrodynamic transients in core, which are changes of coolant flow, coolant and fuel temperature, heat transfer, void formation, pressure balance etc due to power transient, must be precisely taken into account.

In EUREKA, the model was successfully developed to solve those phenomena with reasonable assumptions and has demonstrated reliability through the E-core experiment analysis. Those are explained in following chapters in this report.

Since EUREKA can calculate adequate coolant transient phenomena and feedbacks, EUREKA can handle following transients besides fast power transients represented by rod drop accident in BWR and rod ejection accident in PWR.

(1) General reactivity initiated transient
(2) Coolant flow coast down transient
(3) Transient caused by coolant temperature change

2. Description of Mathematical Model

2.1 General Model Description

The core considered in EUREKA model can be divided into up to maximum five regions (channels) radially and 20 regions (21 nodes) axially, as shown in **Fig. 1.1**. Each subdivision must be given its own power generation rate and reactivity feedback weighting factor for an application to point kinetics calculation. Each channel is represented a fuel rod which has three materials (fuel meat, gas gap and cladding) and associated coolant, being subdivided into up to maximum 25 nodes in radial direction (shown in **Fig. 1.2**). These are provisions to calculated thermal-hydrodynamics of channels and temperature profiles in fuels.

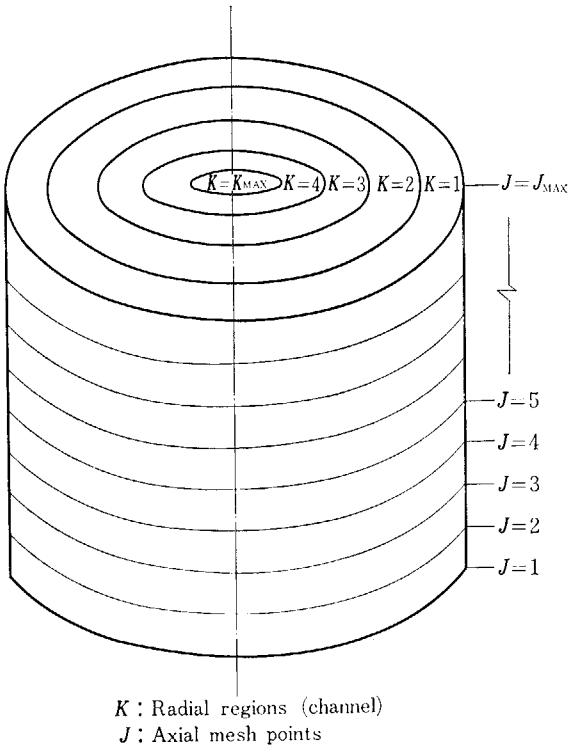

Fig. 1.1 Schematic reactor core subdivided into channels and axial mesh point in EUREKA.

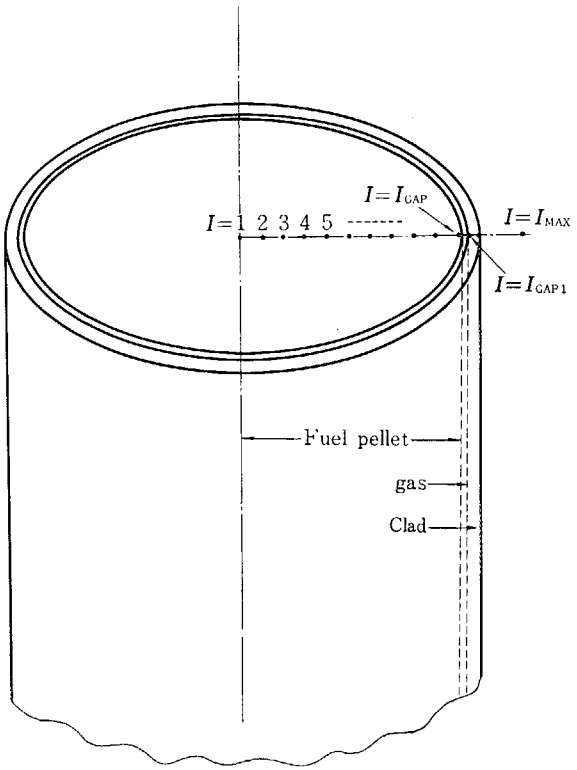

Fig. 1.2 Radial mesh point layout of fuel rod.

The transient power is determined through a numerical solution of the one point kinetics equation. The temperature distributions in each fuel are computed on the basis of a one-dimensional heat conduction equation. Local heat generation is determined from reactor power and specified weighting factors. Heat transfer correlations at the clad-coolant interface are employed in each of the various heat transfer regimes, such as convection, nucleate, transition and film boiling. The hydrodynamics in each coolant channel are solved from a one-dimensional conservation equations of mass, momentum and energy.

The main program is composed of two parts. The first part calculates the initial steady states of neutronics and thermal hydrodynamics and the second part performes the repeated transient calculations. The flow chart of the EUREKA is shown in **Fig. 2.1**. The initial conditions

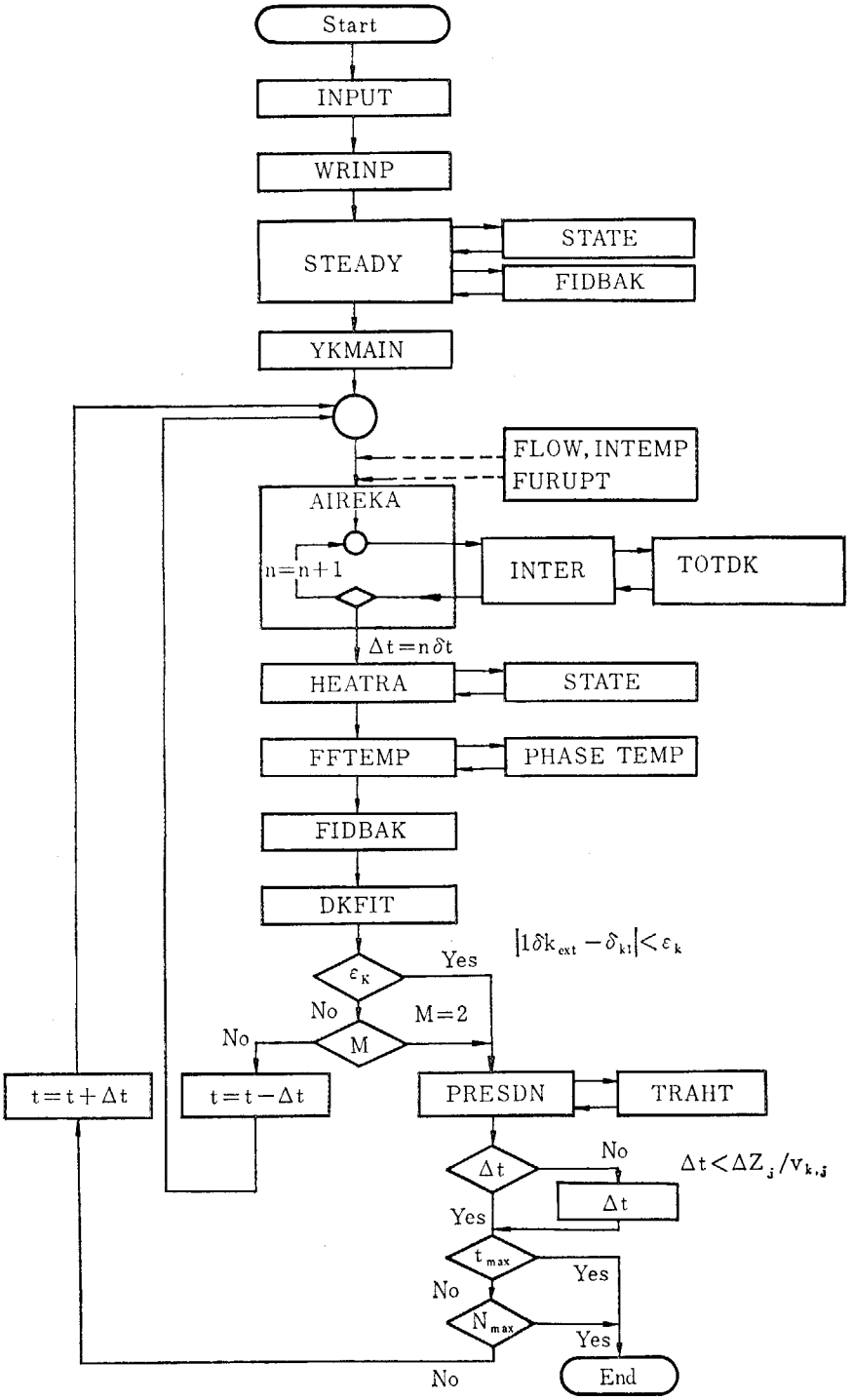

Fig. 2.1 Flow chart of EUREKA

of the core are calculated by subroutine STEADY in which thermal hydraulic geometry of system and physical properties of fuel and coolant are determined by using subroutine STATE (steam table) and PHASE (temperature dependent function of fuel and cladding material properties). Coolant flow rate, enthalpy rise, coolant temperature and void distribution are also calculated in subroutine STEADY. After the steady state conditions of thermal hydrodynamics are set, initial kinetic condition of reactor is calculated in subroutine YKMAIN. For transient calculation of reactor kinetics, subroutine AIREKA which consists of numerical method of the modified Runge Kutta is used. The values of amount reactor feedbacks in each time step are calculated from subroutine FIDBAK. The transient calculations of coolant enthalpy rise, coolant temperature and void distributions, and heat transfer coefficients in each axial nodes in each coolant channel are

performed in subroutine HEATRA. Profiles of transient temperature in each fuel rod are calculated using subroutine FFTEMP, and its associated subroutine TEMP (numerical method of implicit) and subroutine PHASE. Finally, pressure drops of each channel, such as acceleration, friction and head, are solved in subroutine PRESDN in order to decide inlet coolant velocity.

Since power behavior is rapid in comparison with thermal hydrodynamic behavior, it is required to use shorter time increment for the accurate calculation of power behavior. Then, two kinds of time increment are considered in EUREKA in the process of transient calculation. Relation between the thermal-hydrodynamics and reactor kinetics time increments is defined by $\Delta t = n_k \cdot \delta t'$, where Δt, $\delta t'$ and n_k are the thermal hydrodynamics time increment, the reactor kinetics time increment and the pre-determined integer, respectively. In the first stage of transient calculation at time, t, reactor kinetics calculations are repeated n_k times, increasing time by one kinetics time increment at each time using an extrapolated feedback reactivity, $\delta k_{\text{est}}(t)$, which is estimated by four point extrapolation method based on the past reactivity data. Then, the thermal hydrodynamics time increment is determined and the thermal hydrodynamic transient calculation is done one time. After the fuel temperature profiles and thermal hydrodynamic state of coolant are computed, the feedback reactivity at this time, $\delta k(t)$, is calculated. When the error between the extrapolated and newly calculated reactivity is less than an allowable limit, ε_k, i.e,

$$|\delta k_{\text{est}}(t) - \delta k(t)| < \varepsilon_k$$

the extrapolation is considered allowable, and next transient calculation are continued. When it is greater than the allowable, $\delta k_{\text{est}}(t)$ is newly assumed and the time step is cut back to $t - \Delta t$ to repeat all transient calculation from reactor kinetics to feedback reactivity.

As it is well known, the thermal hydrodynamics time increment, Δt, and space mesh width, ΔZ_j, should maintain the relation $\Delta t < \Delta Z_j / v_{j,k}$, so as to keep stability of numerical solution of thermal hydrodynamics differential equations by difference approximations, where $v_{j,k}$ are coolant flow velocities.

2. 2 Steady State Calculations

Subroutine STEADY calculates the steady state thermal hydraulic performances of the core as the initial condition of transient calculation. Physical properties of coolant are, as stated in Section **2. 3**, calculated by quadratic fittings of steam table in subroutine STATE corresponding to system pressure and enthalpy given by input. The details of steady state calculation are described below.

2. 2. 1 Heat Balance

The initial reactor power, P, is correlated to power densities in core subregions:

$$P = \sum_{j,k} P_{j,k} \tag{1}$$

$$P_{j,k} = K_1 (\sum_i \mu_i \cdot \Sigma_{fi} \cdot \phi_i)_{j,k} \cdot \Delta V_{j,k} \tag{2}$$

where

$P_{j,k}$: power in subregion (j, k)
$\Sigma \mu_i \Sigma_{fi} \phi_i$: power density (input data) in subregion (j, k)
$\Delta V_{j,k}$: volume of subregion (j, k)
K_1 : conversion constant.

Steady state heat balance in coolant is described by the expression:

$$h_{j+1,k} = h_{j,k} + \frac{P_{j,k}}{A_w \cdot v_{j,k} \cdot \rho_{j,k}} \tag{3}$$

Heat transfer to coolant is described by the following expression:

$$P_{j,k}=A_{j,k}\cdot H_{j,k}\cdot(Tc_{j,k}-Tw_{j,k}) \tag{4}$$

where

$h_{j,k}$: coolant enthalpy at inlet to node j
$h_{j+1,k}$: coolant enthalpy at exit of node j
A_w: coolant flow area
$v_{j,k}$: coolant velocity
$\rho_{j,k}$: coolant density
$A_{j,k}$: heat transfer area
$H_{j,k}$: heat transfer coefficient
$Tc_{j,k}$: cladding surface temperature
Tw: coolant temperature
j: axial node index in a coolant channel
k: channel region number

The heat transfer coefficient is calculated in accordance with coolant flow condition, as stated in Section **2. 2. 4**.

2. 2. 2 Fuel Rod Temperature Distribution

In the analyses of a reactivity accident, it is the most important to calculate in detail the temperature of the fuel for evaluating the feedback effects that influence the power burst. In EUREKA, to calculate the temperature distribution in the fuel rod, as stated in Chapter 1, the fuel rods of the core are divided into up to maximum five regions (channels) in accordance with the radial power distribution. Each fuel rod is divided radially into three subregions (fuel meat, gas gap and cladding), which can be further subdivided into up to maximum 24 intervals (25 node points). It must be noted that in the gas gap subregion node point is not allowed. The interval in the axial direction can be divided into up to maximum 20 intervals (21 node points), as shown in **Fig. 2. 2**.

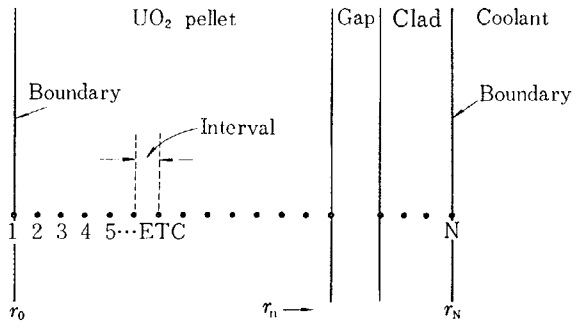

Fig. 2. 2 Radial mesh point pattern for thermal model

Heat transfer in each fuel rod is determined based on the one-dimensional conduction equation. The partial differential equation for the diffusion of heat within each fuel rod is

$$\nabla k(u, r)\nabla u(r)+S(r)=0, \tag{5}$$

where the symbol $u(r)$ represents temperature as a function of radial position, r. Volumetric heat capacity and thermal conductivity are denoted by the symbols $g(u, r)$ and $k(u, r)$, respectively, and are treated as functions of both position and temperature. The heat source per unit volume, $S(r)$, is assumed to be a separated function of space. The magnitude of the local heat source in each node is calculated from the specified average core power level and preassigned axial and radial weighting factors given by the input.

When the equation (5) is solved for the fuel rod, the cladding surface temperature has to be assumed as the boundary condition. The cladding surface temperature is calculated by using the heat transfer coefficients which are chosen in accordance with five regimes of coolant and a heat flux determined from the heat generation and dimension of the fuel rod. Also, the gas gap heat transfer coefficient between a pellet and a cladding is calculated by a fitting formula as function of gap clearance and gap average temperature as stated in Section **2. 2. 5.**

The numerical method of the equation (5) is described in Section **2. 8** in detail, and that is used in the calculation of the temperature distribution both of steady state and transient conditions in the same manner.

2. 2. 3 Channel Pressure Drop

The channel flow distribution in the core is determined so as to maintain the channel pressure drop equal for all channels. The total coolant flow rate is given by

$$G_{\text{total}}=\sum_{k=1}^{k_{\max}} G(k)=\sum_{k=1}^{k_{\max}} \rho_{\text{in}}\cdot A_{\text{w}}(k)\cdot v_{\text{in}}(k). \tag{6}$$

The channel pressure drop for each channel is

$$p_{\text{total}}(1)=\cdots\cdots=p(k)=\cdots\cdots p(k_{\max}), \tag{7}$$

where

G_{total} : total coolant flow rate
$G(k)$: mass flow rate in channel k
ρ_{in} : coolant density at channel inlet
$A_{\text{w}}(k)$: coolant flow area in channel k
$v_{\text{in}}(k)$: coolant velocity at channel k inlet
p_{total} : channel pressure drop.

The channel pressure drop, p_{total}, consists of the various terms in equation (8), which are the functions of coolant velocity, density and viscosity. Therefore, the channel pressure drop is calculated when coolant physical properties, coolant velocity and channel power are given. The coolant physical properties are derived by subroutine STATE (Ref. to Section **2. 3**) and the channel power is calculated by equation (2), so that the channel flow distribution is obtained by iterative calculations of equations (7) and (8) with assumed coolant inlet velocities :

$$p_{\text{total}}(k)=p_{\text{fric}}+p_{\text{head}}+p_{\text{acc}}+p_{\text{in}}+p_{\text{out}} \tag{8}$$

Where

$$p_{\text{fric}}=\int_0^l \rho\cdot\frac{v^2}{2g}\cdot\frac{\lambda}{De}\cdot dl \tag{9}$$

$$p_{\text{head}}=\int_0^l \rho dl \tag{10}$$

$$p_{\text{acc}}=\int_0^l \rho\cdot v\left(\frac{dv}{dl}\right)dl \tag{11}$$

$$p_{\text{in}}=\rho_{\text{in}}\frac{v_{\text{in}}^2}{2g}\left(K_{\text{in}}+\frac{l_{\text{in}}}{De}\lambda_{\text{in}}\right) \tag{12}$$

$$p_{\text{out}}=\rho_{\text{out}}\frac{v_{\text{out}}^2}{2g}\left(K_{\text{out}}+\frac{l_{\text{out}}}{De}\lambda_{\text{out}}\right) \tag{13}$$

and

p_{fric} : friction pressure loss
p_{head} : density head loss
p_{acc} : acceleration pressure loss
p_{in} : inlet disturbance pressure loss

p_{out} : exit disturbance pressure loss
ρ : coolant density
v : coolant velocity
g : gravity constant
λ : friction coefficient
De : equivalent hydraulic diameter
l : effective fuel length
K : contraction or expansion loss coefficient.

2.2.4 Heat Transfer Coefficient

The heat transfer coefficient between fuel cladding and coolant is calculated based upon one of the following five different coolant flow conditions:

1) Single phase (liquid) region[9]

In case of turbulent coolant flow ($Re>2000$),

$$H=0.023\,Re^{0.8}\cdot Pr^{0.4}\cdot(\lambda/De) \tag{14}$$

In case of laminar coolant flow[10] ($2000>Re>200$),

$$H=1.02\,Re^{0.45}\cdot Pr^{0.33}\cdot(De/L)^{0.4}\cdot(\nu(T_c)/\nu(T_w))^{0.14}\cdot(\lambda/De) \tag{15}$$

In case of pool cooling,[7),11)] (16)

$$H=\eta\cdot H_{laminer}\cdot(T_c-T_w)^n.$$

Where

η : coefficient calculated from flow rate
n : 1/3 or 1/4.

2) Nucleate boiling region (including subcooled boiling)

Nucleate boiling starts when cladding surface temperature exceeds so-called Jens-Lottes temperature.[12),13)] Transition boiling is defined to occur at the time when surface heat flux exceeds the DNB (departure from nucleate boiling) heat flux.

Jens-Lottes temperature, T_{JL} is defined by

$$T_{JL}=T_{sat}+\Delta T_{JL} \tag{17}$$

$$\Delta T_{JL}=0.819\cdot e^{-(p/63.3)}\cdot q^{1/4}. \tag{18}$$

DNB heat flux[14] is calculated by

$$q_{DNB}=2.8\times(0.236\times10^6+0.0188G)\cdot[3.0+0.018(T_{sat}-T_w)]\times[0.435+1.23e^{-(0.0093z/De)}]\cdot(1.7-1.4e^{-A}] \tag{19}$$

$$A=0.532\times(\rho_f/\rho_g)^{1/3}. \tag{20}$$

The heat transfer coefficient in the nucleate boiling region is assessed by the method described in Section **2.7.2.**

3) Transition boiling region

The transition boiling region is bounded by the DNB heat flux point at the lower and film boiling initiation point at the upper end. It is assumed that film boiling occurs when cladding surface temperature exceeds coolant temperature by more than 60 degrees centigrade (Ref. **Fig. 2.3**).[15]

The heat transfer coefficient in the transition boiling region, H_{TB}, is given by

$$H_{TB}=\frac{q_{DNB}-q_{TB}}{T_{TB}-T_{DNB}}, \tag{21}$$

where

q_{DNB} : DNB heat flux
q_{TB} : heat flux at initiation of film boiling
T_{TB} : $T_{sat}+60°C$

T_{DNB} : cladding surface temperature at DNB heat flux.

The heat flux at initiation of film boiling is assumed to be 1.44×10^5kcal/m^{2}hr in this program.

4) Film boiling region

The lower bound of the film boiling region is at the point where cladding surface temperature exceeds T_{TB} and the upper bound at the point where bulk coolant enthalpy reaches saturated steam enthalpy.

The heat transfer coefficient in this region is calculated by

$$H_{FB}=0.023\,Re^{0.8}Pr_{gas}^{0.4}\ (\lambda_{gas}/De), \tag{22}$$

where

λ_{gas} : thermal conductivity of steam

Pr_{gas} : Prandtl number of steam.

5) Gaseous region

In the case bulk coolant enthalpy exceeds saturated steam enthalpy the heat transfer coefficient is given by the formula (22).

2.2.5 Physical Properties of Fuel and Cladding

Physical properties of fuel and cladding materials required for EUREKA are thermal conductivity, specific heat and thermal expansion coefficient. These physical properties are given in quadratic fittings versus temperaure in MKH unit, except for thermal conductivity of fuel and gap heat transfer coefficient.

The thermal conductivity of UO_2 pellet is calculated by the fitting formula :

$$\lambda_{UO_2}=a_0+a_1T+a_2T^2+a_4/(T+a_5) \tag{23}$$

The gap heat transfer coefficient is calculated by the fitting formula :[8]

$$H_{gap}=\frac{a_0+a_1T+a_2T^2}{(a_4+\Delta x\times10^{-6})} \tag{24}$$

where

$a_0\sim a_5$: coefficients given as input data

T : temperature

Δx : gap clearance in meter unit.

In Appendix-B are given pertinent physical properties of fuel and cladding materials commonly used in light water power reactors.

2.3 Coolant Flow State and Physical Properties

Coolant physical properties are derived from subroutine STATE. In the boiling region the following procedures are applied based on physical properties of saturated steam and water calculated by STATE.

1) Coolant temperature

In the case coolant enthalpy, h, is less than saturated enthalpy, h_{sat}, such as in the subcooled boiling region, coolant temperature is calculated by subroutine QUAFIT used a least squares method. In the case coolant is completely vaporized coolant temperature is assumed to be at the saturated steam temperature :

$$\begin{aligned} &h<h_{sat} && T_w=f(h)\\ &h_{sat}\leq h<h_{gas} && T_w=T_{sat}\\ &h\geq h_{gas} && T_w=T_{gas}=T_{sat}. \end{aligned} \tag{25}$$

2) Steam quality, void volume fraction and density

Steam quality, x, is defined by

$$x=\frac{h-h_{sat}}{h_{gas}-h_{sat}}. \tag{26}$$

Void volume fraction, α, is defined by

$$\alpha=\frac{x/\rho_{gas}}{(1-x)/\rho_{sat}+x/\rho_{gas}}. \tag{27}$$

In the subcooled boiling region, steam quality is set to be zero and void volume fraction, α, is calculated by

$$\alpha=\frac{1}{1+\frac{1}{\beta}} \tag{28}$$

$$\beta=1-12.0\ (\Delta t_{sub}/q)^{0.25}p^{-0.07}, \tag{29}$$

where

Δt_{sub} : subcool temperature

q : heat flux

p : pressure.

Coolant density in the boiling state, ρ, is defined by

$$\rho=x\rho_g+(1-x)\rho_f. \tag{30}$$

3) Viscosity

Coolant viscosities for single phase and gaseous states are derived from STATE. Coolant viscosity in the two phase region is defined by void-fraction-weighted average of the liquid and gas phase values.

Single phase region	$\nu=f(h)$
Two phase region	$\nu=\nu_{sat}$
Gaseous region	$\nu=\nu_{gas}$.

(31)

4) Thermal conductivity

Since coolant thermal conductivity is used only for computation of heat transfer coefficient at the cladding outer surface, the conductivity is defined as follows in accordance with boiling conditions :

Single phase region	$\kappa=f(h)$
Nucleate boiling region	$\kappa=\kappa_{sat}$
Film boiling region	$\kappa=\kappa_{gas}$
Gaseous region	$\kappa=\kappa_{gas}$.

(32)

5) Friction pressure loss coefficient

Single phase friction coefficient[11] for pressure loss calculation is a function of Reynolds number :

$$\lambda=0.3164\ (Re)^{0.25}. \tag{33}$$

In the two phase region Reynolds number is computed by physical properties at the saturated condition. Martinelli-Nelson's two phase friction factor[17] is computed by use of Shiba-Yamazaki's formula[18] :

$$k_{MN}=(1-a)^{-0.875} \tag{34}$$

$$a=\left[2+\frac{1}{\beta}-\sqrt{\left(2+\frac{1}{\beta}\right)^2-4}\right]2.0 \tag{35}$$

$$\beta=\frac{\rho_{sat}\cdot x}{\rho_{gas}\cdot(1-x)} \tag{36}$$

where $a=\alpha$ in the subcooled region.

2. 4 Reactor Kinetics Calculation

2. 4. 1 General Description

Subroutine AIREKA calculates reactor power excursion caused by reactivity perturbations. The method of numerical solution is based on the paper presented by E. R. Cohen[21] at the Second Geneva Conference.

This subroutine is composed of eight smaller subroutines: YKMAIN sets initial conditions, AIREKA controls these reactor kinetics subroutines, INTER and its subordinates CNFBT and RNFBT perform numerical solution by Cohen's method, DIREC checks improper time increments, RANAL computes reactivity and TEST defines end of calculations.

The external reactivity insertion as a function of time is transformed in dollar unit. The neutron density, energy release and delayed neutron precursor densities of maximum six groups are obtained at each time step.

Since the reactor kinetics time increment is adjusted by the main program, AIREKA subroutine informs the main program the proper time increment, if any.

2. 4. 2 Reactor Kinetics Equations

The basic differential equations of reactor kinetics dealt with by subroutine AIREKA are

$$\frac{dN(t)}{dt}=\frac{\rho(t)-\beta}{l}N(t)+\sum_i \lambda_i C_i(t)+S_0 \tag{37}$$

$$\frac{dC_i(t)}{dt}=\frac{\beta f_i}{l}N(t)-\lambda_i C_i(t) \quad (i=1, \cdots, 6) \tag{38}$$

$$\frac{dE(t)}{dt}=N(t) \tag{39}$$

where

t : time
$N(t)$: neutron density
$C_i(t)$: delayed neutron precursor density of i-th group
$\rho(t)$: reactivity
β : effective delayed neutron fraction
f_i : β_i/β
β_i : delayed neutron fraction of i-th group
l : prompt neutron life time
λ_i : decay constant of delayed neutron precursor of i-th group
S_0 : neutron source density
$E(t)$: time integral of neutron density or fission energy.

Equations (37) and (38) are modified by use of the following substitutions:

$$\frac{\rho(t)}{\beta}=r(t)$$

$$\frac{l\lambda_i}{\beta f_i}C_i(t)=W_i(t)$$

$$\frac{l}{\beta}S_0=S^* \tag{40}$$

$$\frac{dN(t)}{dt}=\frac{\beta}{l}\{[r(t)-1.0]N(t)+\sum_i f_i W_i(t)+S^* \tag{41}$$

$$\frac{dW_i(t)}{dt}=\lambda_i N(t)-\lambda_i W_i(t) \tag{42}$$

Equations (39) and (42) are commonly described by the following standard form :

$$\frac{dF_j(t)}{dt}=A_jN(t)+B_jF_j(t) \tag{43}$$

Therefore, equations (41) and (43) are solved in a generalized form in this program.

2.5 Calculation of Feedback Reactivities

In EUREKA, four kinds of feedback reactivities, are taken into account, which are induced by the changes of reactor thermal hydraulic characteristics.

They are

(1) δk_D induced by change of fuel temperature T_{FA}

(2) δk_T induced by change of moderator temperature T_W

(3) δk_α induced by change of void volume fraction α

and (4) δk_E induced by thermal expansion of fuel cladding.

These feedback reactivities are fitted to formulae in power series with proper variables, as shown in the following, which are calculated numerically in subroutine FIDBAK :

$$\delta k_D(z_{j,k})=a_{D_1}+a_{D_2}T_{FA}(z_{j,k})+a_{D_3}T_{FA}{}^2(z_{j,k})+a_{D_4}T_{FA}{}^3(z_{j,k})+a_{D_5}\{T_{FA}(z_{j,k})\}^{a_{D_6}} \tag{44}$$

$$\delta k_T(z_{j,k})=a_{T_1}T_W(z_{j,k})+a_{T_2}T_W{}^2(z_{j,k})+a_{T_3}T_W{}^3(z_{j,k}) \tag{45}$$

$$\delta k_\alpha(z_{j,k})=a_{\alpha_1}\alpha(z_{j,k})+a_{\alpha_2}\alpha^2(z_{j,k}) \tag{46}$$

$$\delta k_E(z_{j,k})=2\lambda_C(V_F/V_M)a_{E_1}T_{CA}(z_{j,k}) \tag{47}$$

where a_{Di}, a_{Ti}, $a_{\alpha i}$ and a_{Ei} are fitting coefficients in the reactivity feedbacks, which are given in EUREKA as input data; λ_C is linear expansion coefficient of cladding material and V_F/V_M is volume ratio of fuel to moderator in the unit rod cell.

The variables, $T_{FA}(z_{j,k})$ and $T_{CA}(z_{j,k})$ are volume weighted average temperature of fuel and cladding respectively, at the height z_j of the k-th channel in the core.

These variables are calculated in the following manner. For example, fuel temperature T_{FA} is calculated by

$$T_{FA}(z_{j,k})=\frac{\sum_i T(r_i, z_{j,k})\cdot\Delta V(r_i)}{\sum_i \Delta V(r_i)}. \tag{48}$$

In the calculation of δk_D, which is induced by the change of fuel temperature, T_{FA}, $(z_{j,k})$ is used, implying that Doppler effect is assumed to be expressed with volume weighted average fuel temperature.

As seen from the above formulae, the feedback reactivities are given at each mesh point in the core. In EUREKA, however, nuclear transient is treated by a point kinetics equation. Therefore, the feedback reactivity used in the kinetics equation must be calculated by summing the reactivities at mesh point with weighting factors of neutron and adjoint fluxes.

Thus the total feedback reactivity is calculated in the following formulae :

$$\delta k(t)=\delta k_D(t)+\delta k_T(t)+\delta k_\alpha(t)+\delta k_E(t) \tag{49}$$

$$\delta k_D(t)=\sum_{j,k}\delta k_D(z_{j,k})W_{res}(j, k) \tag{50}$$

$$\delta k_T(t)=\sum_{j,k}\delta k_T(z_{j,k})W_{th}(j, k) \tag{51}$$

$$\delta k_\alpha(t)=\sum_{j,k}\delta k_\alpha(z_{j,k})W_{th}(j, k) \tag{52}$$

$$\delta k_E(t)=\sum_{j,k}\delta k_E(z_{j,k})W_{th}(j, k) \tag{53}$$

$$W_{res}(j, k)=(\phi_{res}\cdot\phi_{res}{}^*)_{j,k}\cdot\Delta V_{j,k} \tag{54}$$

$$W_{th}(j, k)=(\phi_{th}\cdot\phi_{th}{}^*)_{j,k}\cdot\Delta V_{j,k} \tag{55}$$

where $W_{res}(j, k)$ and $W_{th}(j, k)$ are the normalized weights given by the product of neutron and adjoint fluxes and volume element $\Delta V(j, k)$ at the z_j-th nodal point of the k-th channel.
All the feedback reactivities mentioned above are computed in subroutine FIDBAK.

As is explained previously in Section **2. 1**, the extrapolated feedback reactivity at time t, and is calculated in subroutine DKFIT, utilizing a quadratic fitting formula.

Namely, feedback reactivities δk_1, δk_2 and δk_3 at successive time mesh points t_1, t_2 and t_3 just before the time t, being given, the extrapolated reactivity $\delta k_{ext}(t)$ at t in the quadratic formula is obtained by

$$\delta k_{ext}(t)=\delta k_1\frac{(t-t_2)(t-t_3)}{(t_1-t_2)(t_1-t_3)}+\delta k_2\frac{(t-t_3)(t-t_1)}{(t_2-t_3)(t_2-t_1)}+\delta k_3\frac{(t-t_1)(t-t_2)}{(t_3-t_1)(t_3-t_2)}. \tag{56}$$

When the difference between the extrapolated reactivity $\delta k_{ext}(t)$ and computed feedback $\delta k(t)$ at time t is greater than an allowable limit of ε_k, the extrapolated reactivity and kinetic calculation are recomputed to replace the $\delta k_{ext}(t)$ by the $\delta k(t)$.

The EUREKA's test run results show that recalculations are necessary only around peak power time with error tolerance value of 0.5cent. Therefore it can be said that this quadratic formula extrapolation technique is fairly good estimation.

The reactivity used in subroutine INTER, which computes the kinetics equation is the difference between the inserted and feedback reactivity. This subtraction is performed in subroutine TOTDK.

In EUREKA, externally inserted reactivity is given as input data by consecutive linear fitting with as many as ten break points. When the time t is between the time break point t_B and t_E, and the corresponding inserted reactivities are δk_B and δk_E, respectively, the inserted reactivity at t is given by linear interpolation:

$$\delta k_s(t)=\frac{\delta k_E-\delta k_B}{t_E-t_B}(t-t_B)+\delta k_B. \tag{57}$$

The extrapolated reactivity $\delta k_{ext}(t)$ is obtained in subroutine DKFIT, and the net reactivity δk_{net} which is used in the kinetics calculation is given by

$$\delta k_{NET}=\delta k_S(t)-\delta k_{ext}(t). \tag{58}$$

2. 6 Calculation of Transient Coolant Flow Rate

2. 6. 1 Fundamental Equations[19]

The calculation of transient coolant flow rate is based on the continuity equation and the law of conservation of momentum. When heat transfer rate to coolant, coolant flow rate and coolant temperature at the core inlet are known at time t, the transient in-channel continuity equation is expressed by

$$\frac{\partial m}{\partial t}+\frac{\partial(mv)}{\partial z}=0. \tag{59}$$

where

$$m=A\rho. \tag{60}$$

In the case when the flow area in the channel is constant, A, then equation (59) becomes

$$\frac{\partial \rho}{\partial t}+\frac{\partial(\rho v)}{\partial z}=0. \tag{61}$$

From the momentum balance,

$$\frac{\partial p}{\partial z}+\rho\cdot g+\frac{\kappa}{2D_e}\rho v^2+\rho\left[\frac{\partial v}{\partial t}+v\frac{\partial v}{\partial z}\right]=0. \tag{62}$$

where

ρ : coolant density
v : coolant velocity
p : coolant pressure
g : gravity constant
$\kappa/2D_e$: friction coefficient
t : time
z : channel axial coordinate.

By integrating equation (62) in the interval of channel l,

$$\int_0^l \partial p+\int_0^l \rho\cdot g dz+\frac{\kappa}{2D_e}\int_0^l(\rho v^2)dz+\int_0^l \rho\left(\frac{\partial v}{\partial t}\right)dz+\int_0^l \rho v\left(\frac{\partial v}{\partial z}\right)dz=0 \tag{63}$$

and equation (63) is rewritten into

$$\int_0^l \rho\left(\frac{\partial v}{\partial t}\right)dz+\int_0^l \rho v\left(\frac{\partial v}{\partial z}\right)dz=p_{in}-p_{out}-\int_0^l(\rho g)dz-\frac{k}{2D_e}\int_0^l(\rho v^2)dz. \tag{64}$$

As is explained later in Section **2.7** since physical properties of coolant at each mesh point are already calculated, the coolant velocity at the point is given by

$$v(z, t)=v_{in}(t)+\int_0^z\left(\frac{\partial v}{\partial z}\right)dz, \tag{65}$$

therefore,

$$\frac{\partial v}{\partial t}=\frac{\partial v_{in}}{\partial t}+\frac{\partial}{\partial t}\int_0^z\left(\frac{\partial v}{\partial z}\right)dz. \tag{66}$$

From equation (66), the first term in the left hand side in equation (64) is

$$\int_0^l \rho\left(\frac{\partial v}{\partial t}\right)dz=\int_0^l \rho\frac{\partial v_{in}}{\partial t}dz+\int_0^l \rho\frac{\partial}{\partial t}\int_0^z\frac{\partial v}{\partial z}dz\cdot dz. \tag{67}$$

By substituting equation (67) into equation (64), $\partial v_{in}/\partial t$ is obtained as follows.

$$\frac{\partial v_{in}}{\partial t}=\left[p_{in}-p_{out}-\int_0^l(\rho g)dz-\frac{\kappa}{2D_e}\int_0^l(\rho v^2)dz-\int_0^l \rho v\left(\frac{\partial v}{\partial z}\right)\partial z-\int_0^l \rho\frac{\partial}{\partial t}\int_0^z\frac{\partial v}{\partial z}\cdot dz\cdot dz\right]\Big/\left[\int_0^l \rho dz\right]. \tag{68}$$

To solve equation (68), it is necessary to assume

$$\frac{\partial}{\partial t}\int_0^z\frac{\partial v}{\partial z}dz=\int_0^z\frac{\partial}{\partial t}\left(\frac{\partial v}{\partial z}\right)dz. \tag{69}$$

This assumption may not be strictly correct in the case of sudden boiling occurence, but is necessary to reduce the difference equations.

From the continuity equation (61),

$$\frac{\partial v}{\partial z}=-\frac{1}{\rho}\left[v\frac{\partial \rho}{\partial z}+\frac{\partial \rho}{\partial t}\right]. \tag{70}$$

Therefore,

$$\frac{\partial}{\partial t}\left(\frac{\partial v}{\partial z}\right)=\frac{\left(\frac{\partial v}{\partial z}\right)_{t=(t)}-\left(\frac{\partial v}{\partial z}\right)_{t=(t-\Delta t)}}{\Delta t}. \tag{71}$$

By permitting the assumption of equation (69), it is possible to solve equation (68).

The channel inlet velocity at each time step, $v_{in}(t_1)$ is given by

$$v_{in}(t_1)=v_{in}(t_0)+\int_{t_0}^{t_1}\frac{\partial v_{in}(t_0)}{\partial t}dt. \tag{72}$$

Then equation (65) can be solved with aid of equation (72), and thus the velocity, $v(z, t)$, at each mesh point in a chnnel is computed. Since all the coolant velocities at time t are now obtained, the in-channel pressure loss $\Delta p(t)$ is calculated by

$$\Delta p(t)=p_{in}(t)-p_{out}(t)$$

$$=\int_0^l(\rho g)dz+\frac{\kappa}{2D_e}\int_0^l(\rho v^2)dz+\left[\frac{\partial v_{in}}{\partial t}\int_0^l\rho dz+\int_0^l\rho v\left(\frac{\partial v}{\partial z}\right)dz+\int_0^l\int_0^z\rho\frac{\partial}{\partial t}\left(\frac{\partial v}{\partial z}\right)dz\cdot dz\right]. \quad (73)$$

2.6.2 In-channel Pressure Loss and Inlet Flow Rate Calculation

In the analysis of coolant flow rate distribution in the core of light water reactor, it is common to calculate the coolant flow distribution of the channels so as to make pressure differences between upper and lower plenum the same. In the steady state calculation, the initial flow rate of each channel is determined in this way.

It will be possible to obtain channel flow rate even at transient condition likewise the steady state calculation by repeating the above processes. But it is not only ineconomical to repeat the iterative calculation at each time step, but also is not always correct representation of the phenomena. As a matter of fact if sudden boiling takes place in a channel due to power burst, the pressure in this channel may be probably greater than the others. For this reason, in EUREKA, it is avoided to repeat the pressure balance calculation at every time step, and the method to give inlet flow rate at each time step is introduced.

As can be understood from equation (68), the channel inlet flow rate is governed by the coolant velocity at each mesh point, the coolant variables like physical properties, which are computed at each time and mesh point, and by the pressure difference between the channel inlet and outlet(p_{in}-p_{out}). In other words, to obtain an approximate solution of coolant velocity at each mesh point without iterative calculation, it is necessary to assume one of the three variables, the in-channel pressure loss, physical properties of coolant and the inlet velocity, since these three variables are dependent with each other.

As the first approximation, one may think that it will be most acceptable to assume the pressure difference between the upper and lower plenum, if the last time step is kept constant to next time step. This method is commonly used in the single channel calculation. In this case[19], the inlet flow rate change is given from equation (68) by assuming the "p_{in}-p_{out}" of previous time step.

Analysing the multi-channel problem, it will be necessary to make an another assumption in order to satisfy the inter-channel relationship. EUREKA uses a standard pressure loss method multi-channel analysis. This standard pressure loss select the channel, which is thought to receive the least transient pressure effect due to temperature change of coolant, and usually this channel is the outermost one in the core. In this method it is assumed the inlet velocity of the standard channel remains constant during the transient period.

From equation (68), the channel inlet flow rate is given,

$$\frac{\partial v_{in}(k,\ t_0)}{\partial t}=\frac{\Delta p(Ref.,\ t_0)-\Delta p(k,\ t_0)}{\int_0^l\rho(k)\cdot dz} \quad (74)$$

and

$$v_{in}(Ref.,\ t)=\text{const.}$$

$$v_{in}(k,\ t_1)=v_{in}(k,\ t_0)+\frac{\partial v_{in}(k,\ t_0)}{\partial t}(t_1-t_0). \quad (75)$$

where $v_{in}(Ref.,\ t_1)$ and $v_{in}(k,\ t_1)$ are the inlet velocities at time t_1 of the standard and the k-th channels, respectively.

The pressure loss of each channel at time t_1 is given by the use of the inlet velocity obtained from equation (76)

$$\Delta p(k,\ t_1)=p_{in}(k,\ t_1)-p_{out}(k,\ t_1) \quad (76)$$

Therefore, by use of equation (73), the variables mentioned in Section **2. 6. 1** are computed at every time step.

In the case when coolant flow rate is changing with time, equation (75) are modified as follows.

As the change of the coolant flow rate is given by the input, the ratio of the flow change between successive two time step, s, is known.

Therefore,

$$v_{in}(Ref., t_1)=s\cdot v_{in}(Ref., t_0)$$

$$v_{in}(k, t_1)=s\cdot\left[v_{in}(k, t_0)+\frac{\partial v_{in}(k, t_0)}{\partial t}(t_1-t_0)\right]. \tag{77}$$

where the ratio s is set to interval of 0.97~1.03 in the code by adjusting the time step width, to avoid calculational error due to violent pressure change.

The above calculation is performed mainly in subroutines PRESDEN and HEATRA. The coolant physical properties are derived in STATE from enthalpy h obtained in Section **2. 7.**

2. 7 Calculation of Transient Coolant Temperature

2. 7. 1 Fundamental Equations

In this section, the method of calculation, the heat transfer rate to coolant and coolant physical properties are described, which are assumed to be known in the previous section. To estimate the heat transfer rate to the coolant it is necessary to take into account the direct heat production in coolant (due to neutron slowing down and attenuation of gamma rays), in addition to the heat transferred from fuel to coolant.[1)~5)]

The heat transfer rate Q_H is calculated by heat flux of the previous time step for the computational convenience, which is obtained in subroutine FFTEMP (2.8). Although heat flux changes in the transient period, the time constant of the fuel is considerably large. Therefore it seems reasonable to use the heat flux data at the previous time in order to avoid iterative calculation.[1)]

Heat production Q_{PMH} in the coolant is almost prompt in phenomena, thus heat source can be treated as proportional to the power distribution in the core, since the heat production by the neutron slowing down is much greater than that by the attenuation of gamma rays.

Whence additional heat to the coolant in the interval of j-th and $j+1$th mesh is

$$h_{j+1,k}(t_1)=\frac{h_{j,k}(t_1)\cdot\left[\frac{v_{j,k}(t)\cdot\Delta t}{\Delta t}\right]+h_{j+1,k}(t_0)+\left[\frac{Q_{j,k}(t_1)}{\rho_{j,k}\Delta z\cdot A_w}\right]}{\left[1.0+\left(\frac{v_{j,k}(t)\cdot\Delta t}{\Delta z}\right)\right]}. \tag{78}$$

where

$$Q_{j,k}(t_1)=Q_{H_{j,k}}(t_1)+Q_{PMH_{j,k}}(t_1) \tag{79}$$

$$Q_{H_{j,k}}(t_1)=(2\pi r_c\cdot\Delta z)\cdot\left[\frac{q_{j,k}(t_0)+q_{j+1,k}(t_0)}{2}\right]\Delta t \tag{80}$$

$$Q_{PMH_{j,k}}(t_1)=\eta_{PMH}\int_{t_0}^{t_1}\left(\frac{p_{j,k}(t)+p_{j+1,k}(t)}{2}\right)dt \tag{81}$$

and

h : enthalpy of coolant
v : coolant velocity
z : mesh length
Δt : $\Delta t=t_1-t_0$ time interval

$Q_{j,k}(t_1)$: heat produced at time to t_1 in the j=1th mesh
r_c : clad radius
q : heat flux
P : regional core heat output
η_{PMH} : fraction of the moderator heat production.

As mentioned previously, the heat flux q at the previous time step is given from subroutine FFTEMP, and the core heat output is calculated in subroutine AIREKA at the every time step. The heat transfer rate to the coolant can be obtained using equation (79) in step wise.

As $v_{in}(t)$ is known as a boundary condition, v_{j-1} is calculated by solving equations (78) and (65) and (70), alternately. These are done in subroutine HEATRA.

In the next paragraph the relations between the transient heat transfer to coolant and the transient fuel temperature calculations are discussed.

As was previously mentioned, the coolant temperature and physical properties are obtained in subroutine STATE, and heat transfer coefficient for the next time step is also obtained, which will be discussed in datail in the next Section **2. 7. 2.** In addition heat increase in the fuel is already known it is possible to get new temperature profile in the fuel based on the previous profile. The new clad surface temperature is obtained, and heat flux for next time step can be computed using the coolant temperature and heat transfer coefficient.

By the way, in these procedures, gap heat transfer coefficient[8] between the pellet and clad is very controvertible and must be treated carefully. Subroutine GAHT takes account of this coefficient as a function of gap width and gap temperature, which is also used in the steady state calculation.

The physical properties of coolant and the pressure loss coefficients necessary to the pressure loss calculation described in the previous section are also computed from the coolant enthalpy at each mesh point.

2. 7. 2 Calculation of the Heat Transfer Coefficient

In the case of single phase flow problem, the heat transfer coefficient is obtained from the coolant hydraulic-thermal condition (Ref. **2. 3. 4.**).

In the nucleate boiling region, the relation between the heat flux and the clad surface temperature T_c,[12] and the coolant saturation temperature T_{sat} is given by the correlation of Jens-Lottes correlation,

$$T_c - T_{sat} = \beta \cdot q^{1/4}. \tag{82}$$

where

$$\beta = 0.819 e^{-p/63.3}.$$

From the relationship of the heat flux, cladding and coolant temperature, and the heat transfer coefficients, H, is expressed by

$$T_c - T_w = q/H. \tag{83}$$

where $q(t)$ and $q(t+\Delta t)$ are the heat fluxes at time t and $t+\Delta t$, respectively. Let $q(t+\Delta t)$ express in Taylor's series neglecting higher order terms,

$$q(t+\Delta t) \fallingdotseq q(t) + \Delta t \cdot q'(t) \tag{84}$$

hence

$$q(t+\Delta t)^{1/4} = q(t)^{1/4} + \frac{\Delta t \cdot q'(t)}{4q(t)^{3/4}}. \tag{85}$$

Substituting equation (85) into equation (82), it becomes,

$$T_c(t+\Delta t) - T_{sat} = \beta \cdot q(t)^{1/4} + \beta \cdot \frac{\Delta t \cdot q'(t)}{4q(t)^{3/4}} \tag{86}$$

$$T_c(t) - T_{sat} = \beta \cdot q(t)^{1/4}. \tag{87}$$

Subtracting equation (87) from equation (86), the following equation is obtained,

$$T_c(t+\Delta t)-T_c(t)=\beta\cdot\frac{\Delta t\cdot q'(t)}{4q(t)^{3/4}}=\frac{q'(t)\cdot\Delta t}{4q(t)}\cdot(T_c(t)-T_{sat}). \tag{88}$$

As is discussed previously, the heat flux change is relatively slow, $q'(t)$ at the time t can be estimated from the previous values, and cladding surface temperature $T_c(t+\Delta t)$ at the next time step can be estimated utilizing the result at time t.

And by solving equation (82), it is possible to get heat flux corresponding to the temperature $T_c(t+\Delta t)$, when the heat transfer coefficient is computed from equation (83).

2.8 Calculation of Fuel Rod Temperature

2.8.1 Heat Conduction Model

Temperature distribution in a fuel rod is determined by solving the one-dimensional heat conduction equation in cylindrical geometry. The conduction model and method of solution are based on HEAT-1 code.[23)~26)] The core is divided into up to maximum 5 types of channels which are represented by a single fuel pin plus its associated coolant area. The fuel rod consists of three components (fuel, gas gap, and clad) and subdivided into a maximum of 25 radial mesh points. **Fig. 1.2** illustrates the allocation of radial mesh points at which the temperatures will be calculated.

The heat transfer at the fuel-clad boundary is treated by Anderson-Leichter equation which is a function of both temperature and gap distance (Appendix B). The clad-coolant boundary conditions employed at each axial mesh points are derived from the heat transfer model, described in Section **2.2**.

In EUREKA, the thermal properties of components are represented by functions of temperature.

2.8.2 Derivation of the Difference Approximation to the Numerical Calculation

The heat conduction calculation in the fuel rod is assumed to be one-dimensional; radial conduction are allowed but axial conduction is ignored. The partial differential equation for both transient and steady state heat conduction, is given below.

$$\frac{\partial}{\partial t}(g(u, r)\cdot u(r, t))=\nabla k(u, r)\cdot\nabla u(r, t)+S(r, t). \tag{89}$$

where

u=temperature
r=space variable
t=time variable
g=volumetric heat capacity
k=thermal conductivity
S=source term per unit volume

To obtain the spatial difference approximation for n-th mesh point, equation (89) is integrated over an incremental volume, shown in **Fig. 2.2**.

$$\iiint_V\frac{\partial}{\partial t}(g(u, r)\cdot u(r, t))dv=\iiint_V\nabla k(u, r)\cdot\nabla u(r, t)dv+\iiint_V S(r, t)dv \tag{90}$$

Mesh points are allocated such that they lie on the external boundaries of the fuel rod, at the interfaces between materials and at equal intervals between the interfaces and/or boundaries. A region is a segment of space which contains the same material and has a constant spacing between mesh points.

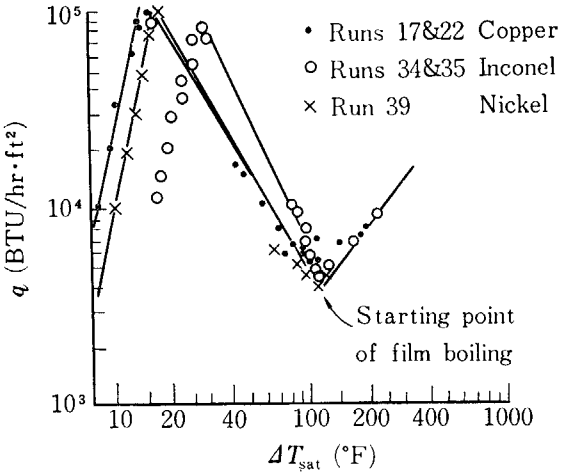

Fig. 2. 3 Starting point of film boiling indicated in experimental results.

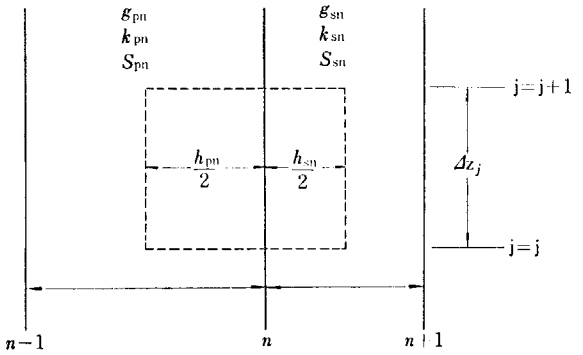

Fig. 2. 4 Two typical radial intervals in thermal model.

Fig. 2. 4 represents three typical mesh points. Subscripts designate space indices and superscripts indicate time indices. Subscripts p and s designate quantities to the left and to the right of the mesh points, respectively. The h's indicate the mesh point spacing, which are not necessarily equal in the different regions. In the region between mesh points, k, g, and S are assumed constant, but k_{pn} is not necessarily equal to k_{sn}, and similar situation occurs for g and s.

Using a foward difference for the time derivative, the first term of equation (90) is approximated by

$$\iiint_V \frac{\partial}{\partial t}(g(u, r)\cdot u(r, t))dv \approx \iiint_V g(u, r)\frac{\partial u}{\partial t}(r, t)dv$$
$$\approx \frac{u_n{}^{m+1}-u_n{}^m}{\Delta t}\left(g_{pn}\frac{h_{pn}}{2}\left(r_n-\frac{h_{pn}}{4}\right)+g_{sn}\frac{h_{sn}}{2}\left(r_n+\frac{h_{sn}}{4}\right)\right). \tag{91}$$

Where the symbols $u_n{}^m$ and $u_n{}^{m+1}$ indicate the temperature at r_n and t_m and at r_n and t_{m+1}, respectively.

The second term of equation (90) becomes

$$\iiint_V \nabla k(u, r)\nabla u(r, t)dv = \iint_S k(u, r)\nabla u(r, t)\overline{ds}$$
$$\approx -\frac{k_{pn}(u_n-u_{n-1})}{h_{pn}}\left(r_n-\frac{h_{pn}}{2}\right)+\frac{k_{sn}(u_{n+1}-u_n)}{h_{sn}}\left(r_n+\frac{h_{sn}}{2}\right). \tag{92}$$

The heat source term is assumed to be a separable function of space and time. The magnitude of this local heat source is determined from the calculated or specified core power level and preassigned by the axial and radial weighting factors. For each axial mesh points, it is thus defined by

$$S(r, t)=P_f\cdot P(t)Q(r). \tag{93}$$

Where P_f is a power factor, $P(t)$ is the time dependent part which is calculated in subroutine AIREKA, and $Q(r)$ is the space dependent weighting factor.

The third term of equation (90) is then approximated as

$$\iiint_V S(r, t)dv \approx S_{pn}\frac{h_{pn}}{2}\left(r_n-\frac{h_{pn}}{4}\right)+S_{sn}\frac{h_{sn}}{2}\left(r_n+\frac{h_{sn}}{4}\right). \tag{94}$$

From the above equations, the following quantities are defined for convenience:

$$h_{pn}{}^V=2\pi\frac{h_{pn}}{2}\left(r_n-\frac{h_{pn}}{4}\right);\quad h_{sn}{}^V=2\pi\frac{h_{sn}}{2}\left(r_n+\frac{h_{sn}}{4}\right);$$
$$h_{pn}{}^S=2\pi\frac{1}{h_{pn}}\left(r_n-\frac{h_{pn}}{2}\right);\quad h_{sn}{}^S=2\pi\frac{1}{h_{sn}}\left(r_n+\frac{h_{sn}}{2}\right);$$
$$h_n{}^b=2\pi r_n \quad ;\quad D_n=g_{pn}h_{pn}{}^V+g_{sn}h_{sn}{}^V$$

Using all the approximated terms to the equation (90), the basic difference equation for the n-th mesh point becomes

$$\frac{({u_n}^{m+1}-{v_n}^{m})D_n}{\Delta t}=-({u_n}^{m}-{u_{n-1}}^{m})k_{pn}{h_{pn}}^{S}+({u_{n+1}}^{m}-{u_n}^{m})k_{sn}{h_{sn}}^{S}$$
$$+(Q_{pn}{h_{pn}}^{V}+Q_{sn}{h_{sn}}^{V})P_fP_t\lambda. \tag{95}$$

Using a foward difference for the time derivative, equation (90) can be approximated by the following difference equation for the n-th interior mesh point at the time node $(m+1)$:

$$a_n{u_{n-1}}^{m+1}+b_n{u_n}^{m+1}+c_n{u_{n+1}}^{m+1}=d_n.$$

where

$$a_n=-\frac{k_{pn}{h_{pn}}^{S}\Delta t}{2},\quad c_n=-\frac{k_{sn}{h_{sn}}^{S}\Delta t}{2},\quad b_n=\sigma D_n-a_n-c_n,$$
$$d_n=-\sigma a_n{u_{n-1}}^{m}+\sigma(D_n+a_n+c_n){u_n}^{m}-\sigma c_n{u_{n+1}}^{m}$$
$$+\Delta tP_f\left(\frac{\lambda^{m+1}+\sigma\lambda^{m}}{2}\right)\cdot(Q_{pn}{h_{pn}}^{V}+Q_{sn}{h_{sn}}^{V}). \tag{96}$$

In equation (96), σ is 1.0 for transient cases and 0 for steady state cases.

2.8.3 Derivation of a Difference Formula to Boundary Conditions

The boundary condition allowed takes the form of

$$A(u)u+B(u)\left(\frac{\partial u}{\partial r}\right)=D(u)C(t). \tag{97}$$

The equation (97) is used to represent the boundary condition of both at the center of fuel and at the cladding-coolant interface. Equation (90) is again used to obtain the difference formula at the boundaries, with the volume of integration. The second term of equation (90) for the boundary condition at $r=r_0$ is

$$\iiint_V\nabla\cdot k(u,r)\nabla u(r,t)dV=\iint_S k(u,r)\nabla u(r,t)\cdot\overline{ds}$$
$$\approx-\frac{k_{s0}}{B_0}(C_0-A_0u_0){h_0}^{b}+k_{s0}(u_1-u_0){h_{s0}}^{S}. \tag{98}$$

The difference equation for the mesh point at $r=r_0$ becomes

$$B_0\left(\frac{{u_0}^{m+1}-{u_0}^{m}}{\Delta t}\right)g_{s0}{h_{s0}}^{V}=-k_{s0}(C_0-A_0u_0){h_0}^{b}+B_0k_{s0}(u_1-u_0){h_{s0}}^{S}+B_0{S_{s0}h_{s0}}^{V}. \tag{99}$$

Difference equations for the boundary at $r=r_N$ are derived in a similar fashion. These equations for the boundary mesh points are converted to the implicit formula in the same manner as for the interior points. Thus, $r=r_0$,

$$b_0{u_0}^{m+1}+c_0{u_1}^{m+1}=d_0. \tag{100}$$

where

$$c_0=-B_0\frac{k_{s0}{h_{s0}}^{S}\Delta t}{2},\quad b_0=B_0\sigma g_{s0}{h_{s0}}^{V}+\frac{k_{s0}A_0{h_0}^{b}\Delta t}{2B_0}-c_0,$$
$$d_0=-\sigma c_0{u_1}^{m}+\sigma\left(g_{s0}{h_{s0}}^{V}+c_0-\frac{k_{s0}A_0{h_0}^{b}\Delta t}{2B_0}\right)u_0$$
$$+\frac{k_{s0}{h_0}^{b}D_0\Delta t(C_0{}^{m+1}+\sigma C_0{}^{m})}{2B_0}+\Delta tP_fP_t\left(\frac{\lambda^{m+1}+\sigma\lambda^{m}}{2}\right)Q_{s0}{h_{s0}}^{V}. \tag{101}$$

at $r=r_N$,

$$a_N{u_{N-1}}^{m+1}+b_N{u_N}^{m+1}=d_N \tag{102}$$

where

$$a_N=-\frac{k_{PN}{h_{PN}}^{S}\Delta t}{2},\quad b_N=\sigma g_{PN}{h_{PN}}^{V}+\frac{k_{PN}A_N{h_N}^{b}\Delta t}{2B_N}-\alpha_N,$$

$$d_N=-\sigma a_N u_{N-1}{}^m+\sigma\left(g_{PN}h_{PN}{}^V-\frac{k_{PN}A_N h_N{}^b\Delta t}{2B_N}+a_N\right)u_N{}^m$$
$$+\frac{k_{PN}h_N{}^b D_N\Delta t(C_N{}^{m+1}+\sigma C_N{}^m)}{2B_N}+\Delta t P_i P_t\left(\frac{\lambda^{m+1}+\sigma\lambda^m}{2}\right)Q_{PN}h_{PN}{}^V. \quad (103)$$

2.8.4 Solution of the Simultaneous Equation

The difference equations for the mesh points, equations (96), (101) and (92), lead to a matrix equation with tridiagonal element

$$\begin{vmatrix} b_0 & c_0 & 0 & 0 & & \\ a_1 & b_1 & c_1 & 0 & 0\text{'s} & \\ 0 & a_2 & b_2 & c_2 & & \\ & \cdot & \cdot & \cdot & & \\ & & \cdot & \cdot & \cdot & \\ & & & \cdot & \cdot & \cdot \\ & 0\text{'s} & a_{N-1} & b_{N-1} & c_{N-1} & \\ & & 0 & a_N & b_N & \end{vmatrix} \begin{vmatrix} u_0{}^{m+1} \\ u_1{}^{m+1} \\ u_2{}^{m+1} \\ \cdot \\ \cdot \\ \cdot \\ u_{N-1}{}^{m+1} \\ u_N{}^{m+1} \end{vmatrix} = \begin{vmatrix} d_0 \\ d_1 \\ d_2 \\ \cdot \\ \cdot \\ \cdot \\ d_{N-1} \\ d_N \end{vmatrix}. \quad (104)$$

Although with the general boundary condition form of equation (97), the coefficient matrix is nearly symmetric with equation (98), the matrix is always symmetric.

The solution to the above equations is obtained by applying the Gaussian eliminations, ie :

(1) From $E_0=\frac{c_0}{b_0}$ and $F_0=\frac{d_0}{b_0}$ (105)

(2) From $E_j=\frac{c_j}{b_j-a_jE_{j-1}}$ (106)

and

$$F_j=\frac{d_j-a_jF_{j-1}}{b_j-a_jE_{j-1}} \quad (107)$$

for $j=1, 2, 3, \ldots, N-1$

(3) From $u_N{}^{m+1}=\frac{d_N-a_NF_{N-1}}{b_N-a_NE_{N-1}}$ (108)

(4) From $u_j{}^{m+1}=-E_ju_{j+1}+F_j$ (109)

for $j=N-1, N-2, N-3, \ldots, 2, 1, 0$.

3. Test Results

3.1 General

In order to verify EUREKA model reliability, many of test run calculations have been performed on the SPERT-III E-core transient tests. The SPERT-III E-core is a small PWR reactor with oxide fuels, however, characteristics of the core are generally similar to typical PWR currently designed. Since tests cover various reactivity transients from different operational modes of PWR, the SPERT-III transient tests will be proper selection to examine EUREKA reliability.

The SPERT-III E-core tests can be divided into three major phases as listed in the TABLE 3.1. These depend on initial test conditions of reactor, namely, cold-startup, hot-startup and power operating condition. The cold-startup test which is called fiducial test in the SPERT, was performed to prove that SPERT-III E-core has similar kinetic characters with other SPERT kinetic tests. In this test phase, SPERT reports do not mention that any special kinetic character of the SPERT-III E-core were found in comparison with other SPERT reactors. The other two test phases which simulate reactivity accident initiated from hot-startup conditions and power operating conditions were the foremost tests performed by the SPERT-III E-core.

TABLE 3.1 SPERT-III·E core experiments

Reactor initial condition		
Reactor power	(MW)	$5\times10^{-5}\sim20$
Pressure	(kg/cm^2g)	$1\sim100$
Temperature	(°C)	$20\sim260$
Flow velocity	(m/sec)	$0\sim7.5$
Transient condition		
Inserted reactivity	($)	$0.6\sim1.3$
Reactor period	(sec)	$2\sim0.01$
Insertion rate	($/sec)	$\fallingdotseq15$

All sample calculation results of the EUREKA meet the SPERT transient tests with good accuracy. General difference between EUREKA calculations and SPERT experiments are approximately 10~15% and these differences are within experimental uncertainties as listed in the TABLE 3.2. One remarkable case, in which approximately 30% of differences was obtained, is in an analysis of the transient from 20MW full power operation, however, it should be noted that there were several unknown inputs including doppler temperature as discussed in the Appendix A-2. Therefore it is believed that, if the calculational conditions were clear enough, differences between analysis and experiment in this case would be much less than those results. Thus it can be generally concluded that EUREKA could calculate light water power reactor kinetic behaviors within 15% of uncertainty, when inputs were adequate.

TABLE 3.2 EUREKA analysis to the SPERT-III E-core experiment

Case. No.		1—1	1—2	1—3	1—4	1—6	1—9	3—2
Initial condition								
Pressure	psi	1500	1500	1500	1500	1500	Atm.	1500
Temperature	°F	500	500	500	500	500	70	500
Flow rate	f/s	14	14	14	14	14	0	2.8
Reactor power	MW	5×10^{-5}	5×10^{-5}	5×10^{-5}	1	20	5×10^{-5}	5×10^{-5}
Transient condition								
Inserted reactivity	$	1.21 (1.23 ±0.05)	1.10 (1.10 ±0.04)	1.04 (1.04 ±0.04)	1.21 (1.25 ±0.04)	1.17 (1.17 ±0.05)	1.21 (1.21 ±0.05)	1.21 (—)
Initial period	ms	10 (~9.7)	20 (~20.6)	40 (~41.6)	~10 (~)	~ (~)	10 (~10.0)	10 (—)
Reciprocal period	sec^{-1}	100 (~111)	50 (~49)	25 (~24)	~100 (~)	~ (~)	100 (~100)	100 (—)
Peak power	MW	458 (410±41)	123 (97±10)	37 (35±4)	498 (~)	(610±60)	312 (280±42)	485 (—)
Energy*	MW-S	9.1 (8.5±1.1)	5.5 (4.5±0.6)	3.3 (3.1±0.4)	9.1 (~)	(17±2)	6.1 (6.0±1.0)	9.1 (—)
Peak power time	sec.	0.22 (~0.227)	0.35 (~0.37)	0.57 (~0.6)	0.12 (~)	(0.11 ±0.05)	0.216 (~0.23)	0.22 (—)
Compensated* reactivity	¢	22.3 (24±3)	12.7 (12±1)	7.8 (8±1)	21.1 (~)	(~22)	22.0 (22±2)	22.6 (—)
reference IDO-17281 SPERT Run No.		(60)	(62)	(56)	(83)	(86)	(43)	(—)

( ) Experimental value
* Value at peak power time

3.2 Detailed Evaluation of EUREKA Results[30),31)]

Fig. 3.1 shows the spectral curve of peak power vs. reciprocal period in all the hot-startup test phase. Experimental result is compared with results of EUREKA, RARET and AIREK where PARET is the coupled nulear, thermal-hydrodynamic kinetics code used for E-core transient analysis in the SPERT, as like as EUREKA, and AIREK is the well known adiabatic kinetics calculation code. As seen in **Fig. 3.1**, both peak powers in EUREKA and PARET show excellent agreement with experiment within 15% of differences in general, but AIREK results have up to 80% of differences. It is understandable that the above difference comes from difference of computational model whether moderator temperature feedback effects are taken into account or not.

Good agreement between EUREKA and experiments is also demonstrated in **Fig. 3.2** which is a spectral curve of burst energy at peak power time vs. reciprocal period. In this figure, differences between EUREKA and experiments are generally within 15% and it is again compared with AIREK results of up to 100% of differences. In general, comparison of the burst energy at the peak power time has the maximum difference in analysis and experiment because the uncertainties of burst power and uncertainties of peak power time are multiplied. This difference of burst energy becomes smaller at runout power and if the burst energy is compared on calculated results, generally in EUREKA differences are less than 10% and AIREK's are up to 50%, respectively.

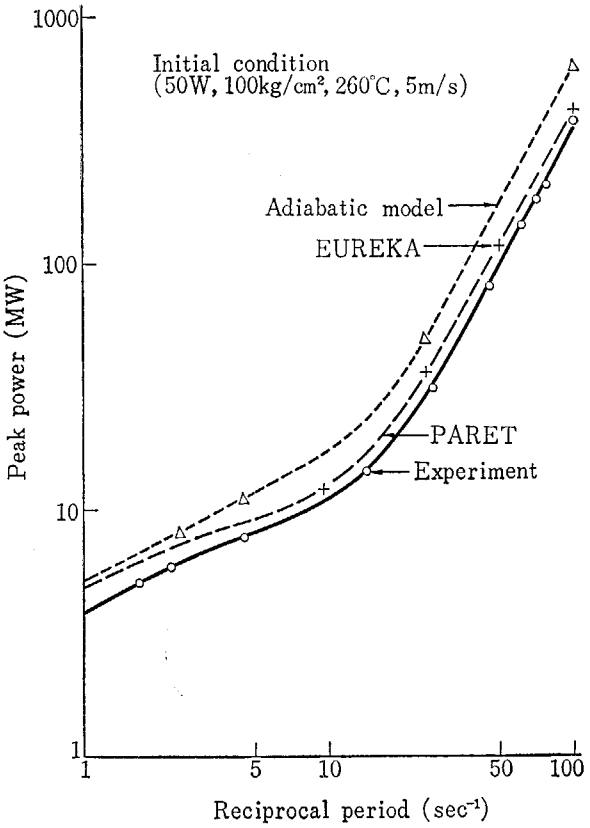

Fig. 3.1 Peak power vs. reciprocal period of SPERT-III transient from hot-startup initial condition (Experimental data and analytical result)

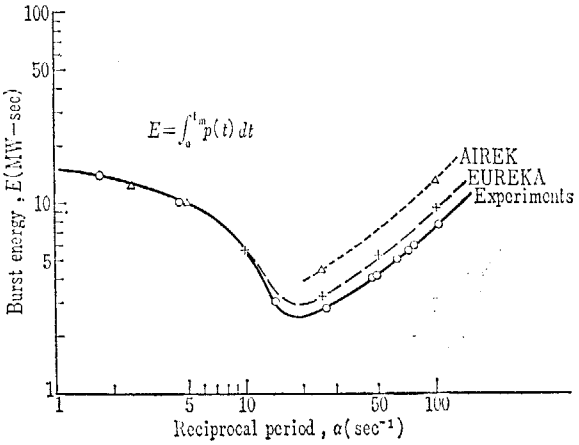

Fig. 3.2 Energy vs. reciprocal period of SPERT-III transient at hot-startup initial condition (Experimental data and analytical results)

Fig. 3.3 shows time dependent power, energy and compensated reactivity curves of the 10 ms transient test on cold-startup. **Fig. 3.4** shows same period transient from hot-startup condition. Both EUREKA and AIREK results are compared in these figures. Significant difference is seen between **Fig. 3.3** and **Fig. 3.4**. In **Fig. 3.3**, all the results of experiment, EUREKA and AIREK show good agreement, but comparing in **Fig. 3.4**, AIREK result is very poor to results of

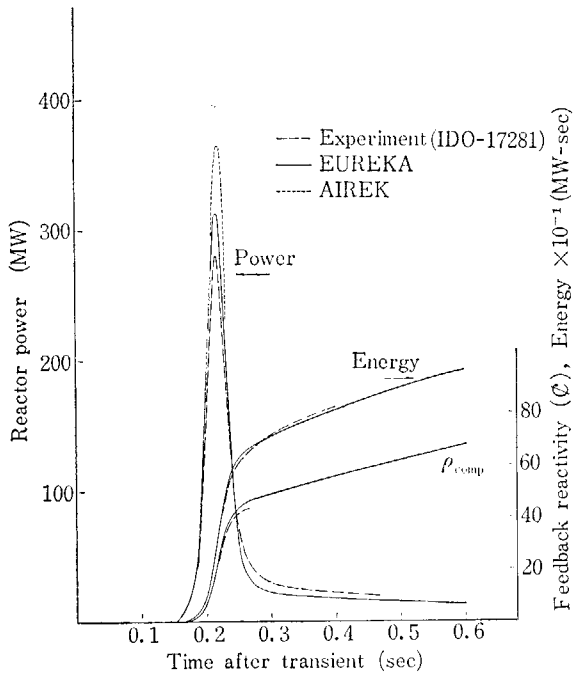

Fig. 3.3 EUREKA analysis (case 1—9), SPERT-III 10 ms transient (70°F, pool water, atmospheric pressure)

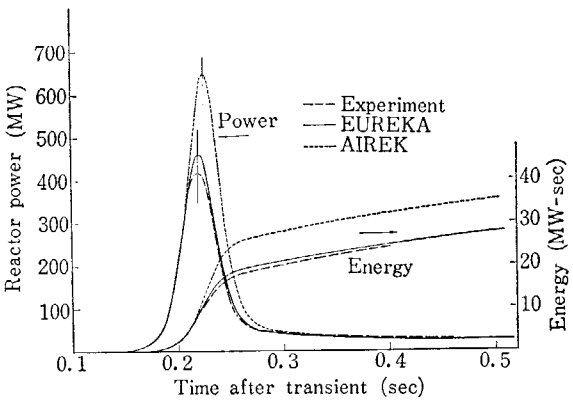

Fig. 3.4 EUREKA analysis (case 1—1), SPERT-III 9.7 ms transient (T=500°F, v=14 t/s, P=1500 psi)

experiment and EUREKA. Again this difference is explained by difference of analysis model whether moderator temperature feedback effects are taken into account or not.

In general, moderator temperature coefficient increases with system temperature rise in light water power reactor, because water specific density change per unit temperature is increased significantly with system temperature rise. In SPERT-III E-core, moderator temperature coefficient at room temperature condition is 0.72¢/°C and it is increased to 7.2¢/°C at hot-startup condition (260°C). This means that unit energy addition to coolant generates ten times larger moderator temperature feedback at the hot-startup transient in the SPERT-III E-core than that of the cold-startup cases. Significant amount of feedback comes out by the prompt moderator heating effect which is mainly due to neutron slowing down at the hot-startup transient to suppress burst power. In the adiabatic kinetic models this reactivity feedback is not taken into account, so that the results become poor at hot-startup analysis as indicated in **Fig. 3. 2.**

Fig. 3. 5 shows comparison of compensated reactivity curves obtained from experiments and analysis in the transient case of **Fig. 3. 4.** EUREKA results shows excellent agreement with experiment but AIREK does not. In addition, it is observed that EUREKA result have an oscillation in compensated reactivity curve as like as observed in experiment. The nature of the oscillation is examined in **Fig. 3. 6.**

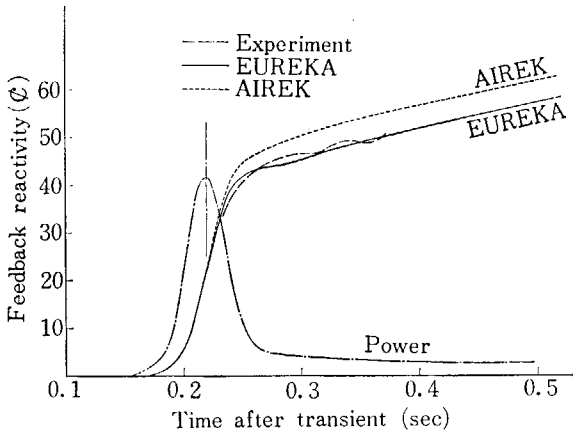

Fig. 3. 5 EUREKA analysis (case 1—1), SPERT-III 9.7 ms transient (T=500°F, v=14 f/s, P=1500 psi)

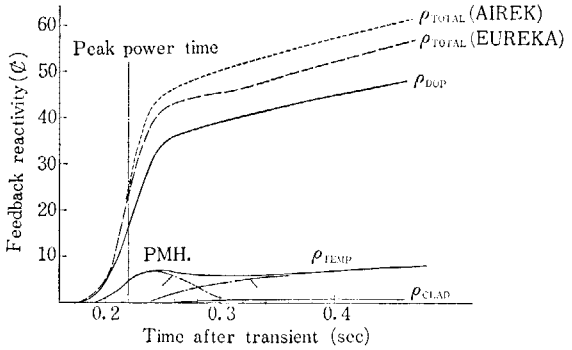

Fig. 3. 6 Compensated feedback reactivity in EUREKA (test run case 1—1)

EUREKA calculates total reactivity feedback from three sources as shown in **Fig. 3. 6.** Doppler effect is dominant and proportional to excursion energy throughout transient time of interest, and clad expansion effect, even though it is small, is increased with clad temperature rise. While moderator temperature feedback has a dip at the time approximately 280 ms after initiation of the transient.

It is observed that a relatively large amount of moderator temperature feedback comes out following to power burst, and decreases for a little while after and again increases slowly when run out power is established. It is understood that this funny moderator temperature behavior based on the reasons that, as indicated with dotted line in **Fig. 3. 5**, the early rapid reactivity feedback is generated by the prompt moderator heat by violent burst power and the later slow reactivity feedback is generated by heat transfer from fuel to coolant. Decrease of moderator feedback at the time of interest is caused by the reason that the warmed up water by prompt moderator heat is swept out from the core by coolant flow, and heat transfer from fuel to coolant is not yet well developed to compensate it. AIREK result is also seen in **Fig. 3. 6** for comparison. The doppler feedback curve of EUREKA and the total feedback of AIREK can be compared in this figure, since AIREK takes into account only doppler feedback as be used in an adiabatic

model. Approximately 6¢ of difference in doppler feedbacks at peak power time is observed between two models, and it must be reffered to approximately 23¢ of total reactivity feedback at the time. In EUREKA calculation, 6¢ of this difference is compensated by moderator feedback, and in AIREK calculation, this 6¢ of reactivity should be compensated by doppler effect which reflect to increase burst power, burst energy and slower power time in calculation.

Fig. 3.7 shows the effect of coolant velocity on moderator feedback. Coolant velocity of 1 m/s is compared with 5 m/s coolant velocity. All other kinetic parameters are set the same in this comparison.

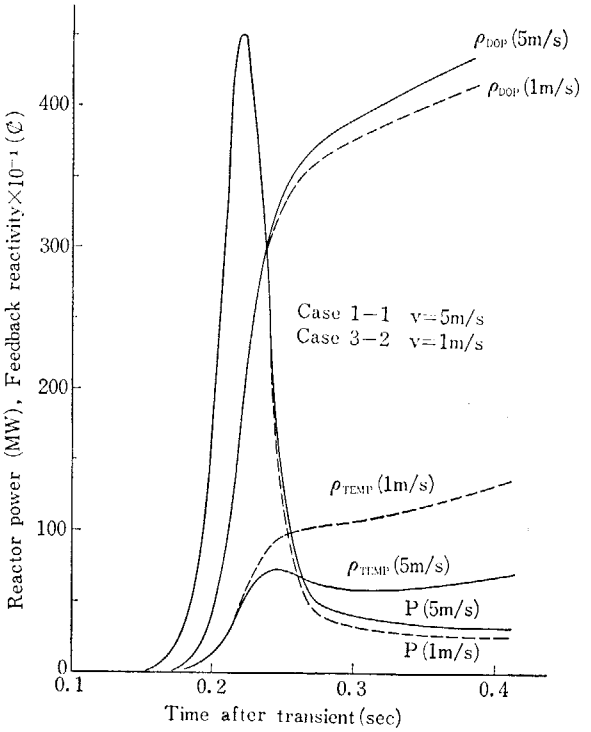

Fig. 3.7 Transient power and feedback reactivity with different flow rate by EUREKA (τ_0=10 ms, P=1500 psi, T=500°F)

As shown in **Fig. 3.7**, coolant velocity only changes run out power is small amount. It can be explained that, if coolant velocity is low, average coolant temperature rise is high, and thus moderator temperature feedback effect becomes large and as a result run out power becomes low. A remarkable result of **Fig. 3.7** is that coolant velocity does not influence on moderator feedback reactivity at power burst period. It can be concluded by this comparison that the prompt moderator heating effect does not lose it's outmost feature of controlling burst power, eventhough coolant velocity comes up to 5 m/s which is considered upmost coolant velocity in current light water power reactors.

As explained in the above paragraphs, several important conclusions obtained from EUREKA on reactor kinetics, by the comparison of SPERT-III E-core transient tests, are that

1) The prompt moderator heating effect is a significant effect to control burst power when reactivity transient occurs in power reactors at hot-startup and power operating condition.
2) Beside the prompt moderator heating effect, moderator feedback due to heat transfer from fuel to coolant gives some influence on run out power behavior.
3) By the above reasons, it is very much important for precise kinetic analysis of light water power reactors to use such a code that multi-regions thermal-hydrodynamics calculations are coupled to neutron kinetics calculation.

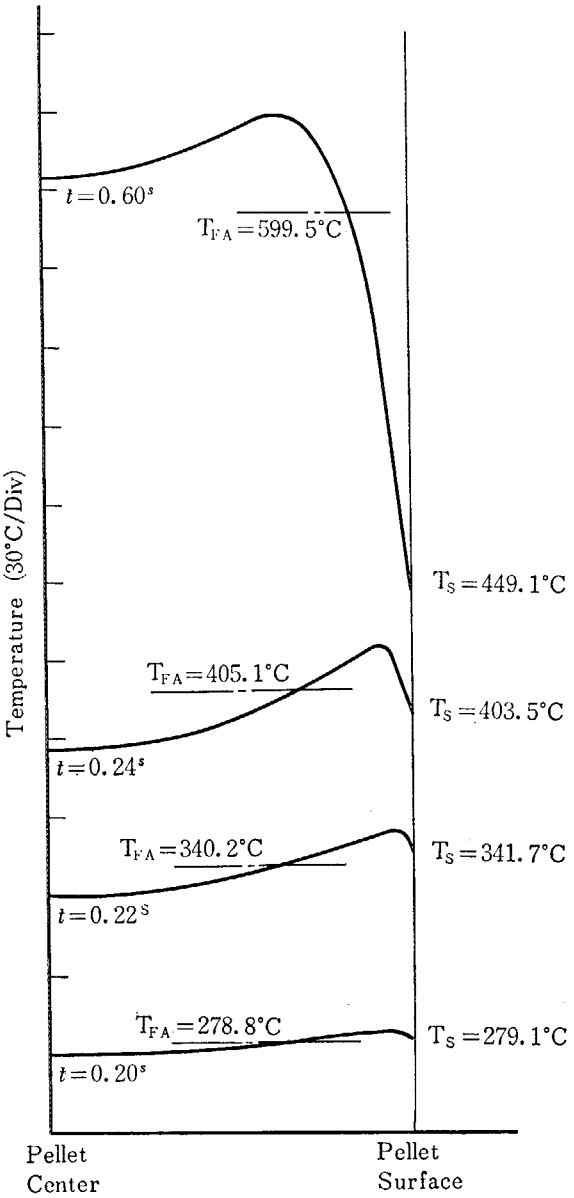

Fig. 3.8 Temperature distribution in fuel pellet

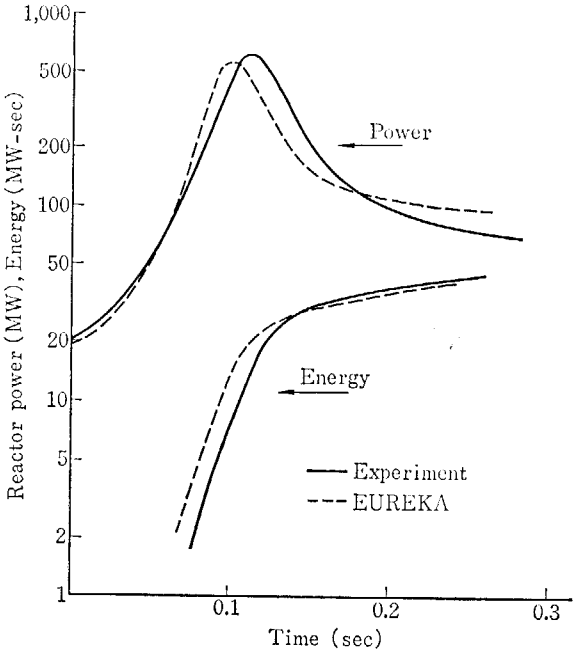

Fig. 3.9 EUREKA analysis (case 1—2) (10 ms, 20 MW, 500°F, 14 ft/s, 1500 psi)

4. Input Explanation

EUREKA inputs are fairly simple but the next three notices must be read carefully.

1) Inlet coolant temperature is controlled by coolant enthalpy, HIN. Coolant reference temperature, TIN, is only used for quadratic fitting calculation to approximate temperature-enthalpy correlation of water from the steam table. Therefore, it is desirable to set TIN value rather lower than the temperature equivalent to HIN.

2) Numbers of delayed neutron, NDLY, should be set six. Even a person who wish to use one delayed neutron group, must set NDLY six and sets five of delayed neutron fraction, DLYER (I), and decay constants, DECAY (I), to be zero.

3) Natural convection factors, ETA and ENU, are one and zero at forced convection problem. These values must be carefully calculated at a natural convection case in accordance with note in Appendix C and sentences discussed in the chapter 3.

EUREKA input explanation

Card 0; Title card. Problem No. (A4), Date (3A4), and Name (13A4).

Card 1; Computing time card. TMAX (6E 12.5).

Card 2; Control parameter card. (I12)

- KDOP; Numbers of set of reactivity inputs is given. When it is not reactivity transient case, KDOP must be set zero. (KDOP$\leq$10)
- KFLOW; Numbers of set of flow transient input is given. When it is not flow transient case, KFLOW must be set zero. (KFLOW$\leq$10)
- KTEMP; Numbers of set of temperature transient inputs is given. When it is not temperature transient case, KTEMP must be set zero. (KTEMP$\leq$10)
- KFRE; Numbers of fuel rupture informations for writeup is given. If user will not use this subroutine, KFRE may set zero. (KFRE$\leq$5)
- KDVBV; When KDVBV is set zero, builtin version performs calculation for normalizing heat generation and feedback importance factor. If user wish to use unnormalized values, KDVBV must be set positive number (any).
- IFDB; When IFDB is set zero, averaged temperature in fuel is used for Doppler feedback temperature. Other number uses surface temperature model.

Card 3; Control card for mesh computing frequency, and write up. (I12) (two sheet)

- IMAX; Maximum number of fuel cell nodes. (IMAX$\leq$25)
- JMAX; Maximum number of axial nodes in core. (JMAX$\leq$20)
- KMAX; Maximum number of flow channel in core. (KMAX$\leq$5)
- LMAX; Maximum number of fuel composition. (LMAX$\leq$5)
- NUMAX; Maximum number of computing frequency controlled by kinetic time. It must be noted that NUMAX is not controlled by hydraulic time TINHY.
- LGAP; Smaller number of fuel compositions between gap is set. Generally LGAP is two.
- NEX; Edit of detail transient information controlled by subroutine OUT 2 is written up every NEX times of hydraulic time.
- NEY; Edit of fuel temperature profile of whole core is written up every NEY times of hydraulic time.

Card 4; Fuel information card.

NFUEL; NFUEL is total numbers of fuel element in core and must be equal to total of FUELN in card 6. (I12)

Card 5; Fuel rod information card. (6E 12.5)

RCELL; Radius of equivalent unit cell. (m)

SRA; Radius of fuel pellet. (m)

SRB; Inner radius of clad. (m)

SRC; Outer radius of clad. (m)

ELIN; Length of noneffective fuel length at inlet. (m)

ELOUT; Length of noneffective fuel length at outlet. (m)

Card 6; FUELN(K) is fuel numbers in channel K. Data to KMAX are required. (6E 12.5)

Card 7; SKIN(K) is inlet pressure drop coefficient of K•th channel. Data to KMAX are required. (6E 12.5)

Card 8; SKOUT(K) is outlet pressure drop coefficient of K•th channel. Data to KMAX are required (6E 12.5)

Card 9; HZ(J) is height of axial fuel mesh J from effective fuel bottom. Therefore HZ(1) is always set zero. Data to JMAX are required. (6E 12.5) (m)

Card 10; Information card of fuel composition. (6I12)

NI(L); Numbers of interval in composition L.

Card 11; Reactor Operating Condition Information card (6E 12.5)

PP; System pressure. (kg/cm^2a)

HIN; Coolant inlet enthalpy. (kcal/kg)

GTOT; Total coolant flow rate in core. (m^3/hr)

TOTPW; Reactor power at initial condition. (MW)

TIN; Reference coolant inlet temperature. (°C)

Card 12; Multiplier and constant for heat calculation. (6E 12.5)

ETA; Multiplier to simulate natural convection heat transfer coefficient. (set 1 for forced convection case)

ENU; Same as ETA. 0.333 is generally used. (Set 0 for forced convection case)

ETADNB; Multiplier to DNB heat flux. EUREKA used Tong's DNB heat flux equation, but if user wishes to change the value, this multiplier is used. (normally 1)

ETHPMH; PMH heat generation rate.

Cards from 13 to 23 are data of fuel properties and recommend data are prepared in App. B.

Card 13; RHOP is density of fuel pellet. (6E 12.5) (kg/m^3)

Card 14; RHOK is density of fuel clad. (6E 12.5) (kg/m^3)

Card 15; Fuel pellet capacity calculation data card (6E 12.5)

Heat capacity (Cp) is calculated with quadratic temperature fitting of $Cp=a_0+a_1T+a_2T^2$ (unit kcal/kg.°C)

CPF 0 is a_0, CPF1 is a_1, and CPF2 is a_2.

Card 16; Fuel clad heat capacity calculation data card (6E 12.5)

Same as the card 16.

CPC 0 is a_0, CPC1 is a_1, and CPC2 is a_2

Card 17; Fuel pellet linear expansion coefficient calculation data card (6E 12.5)

Linear expansion coefficient is calculated with quadratic temperature fitting of $\lambda=a_0+a_1T+a_2T^2$

ALF 0 is a_0, ALF1 is a_1, and ALF2 is a_2.

Card 18; Clad linear expansion coefficient calculation data card. (6E 12.5)

Same as the card 19.
ALC 0 is a_0, ALC1 a_1 and ALC2 is a_2.

Card 19; Fuel pellet thermal conductivity calculation data card (6E 12.5)
Pellet thermal conductivity (λ_f) is calculated by power function with temperature of $\lambda_f=a_0+a_1T+a_2T^2+a_3/(T+a_4)$ (unit kcal/m·hr·°C)
RAMF 0 is a_0, RAME1 is a_1 and etc.

Card 20; Clad thermal conductivity calculation data card (6E 12.5)
Clad thermal conductivity is calculated by quadratic temperature fitting of $\lambda_c=a_0+a_1T+a_2T^2$ (unit kcal/hr·hr°C)
RAMC 0 is a_0, RAMC1 is a_1 and etc.

Card 21; Gap heat transfer coefficient calculation data card (6E 12.5)
The coefficient (h) is calculated by the equation of

$$h=8650\times\left(\frac{-0.79\times10^{-5}T^2+0.0344T+6.35}{22.56+\Delta x\times10^6}\right)$$

from Anderson and Leichter's work[8] (see App. B). Unit of h is kcal/m²·hr·°C. In this equation, T is gap temperature and x is gap distance. These time dependent value are calculated in EUREKA.
RAMG 0 is a_0. RAMG1 is a_1, RAMG2 is a_2 and CONSTG is a_4

Card 22; Kinetic Parameter information card (I12, 5E 12.5)
NDLY; Numbers of delayed neutron group (set 6)
TINC 0; Kinetic time increment. The following equation must be satisfied. (unit in sec)
n×TINCN=TINHY.
n is integer number from 1 to 10.
TINHY; Hydraulic time increment. The following equation must be satisfied. (unit in sec)
TINHY=(z(J)/v(J)) min
where z(J) is axial mesh span and v(J) is coolant velocity at mesh J.
If TINHY does not satisfy the equation, index "Hydraulic time is error" is written up but calculation continues. TINHY is changed to be half just one time during transient calculation when TINHY is over (z_j/v_j) min but never goes down more than one time.
PROT; Prompt neutron life time l (sec)
EFDLYD; Effective delayed neutron fraction β.

Card 23; Card of delayed neutron information (6E 12.5).
DLYER(I) is percentage of i-th delayed neutron β_i.

Card 24; Card of Delayed Neutron decay constant (6E 12.5)
DECAY(I) is decay constant of i-th delayed neutron λ_i (unit sec^{-1})

Card 25; Card of heat generating rate in fuel pellet (6E 12.5).
AMU(I) is heat generation rate in i-th mesh point in fuel and clad. Data to IMAX is required.

Card 26; Heat generating information of core (6E 12.5).
FRPW(J, K) is heat generation rate at J-th node (axial) in K-th channel. Sets of data to KMAX which cover data from J=1 to JMAX are required.

Card 27; Doppler feedback importance data in core (6E 12.5).
Same as the card 28.

Card 28; Moderator temperature feedback importance data in core (6E 12.5).

Same as the card 28.

Card 29; Doppler feedback reactivity ρ_{dop} is calculated by the temperature function $\rho_{dop}=a_0+a_1T+a_2T^2+a_3T^3+a_4Ta^5$ and the imput DOPC(1) is a_0 and DOPC(6) is a_5. Where T is fuel temperature. Unit of ρ_{dop} is $\Delta k/k$.

Card 30; Void and clad expansion coefficient (6E 12.5).
These feedback reactivity is calculated by the function of
$\rho_{void}(\text{clad exp.})=a_0\alpha+a_1\alpha^2$ ($\Delta k/k$/% void)
where α is void fraction (clad expansion fraction) in unit cell.
a_0 corresponds to VOIC(1) and a_1 corresponds to VOIC(2) or EXPC(2).

Card 31; Moderator temperature feedback coefficient (6E 12.5).
Moderator temperature feedback reactivity is calculated by the function of
$\rho_{mod}=a_0T+a_1T^2+a_2T^3$ ($\Delta k/k$)
where T is coolant temperature and a_0 corresponds to TEMC(1) and etc.

Card 32; Reativity transient information card (6E 12.5).
If KDOP is zero, skip this card. Set of data reactivity ($\Delta k/k$) and time (sec) data is given up to KDOP sets (less than 10). Time of the last data must be equal to or greater than computing transient time TMAX (card 1).

Card 33; Maximum permissible error in repeating calculation.
EPI1; Nucleate boiling temperature error (0.01°C)
EPI2; Heat flux error (0.001)
EPI3; Feedback reactivity error (0.005)
EPI4; Clad temperature error (0.05°C)
EPI5; Pressure prop error (0.005)
EPI6; Heat transfer coefficient error (0.01)
data in parenthes is used for sample calculation.

Card 34; and 35
Node for special writeup (I12, 5E 12.5).
JEDIT and KEDIT is number of node selected for special write up in OUT 2 and normally same number (less than 6) JPP(J) in card 36 is node number in KPP(K) channel. KPP(J) and KPP(K) are set in card 33 and 34.

Card 36; Flow transient information card (6E 12.5).
If KFLOW is zero (non flow transient case), skip this card. Sets of flow rate (m^3/hr) and time (sec) data is given up to KFLOW sets (less than 10).
Time of the last data must be equal to or greater than computing transient time TMAX (card 1).

Card 37; Coolant temperature transient information card (6E 12.5).
If KTEMP is zero (non coolant temperature transient case), skip this card. Sets of temperature change data is given up to KTEMP sets (less than 10). Time of the last data must be equal to or greater than computing transient time TMAX (card 1).

Card 38; Fuel rupture information writeup. Index card (6E 12.5).
If KFRE is zero, skip this card.
FRE (1); Clad melting temperature is given (°C)
FRE (2); Fuel melting temperature is given (°C)
FRE (3); Water logged fuel rupture energy is given (cal/gr UO_2)
FRE (4); Fuel rupture energy is given (cal/gr UO_2)
FRE (5); Fuel evaporation energy is given (cal/gr UO_2)

Card 39; Volume fraction in each region in core.

If KDVBV is zero, skip this card. If not, volume of each core region (j and k) must be given.

5. Conclusion

The results computed by EUREKA on the SPERT-III E-core showed excellent agreement with experimental results within the range of difference from 10 to 30% over a wide range of different experimental conditions. The reasons lie in the detailed treatment of thermal hydrodynamics, which influences reactor kinetic behavior through feedback reactivity. Also, it is proved from these experimental analyses that the moderator feedback reactivity in hot-standby, hot-startup, and power operating conditions of a reactor has a very important role, and the thermal hydrodynamic model of EUREKA is much suitable for predicting transient response of light water power reactors in comparison with the adiabatic model which has been used generally in reactivity accident analyses.

The thermal hydrodynamic model used in EUREKA has caused numerical instability in certain situations, that is, transient boiling occurred seriously in coolant channel. Also, there are many uncertainties in the areas of transient boiling heat transfer and void volume production. A truely reliable model can not be designed until these uncertainties are overcome. For the above reasons and the fact, the EUREKA must be improved in future.

Acknowledgment

The authors express their appreciation to Dr. K. Sanogawa for his preparation of steam table subroutine, to Mr. I. Nomura and Mr. T. Miura for their aids in programing. They also give thanks to Mr. K. Sato, Mr. T. Taji and Mr. T. Tutui for their advices on coding techniques, to Mr. H. Hatta and Mr. N. Takahashi for their help in huge number of test run calculations. Finally authors extend their thanks to persons, concerned with the SPERT-III E-core experiment, for their courtesy of transmitting us results.

References

1) T. G. Taxelius: Quartery Technical Report-SPERT Project Jan., Fev., Mar. 1968, IDO-17287 (1968).
2) T. G. Taxelius: Quartery Technical Report-SPERT Project July, Aug., Sep. 1967, IDO-17271 (1968).
3) T. G. Taxelius: Quartery Technical Report-SPERT Project Apr., May, June 1967, IDO-17270 (1968).
4) J. E. Houghtaling, M. Ishikawa, J. F. Scott and D. I. Herborn: Temperature Dependent Kinetic Behavior of the SPERT-III·E Core, ANS Trans Act. Vol. 10, No. 2 (1967).
5) J. E. Houghtaling, R. K. McCardell and D. I. Herborn: Reactivity Accident Investigations with a Pressurized Water Reactor Core in the SPERT-III Facility, ANS Trans Act. Vol. 11, No. 1 (1968).
6) C. F. Obenchain and et al.: PARET—A Program for the Analysis of Reactor Transients: Proc. Intern Conf. Research Reactor Utilization and Reactor Mathematics, Mexico City (1967).
7) C. F. Obenchain: PARET—A Program for the Analysis of Reactor Transients, IDO-17282 (1969).
8) W. K. Anderson and G. L. Lechliter: Some Input Properties-Part I Thermal Properties, ANS Trans Act. Vol. 9, No. 2 (1966).

9) W. H. McAdams: Heat Transmission, New York McGraw Hill Book (1954).
10) A. I. Brown and S. M. Marco: Introduction to Heat Transfer, New York McGraw Hill Book, p. 161-172 (1958).
11) J. Japan Soc. Mech. Engrs.: Mechanical Engineering Handbook (Rev. 3), (1951).
12) W. H. Jens and P. A. Lottes: Analysis of Heat Transfer, Burnout, Pressure Drop and Density Data for High Pressure Water, ANL-4627, (1951).
13) Y. Kuge and et al.: KINAK—A Code for One Dimensional, Nuclear, Thermal and Hydraulic Calculation for Boiling Water Reactor, JAERI-1107, (1961).
14) L. S. Tong, H. B. Currin and A. G. Thorp: New DNB (Burnout) Correlations, WCAP-1997 (Rev. 2), (1963).
15) J. Japan Soc. Mech. Engrs.: Boiling Heat Transfer, (1964).
16) P. G. Poletavkin and N. A. Shapkin: Water and Steam Content in Surface Boiling of Water, AERE Lib./Trans 804 (1958).
17) G. W. Maurer: WAPD-BT-19, (1960).
18) M. Shiba and Y. Yamashaki: Trans. Japan Soc. Mech. Engrs., Vol. 32, No. 245 (1966).
19) R. C. Noyes, J. G. Morgan and H. H. Cappel: TRANS-FUGUE-1—A Digital Code for Transient Two-Phase Flow and Heat Transfer, NAA-SR-11008, (1965).
20) NAA-SR-MEMO-4980.
21) E. R. Cohen: Some Topics in Reactor Kinetics, 2nd Geneva Conf., p. 629.
22) Y. Kanbayashi: Reactor Kinetics Code—KIREK, JAERI-memo 3198 (1968).
23) R. J. Wagner: HEAT-1—A One Dimensional Time Dependent or Steady State Heat Conduction Code for the IBM-650, IDO-16867 (1963).
24) R. S. Varga: Numerical Solution of the Two Group Diffusion Equations in x-y Geometry, WAPD-159 (1956).
25) E. L. Wachspress: CURE—A Generalized Two Space Dimension Multigroup Coding for the IBM-704, KAPL-1724 (1957).
26) R. D. Richmyer: Difference Methods for Initial Value Problems, New York Interscience Publishers (1957).
27) R. K. McCardell, D. I. Herborn and J. E. Honghtaling: Reactivity Accident Results and Analysis for the SPERT-III•E Core—A Small Oxide-Fueled, Pressurized-Water Reactor, IDO-17281 (1969).
28) J. P. Stora: Thermal Conductivity of Sintered Uranium Oxide under In-pile Condition, EURAEC-1095 (1964).
29) A. Morishima and et al.: The Design for Power Reactor Fuel Assembly•1 (Design Data of Temperature, Heat Flux Distribution and Mechanical Strength), JAERI-memo 2704 (1967).
30) M. Ishikawa, Y. Kuge, Y. Kanbayashi, E. Takeuchi, N. Ohnishi and H. Hata: Fast Transient Analysis for Light Water Power Reactor by EUREKA, Coupled Nuclear Thermal-Hydrodynamic Kinetic Code, JAERI-1201 (1970).
31) M. Ishikawa: Analysis of Prompt Moderator Heating Reactivity Feedback Effect, JAERI 1214 (1971).

Appendix A. User's Guides for Important Input

A-1. Time Increment

Here, authors wish to add some more sentences to EUREKA explanation for user's convenience. In order to obtain reasonable results by EUREKA, it is noted that the result is significantly dependent on the time increment used in calculation. EUREKA's time increment is definitively controlled with the hydraulic time increment (INPUT), and reasonable kinetic analysis can be obtained when the hydraulic time increment is adequately decided. It is advisable that in general equal or less than half of reactor period is used throughout transient analysis and the provisions are in EUREKA as stated in the chapter 4. It must be recognized that even this time increment is used, calculated peak power should have some percentages of error, because reactor period around peak power time changes violently.

This is because that the major part of compensated reactivity which is the most important for kinetic analysis is generated at around peak power time. Therefore strictly speaking, the above time increment may not be sufficient enough to follow up this violent power generation in accurate, and one who uses finer repeating time increment, will get better results, even though it will increase considerable computing time.

A-2. Doppler Feedback Temperature

As widely used, EUREKA assumes that average fuel temperature is the doppler temperature. This assumption may be good to calculate kinetic behavior starting from low power initial condition in low enriched fuel core.

Since fuel surface heat generation is larger than that in fuel center, transient fuel surface temperature rise becomes larger than average fuel temperature rise when heat transfer from fuel to clad is negligiblly small and in the case when initial fuel temperature profile is not a problemed, such as the case of the cold start-up transient. EUREKA analysis of the cold fiducial test and hot-standby test in the SPERT-III E-core show a good match to experimental results.

However, a significant errors can be expected in this model at the transient analysis from power operating condition where temperature profile in fuel is established. It is remained that in experimental analysis from 20 MW power operational condition, about 30% of calculation difference is brought in at peak power time. One supposed that the reason would be caused by the large temperature profile in fuel established at the time of initial conditions (Fig. 3. 8) of analysis where doppler temperature assumed may be large enough to actual fuel surface temperature that doppler is controlled.

A study to this doppler temperature model problem has been carried by EUREKA. Calculations by two different type of doppler models are used in this study. The one is the fuel average temperature model as stated and the other is so called surface temperature model that the doppler temperature is assumed to be average of fuel surface temperature and fuel average temperature.

Calculated excursion power shape changes significantly depend on doppler model. It also gives some influences on run out power as be seen in the **Fig. 3. 8.** Though any data are not available to justify abequency of these model, however, authors experiences by EUREKA infer that the surface temperature model is rather better than currently used doppler model. Present EUREKA has provision to select either doppler model by user's option.

A-3. Natural Convection Heat Transfer Coefficient

As stated in the chapter 2, EUREKA needs coolant flow rate in INPUT even for a transient

analysis of no flow condition.

Since equations to calculate forced flow heat transfer coefficient is very much different from that of natural convection, the present EUREKA model do not have provision to calculate natural convection heat transfer coefficient exactly. This work is underway, because that thrmal-hydrodynamic calculations to fix natural convection changes considerable structures of the EUREKA model.

In order to compromise the problem, the present EUREKA uses the approximation method for natural convection heat transfer calculation, as stated in the Appendix C. The most important point to use this approximation is to estimate reasonable flow velocity to simulate natural convection. It is quite a difficult problem to user, however it is a quite important input for accurate analysis.

A-4. Multi Region Effect

Heat generations and feedback importance distribution in core of the most important input in EUREKA. These data must be given precisely in each subdivided core regions.

Special emphasises are given to such a case that large flux skew is expected in the core, such as rod ejection accident and rod drop accident analyses. EUREKA experiences infer that heat generation and importance factor distributions at peak power time, is good to analyse burst power and that these data at run out power time are good for run out time analyses. In addition authors recommend to prepare finer subdivided core regions to higher heat generating area in EUREKA calculation.

All the above recommendations come out from author's experiences through SPERT-III E-core tests analysis by EUREKA, and authors believe that EUREKA would calculate reasonable transient behavior of light water power reactor, if proper inputs are used.

Appendix B. Fuel Properties for Input

1. Thermal Conductivity (λ; kcal/m·hr·°C)

1.1 UO_2 pellet (**Fig. B-1**)

Recent Stora's data[28] based on in-pile experiment is used for EUREKA. This data is selected among many thermal conductivity equations for UO_2, since it shows a good agreement with the Lyon's theoretical equation, published in 1964. Stora's data is fitted to quadratic equation with fuel temperature T(°C) so that

$$\lambda_{UO_2}=0.1135\times10^{-5}T^2-0.3352\times10^{-2}T+3.9265+877.63/(T+200) \quad (B-1)$$

1.2 Clad

Here, stainless steel and Zircaloy-II data are presented. For stainless steel

$$\lambda_{SUS}=0.3946\times10^{-2}T+12.967 \quad (B-2)$$

and for Zircaloy-II[8] (Ref. **Fig. B-2**)

$$\lambda_{Zr}=0.010962T+10.5462$$

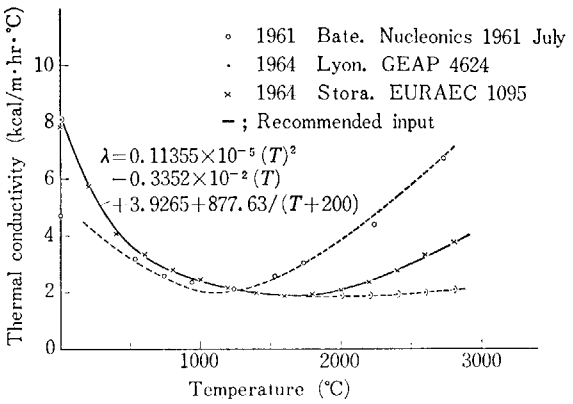

Fig. B-1 UO_2 thermal conductivity (ρ_{UO_2}; 95% T.D.)

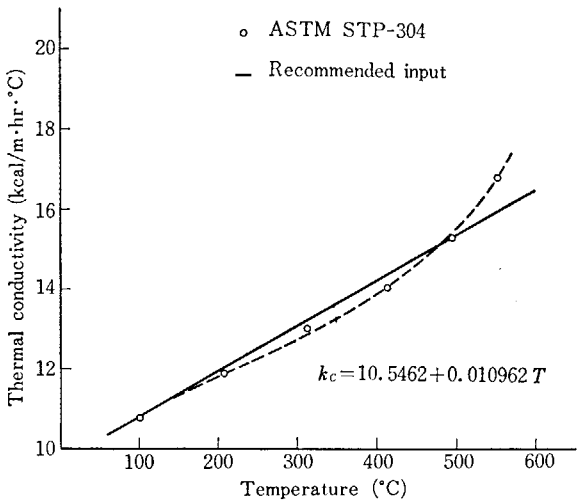

Fig. B-2 Zr-2 thermal conductivity

2. Heat Capacity (Cp; kcal/kg·°C)

2.1 UO_2 pellet

UO_2 with 95 percent of theoretical density is chosen.

$$Cp_{UO_2}=0.8123\times10^{-8}T^2-0.9556\times10^{-6}T+0.0657 \quad (B-4)$$

2.2 Clad

For stainless steel

$$Cp_{SUS}=2.0053\times10^{-5}T+0.12068 \quad (B-5)$$

and for Zircaloy-II[29] (Ref. **Fig. B-3**)

$$Cp_{Zr\text{-}2}=0.25\times10^{-3}T+0.07 \quad (B-6)$$

3. Linear Expansion Coefficient (α, $^0C^{-1}$)

3.1 UO_2 pellet

$$\alpha_{UO_2}=1.0\times10^{-5} \quad (B-7)$$

3.2 Clad

For stainless steel (Ref. **Fig. B-4**)

$$\alpha_{SUS}=1.8\times10^{-5} \quad (B-8)$$

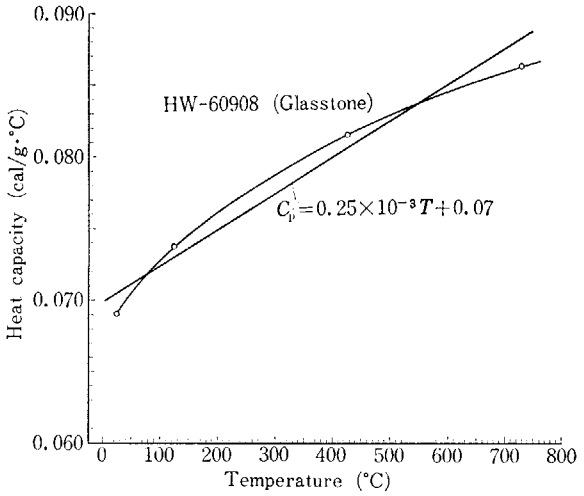

Fig. B-3 Heat capacity of zirconium alloy

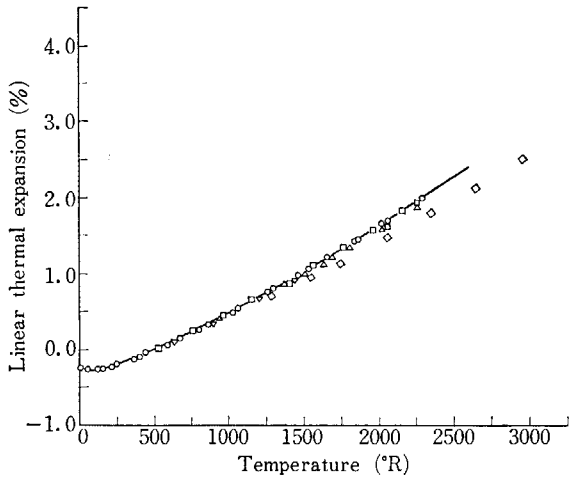

Fig. B-4 Linear thermal expansion rate of stainless steel

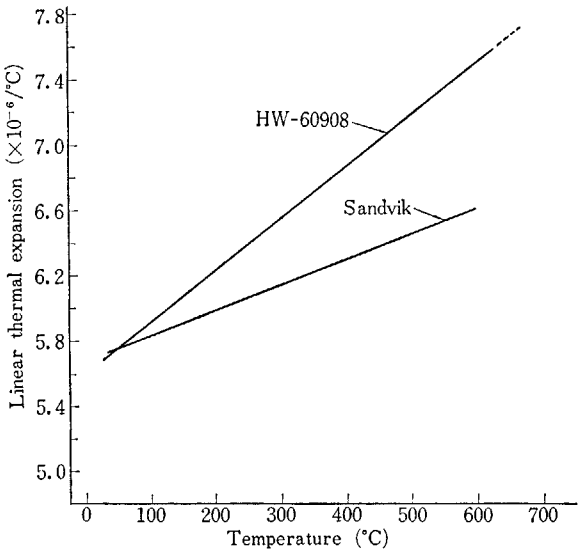

Fig. B-5 Linear thermal expansion rate of Zry-II

and for Zircaloy-II[29] (Ref. Fig. B-5)

$$\alpha_{Zr-2}=0.32\times10^{-8}T+0.56\times10^{-6} \quad \text{(B-9)}$$

4. Gap Heat Transfer Coefficient (H; kcal/m²·hr·°C)

Anderson and Leichter's[8] work is applied in EUREKA. Here, gap heat transfer coefficient H_{gap} is calculated with temperature of gap gas T(°C) and gas clearance $\Delta x(m)$

$$H_{gap}=8650\times\left(\frac{-0.79\times10^{-5}T^2+0.0344T+6.35}{22.56+\Delta x\times10^5}\right) \quad \text{(B-10)}$$

$$\Delta x=r_{\text{clad inner rad.}}-r_{\text{pellet rad.}} \quad \text{(B-11)}$$

where T and Δx are calculated in code. Gap heat transfer coefficient by equation (B-10) are shown in Fig. B-3 with various gap clearance.

5. Fuel Rupture Index

Subroutine FURUPT compares computed fuel status with fuel rupture conditions given by INPUT at every time step and write up fuel rupture when computed value exceeds inputs. Five inputs are required in FURUPT and these data are

FRE (1) is fuel melting temperature 2800°C for UO_2

FRE (2) is clad melting temperature 1800°C for Zr and 1380°C for stainless steel

FRE (3) is fuel rupture enthalpy. SPERT-CDC experiments shows that FRE (3) is 50-60

cal/gr UO_2 for water logged fuel

FRE (4) is UO_2 melting energy approximately 280cal/gr UO_2 for UO_2

FRE (5) is UO_2 evaporating energy approximately 500cal/gr UO_2 for UO_2

$$H=\left(\frac{6.35+0.0344T-0.79\times10^{-5}T^2}{22.56+\Delta x\times10^6}\right)\times8600\,\text{kcal/hr}\cdot\text{m}^2\cdot{}^\circ\text{C}$$

Δx;m 単位

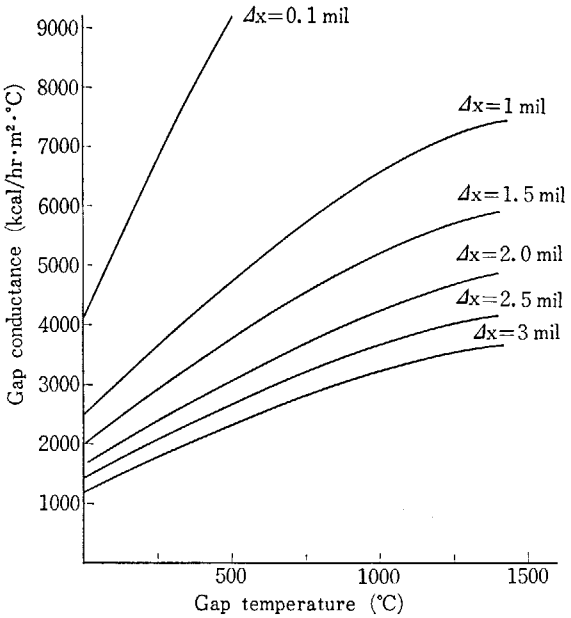

Fig. B-6 Gap heat transfer coefficient

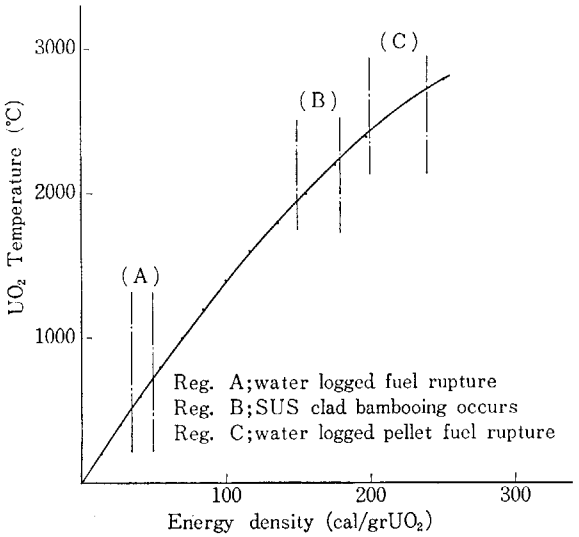

Fig. B-7 UO_2 temperature—energy density curve
$(Cp_{UO_2}(T)=0.8123+10^{-8}T^2-0.9556\times10^{-6}T+0.0657$
$\rho=10.5\,\text{g/cm}^3)$

Appendix C. Natural Convection Heat Transfer

Reactivity accident from cold start up condition would possibly occurs in pool cooling condition and in this case heat transfer coefficient from fuel to coolant must be calculated from time dependent natural convection heat transfer equation.

However, it is difficult to introduce large version of natural convection heat transfer coefficient into present EUREKA constraction and, in addition, if it can be reliable natural convection data for fuel bundle has not been yet published.

SPERT-III E-Core experiment[3] have reported that a forced convection heat transfer equation can approximate natural convection heat transfer with good accuracy by modification. This method is applied in EUREKA.

Natural convection heat transfer equation for thin wire is given

$$Nu_G = 0.129\ (Gr \cdot Pr)^{1/3} \tag{C-1}$$

and can be written into

$$Nu_G = 0.129\left(\frac{g \cdot \beta \cdot d^3}{\nu^2}\Delta t\right)^{1/3} \cdot (Pr)^{1/3} \tag{C-2}$$

where all terms except Δt in the eq. (C-2) are given from reactor condition, and, (C-2) can be written

$$\begin{aligned} Nu_G &= 0.129\left(\frac{g \cdot \beta \cdot \alpha^3}{\nu \cdot a}\right)^{1/3} \Delta t^{1/3} \\ &= k_G \Delta t^{1/3} \end{aligned} \tag{C-3}$$

where, k_G is a known value from reactor condition.

The equation (C-3) is compared with the equation (C-4) which is the equation of forced circulation with Reynold's number of less than two thousands that is thought to be equivalent to natural convection condition.

$$Nu_R = 1.02(Re)^{0.45} \cdot (Pr)^{0.33} \cdot \left(\frac{De}{L_{CH}}\right)^{0.4} \cdot \left(\frac{\nu_{bt}}{\nu_{ct}}\right)^{0.14} \tag{C-4}$$

in the equation (C-4), all terms are given from reactor condition, and coolant velocity, except kinetic viscosity ν_{bt} and ν_{ct}, which has less effect on Nu_R calculation.

Thus, one can write the equation (C-2)

$$Nu_R = \text{constant} = k_R \tag{C-5}$$

Using EUREKA built-in equation (Nu_R) of forced convection heat transfer with Reynold's number of less than two thousands, the equation (C-5) can be written

$$\begin{aligned} Nu_G &= k_G \cdot \Delta t^{1/3} \\ &= \frac{k_G}{k_R} \cdot Nu_R \cdot \Delta t^{1/3} \end{aligned} \tag{C-6}$$

where NUR; calculated in EUREKA by the equation (C-4)

ETA; multiplier to forced circulation (Input) ETA $= k_G/k_R$

ENU; 1/3 for natural convection and zero for forced circulation (Input)

ETA for natural convection is calculated from the equation (C-6), assuming natural convection coolant velocity v. So for as heat transfer is the only problem, the value of v does not alter natural convection heat transfer coefficient very much because of the nature of the equation (C-6), even either v is assumed conservatively or not. If v is assumed smaller, Nu_R become smaller and k become larger and so on. However, in the case that moderator temperature

feedback coefficient is dominate, the value v must be carefully examined to match with natural convection flow velocity. For example, when burst power is a problem, velocity v must be selected to be the natural convection flow velocity at that time, as it is believed that natural convection flow is just started. When run out power is a problem, velocity v must be selected to be the natural convection flow velocity fully developed.

Appendix D. Flow chart

CHART TITLE - MAIN PROGRAM

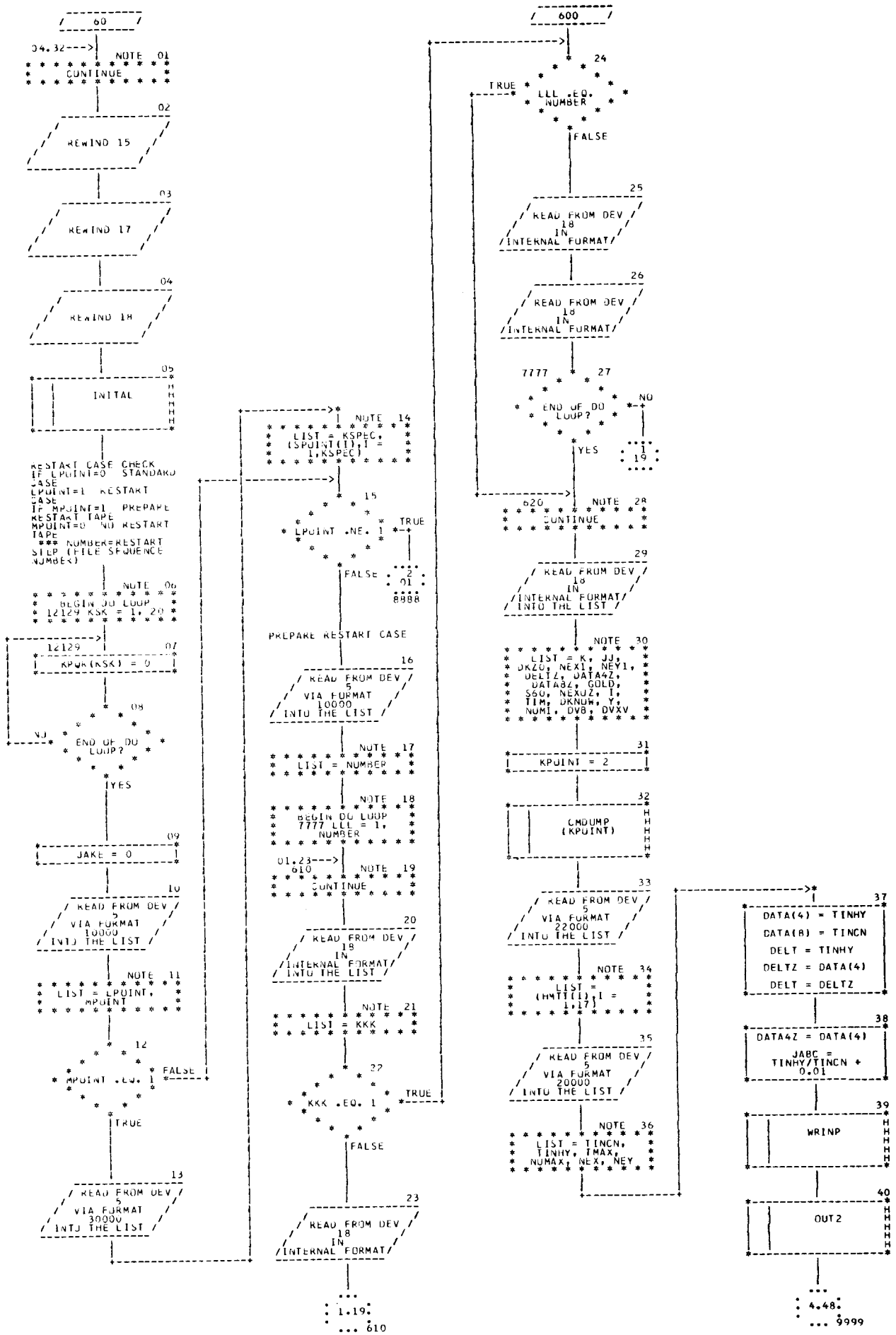

CHART TITLE - PROCEDURES

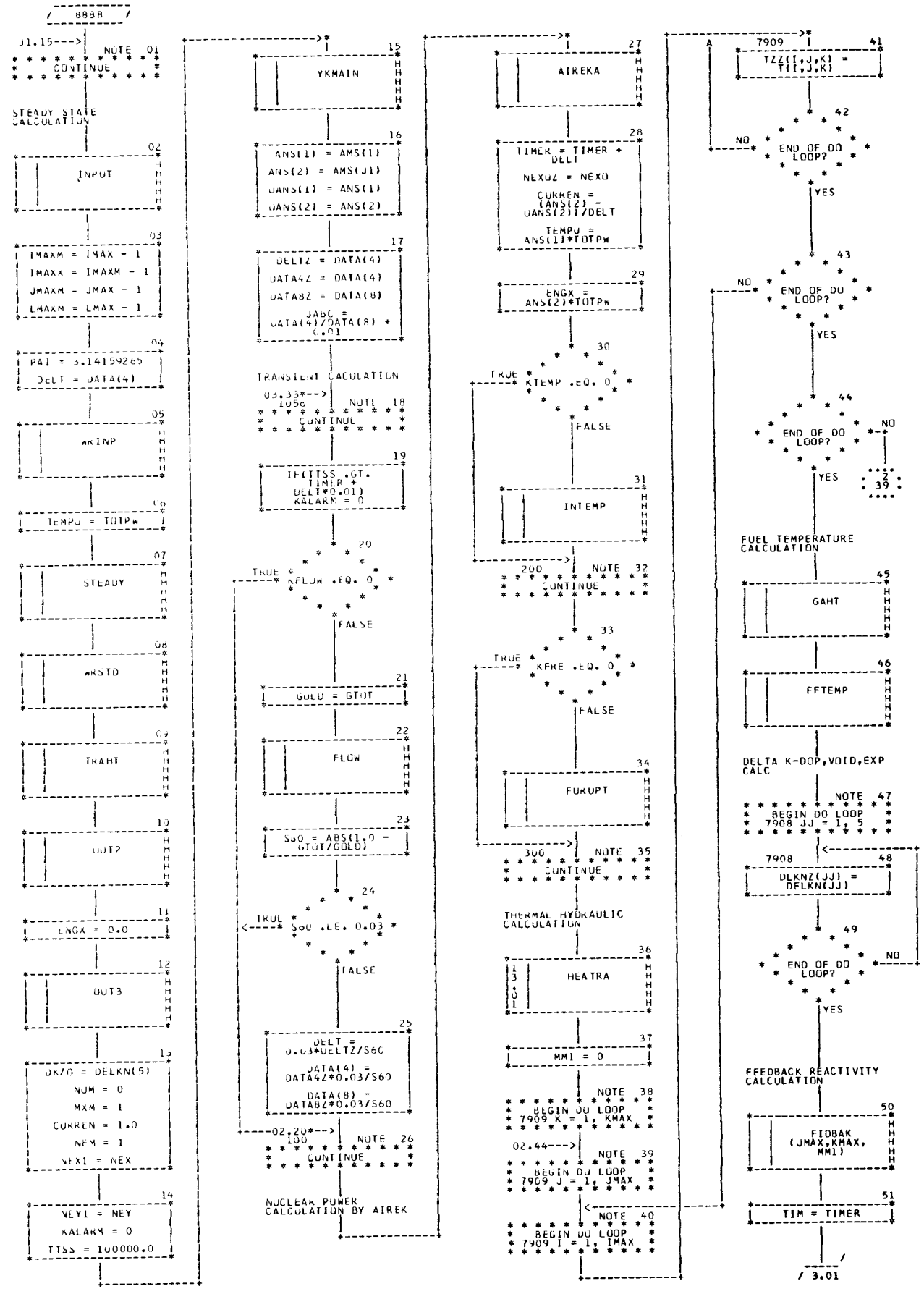

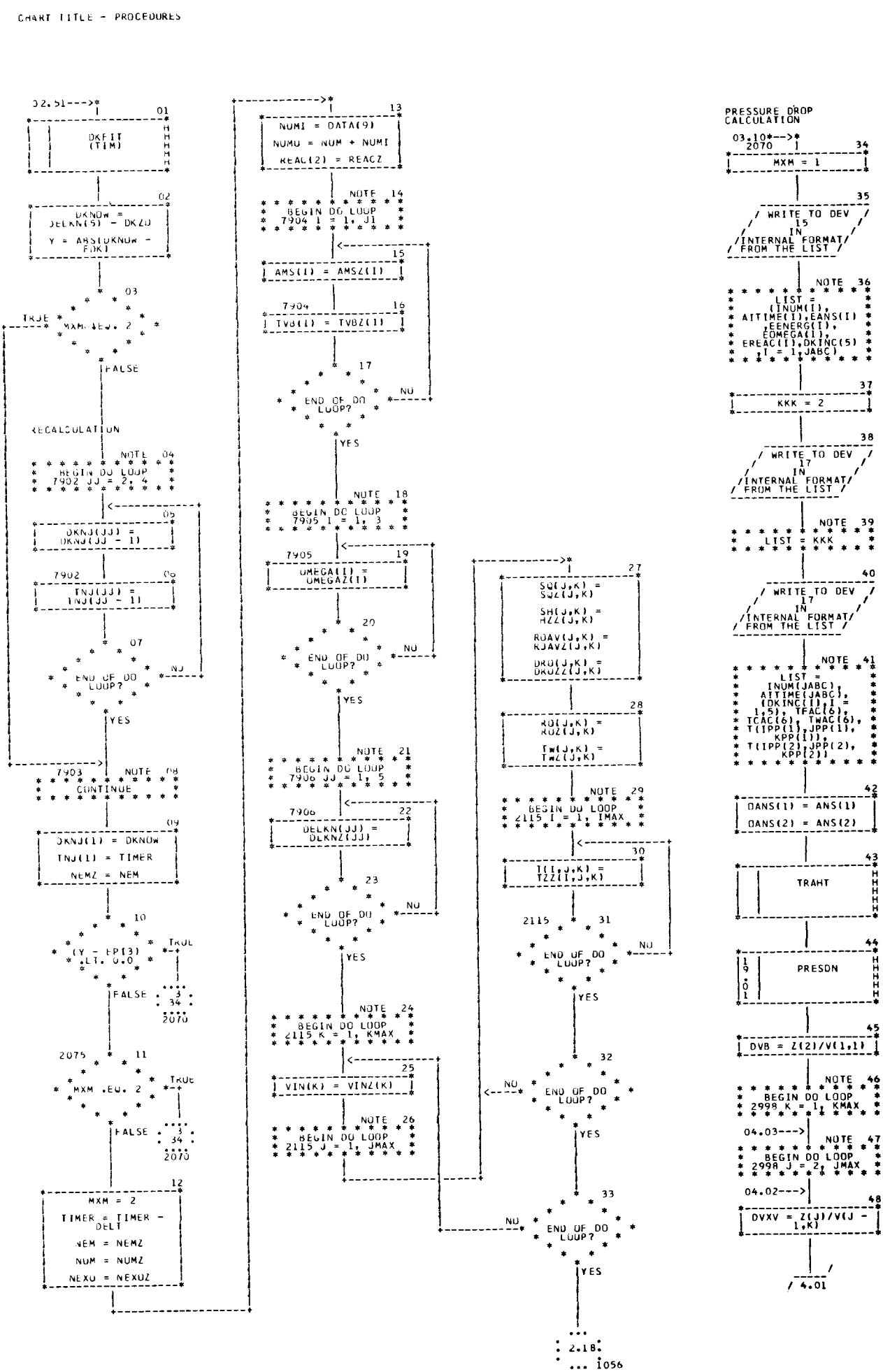
CHART TITLE - PROCEDURES
02.51--->
01
DKFIT (TIM)
02
DKNOW = DELKN(5) - DKZO
Y = ABS(DKNOW - FDK)
03
TRUE
MXM .EQ. 2
FALSE
RECALCULATION
NOTE 04
BEGIN DO LOOP 7902 JJ = 2, 4
05
DKNJ(JJ) = DKNJ(JJ - 1)
7902
06
TNJ(JJ) = TNJ(JJ - 1)
07
END OF DO LOOP?
NO
YES
7903
NOTE 08
CONTINUE
09
DKNJ(1) = DKNOW
TNJ(1) = TIMER
NEMZ = NEM
10
(Y - EPI(3) .LT. 0.0
TRUE
FALSE
2075
11
MXM .EQ. 2
12
MXM = 2
TIMER = TIMER - DELT
NEM = NEMZ
NUM = NUMZ
NEXU = NEXUZ
13
NUMI = DATA(9)
NUMU = NUM + NUMI
REAL(2) = REACZ
NOTE 14
BEGIN DO LOOP 7904 I = 1, J1
15
AMS(I) = AMSZ(I)
7904
16
TVB(I) = TVBZ(I)
17
END OF DO LOOP?
NO
YES
NOTE 18
BEGIN DO LOOP 7905 I = 1, 3
7905
19
OMEGA(I) = OMEGAZ(I)
20
END OF DO LOOP?
NO
YES
NOTE 21
BEGIN DO LOOP 7906 JJ = 1, 5
7906
22
DELKN(JJ) = DELKNZ(JJ)
23
END OF DO LOOP?
NO
YES
NOTE 24
BEGIN DO LOOP 2115 K = 1, KMAX
25
VIN(K) = VINZ(K)
NOTE 26
BEGIN DO LOOP 2115 J = 1, JMAX
27
SQ(J,K) = SQZ(J,K)
SH(J,K) = HZZ(J,K)
ROAV(J,K) = ROAVZ(J,K)
DRO(J,K) = DROZZ(J,K)
28
RO(J,K) = ROZ(J,K)
TW(J,K) = TWZ(J,K)
NOTE 29
BEGIN DO LOOP 2115 I = 1, IMAX
30
T(I,J,K) = TZZ(I,J,K)
2115
31
END OF DO LOOP?
NO
YES
32
END OF DO LOOP?
NO
YES
33
END OF DO LOOP?
NO
YES
2.18
1056
PRESSURE DROP CALCULATION
03.10*-->
2070
34
MXM = 1
35
WRITE TO DEV 15 IN INTERNAL FORMAT FROM THE LIST
NOTE 36
LIST = (INUM(I), AITIME(I),EANS(I) ,EENERG(I), EOMEGA(I), EREAC(I),DKINC(5) ,I = 1,JABC)
37
KKK = 2
38
WRITE TO DEV 17 IN INTERNAL FORMAT FROM THE LIST
NOTE 39
LIST = KKK
40
WRITE TO DEV 17 IN INTERNAL FORMAT FROM THE LIST
NOTE 41
LIST = INUM(JABC), AITIME(JABC), (DKINC(I) I = 1,5), TFAC(6), TCAC(6), TWAC(6), T(IPP(1),JPP(1), KPP(1)), T(IPP(2),JPP(2), KPP(2))
42
OANS(1) = ANS(1)
OANS(2) = ANS(2)
43
TRAHT
44
PRESDN
45
DVB = Z(2)/V(1,1)
NOTE 46
BEGIN DO LOOP 2998 K = 1, KMAX
04.03--->
NOTE 47
BEGIN DO LOOP 2998 J = 2, JMAX
04.02--->
48
DVXV = Z(J)/V(J - 1,K)
4.01

CHART TITLE - PROCEDURES

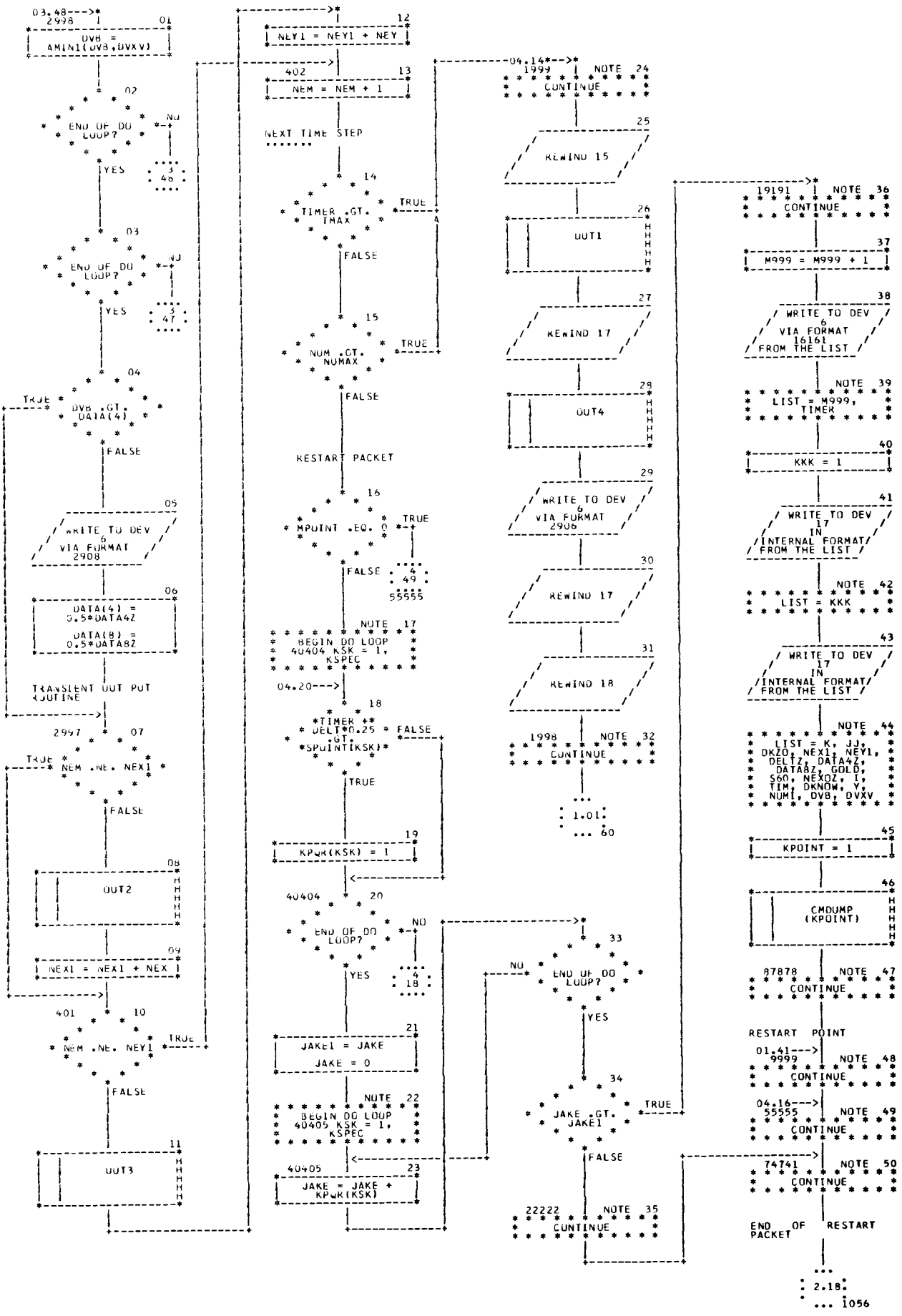

CHART TITLE - PROCEDURES

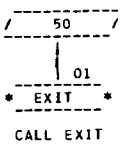

CHART TITLE = SUBROUTINE STPRES(K)

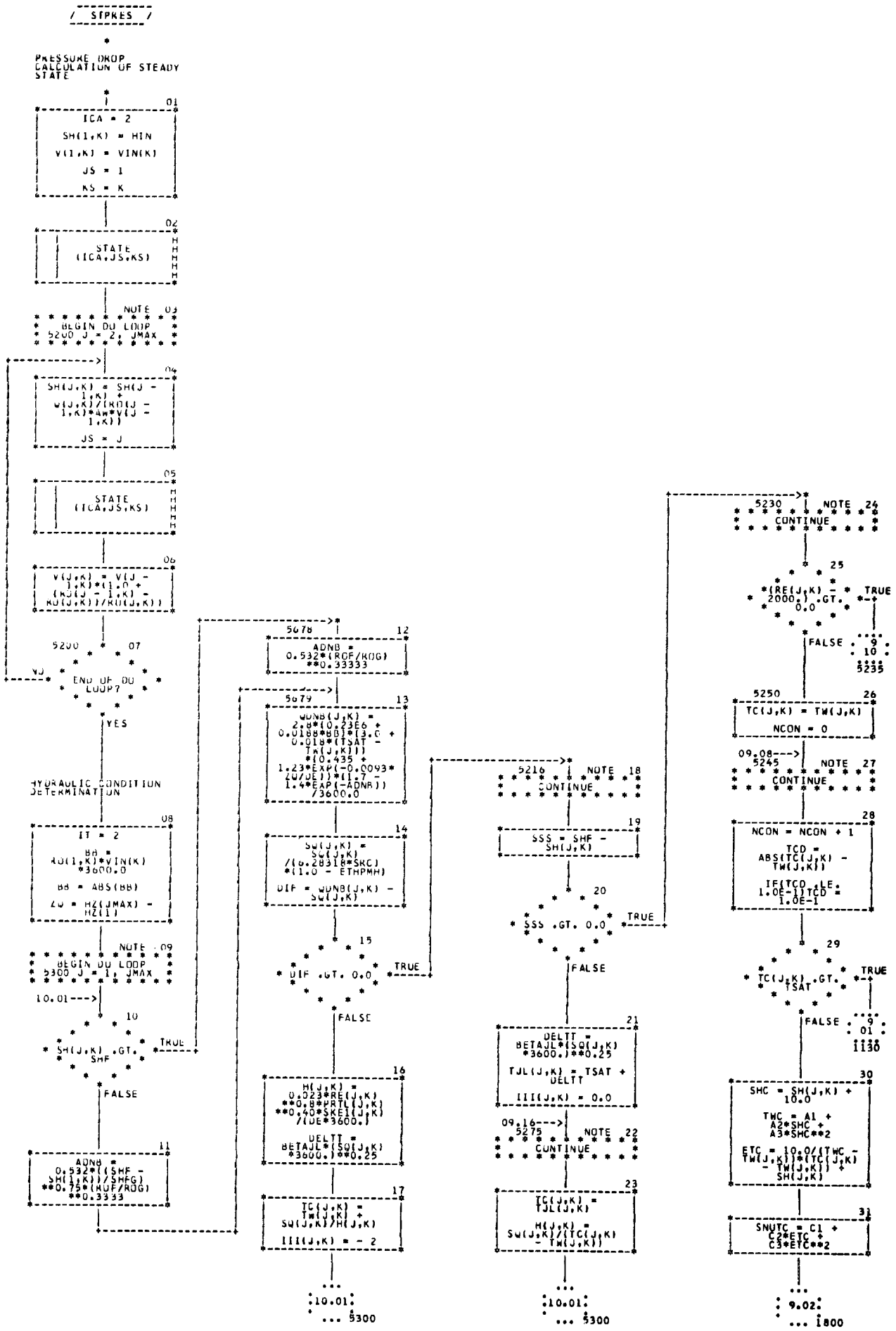

CHART TITLE - SUBROUTINE STPRES(K)

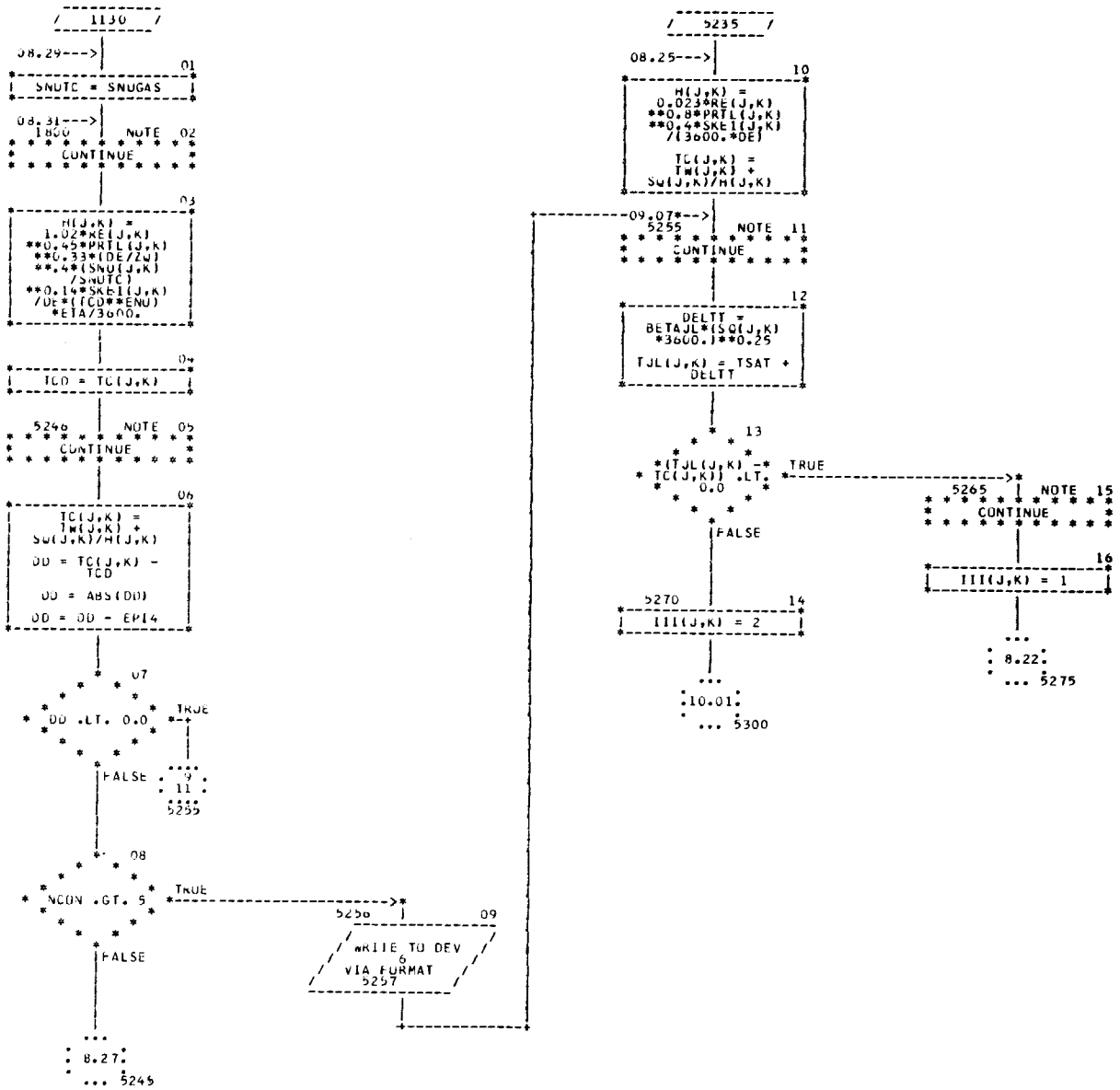

CHART TITLE - SUBROUTINE STPRES(K)

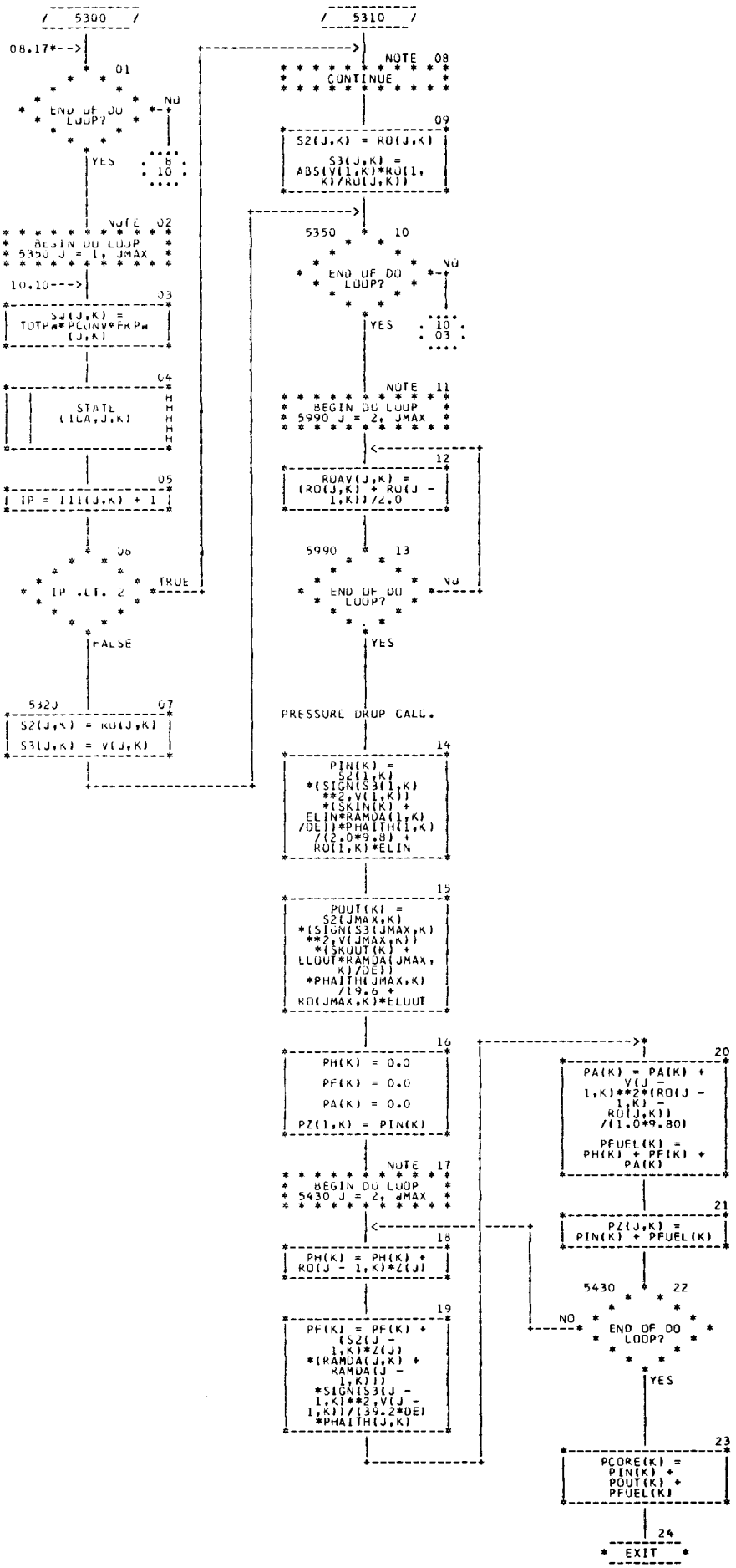

CHART TITLE - SUBROUTINE PRESDN

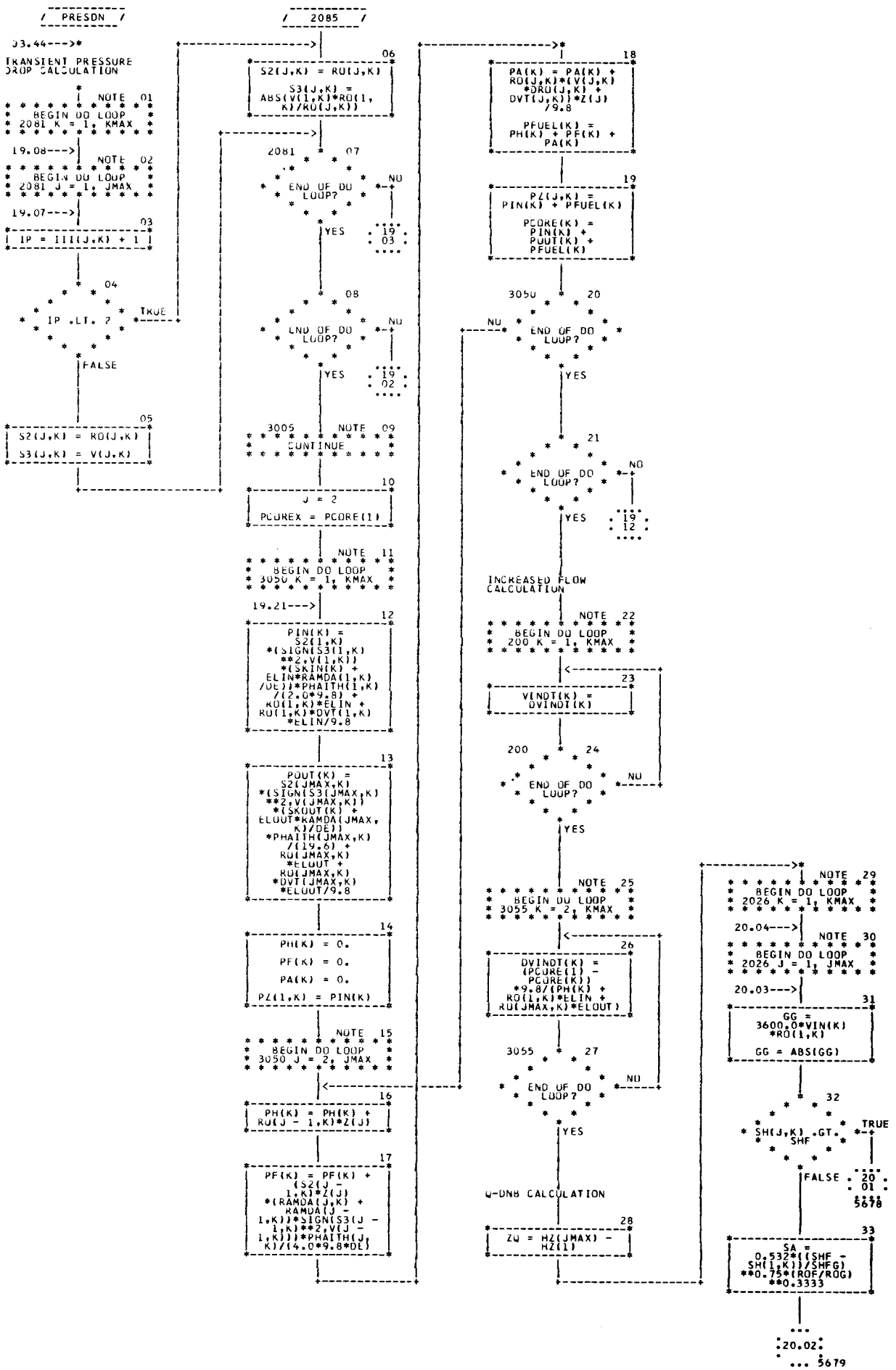

CHART TITLE - SUBROUTINE PRESUN

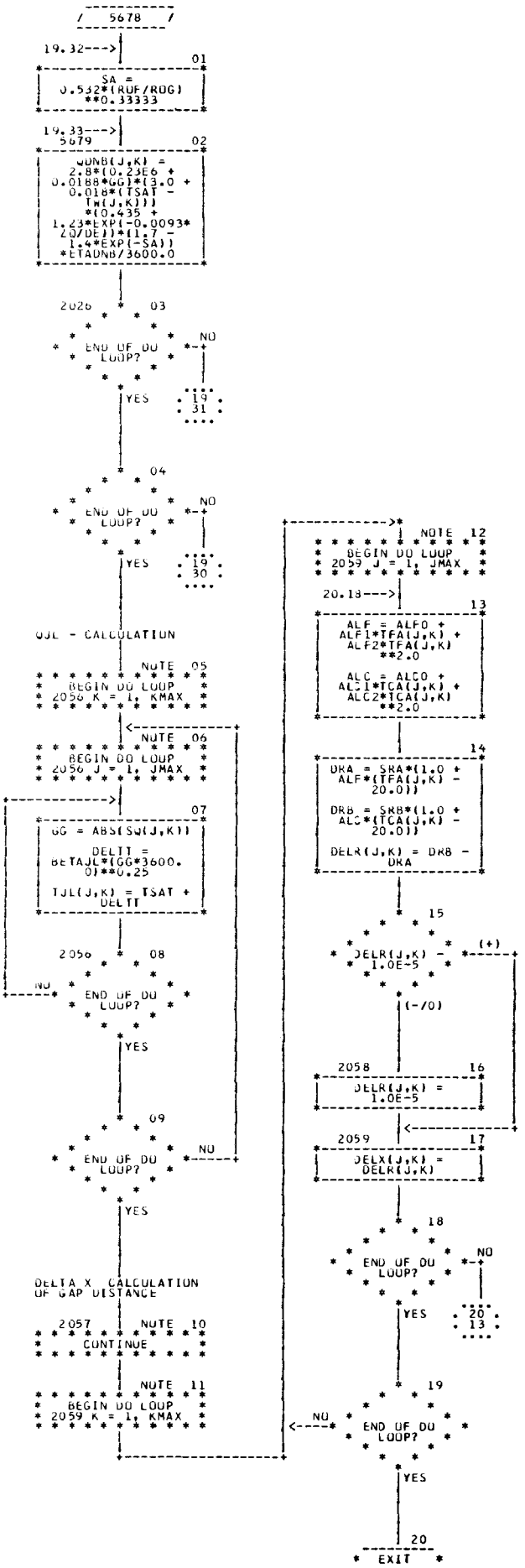

CHART TITLE - SUBROUTINE HEATRA

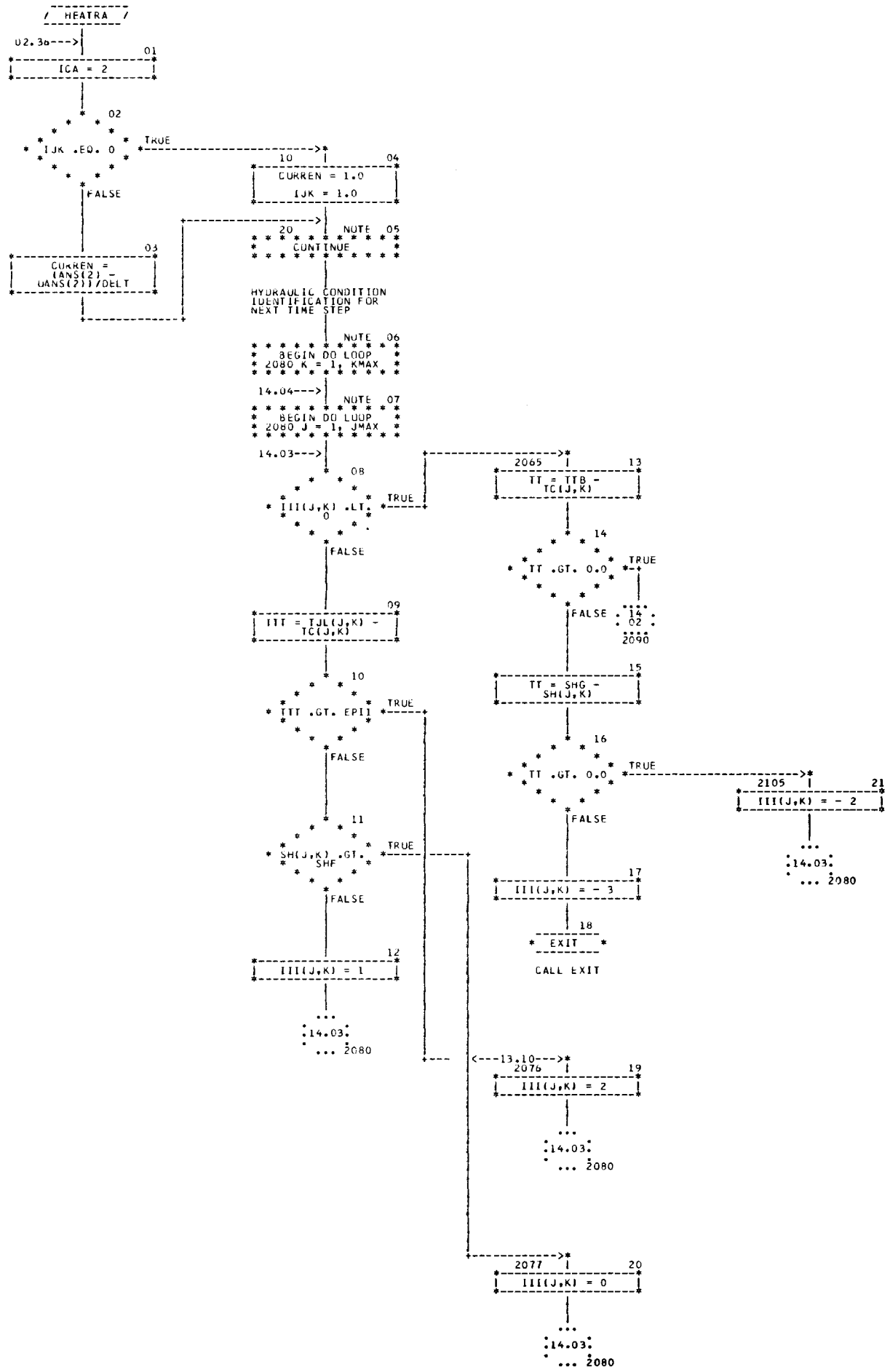

CHART TITLE - SUBROUTINE HEATKA

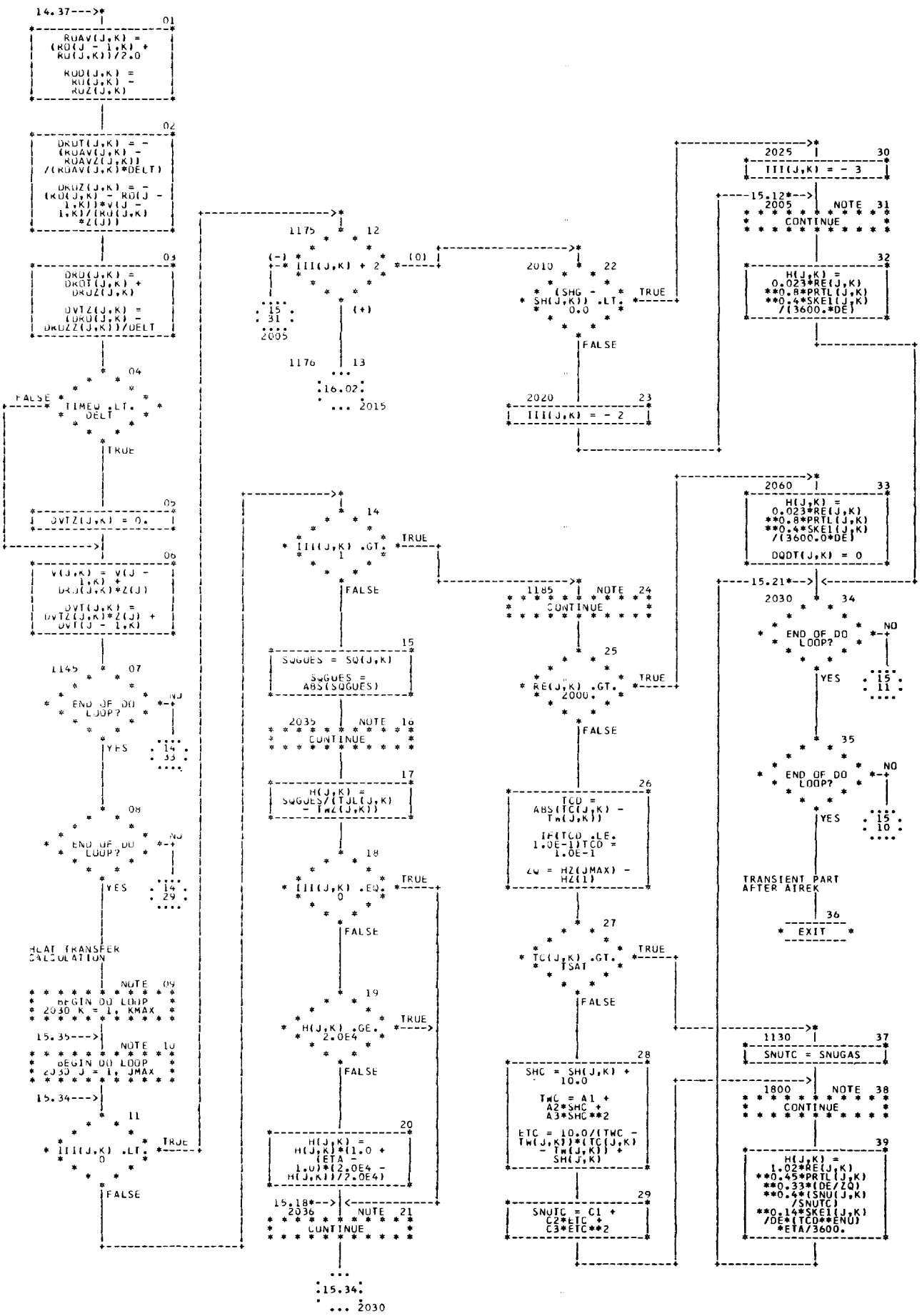

CHART TITLE - SUBROUTINE HEATRA

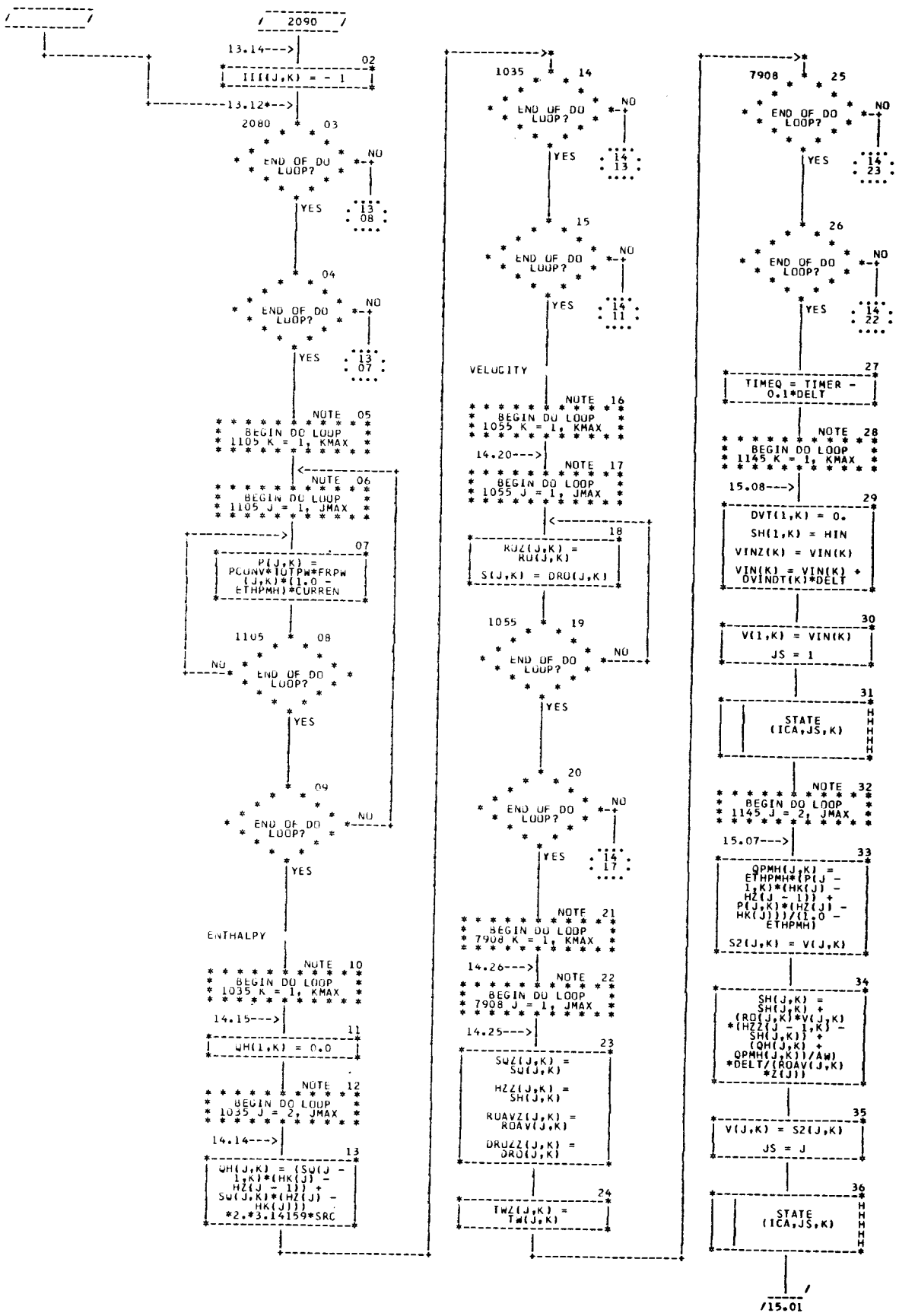

CHART TITLE - SUBROUTINE HEATKA

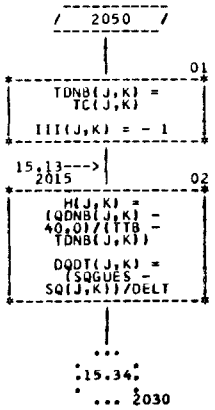

CHART TITLE - SUBROUTINE STEADY

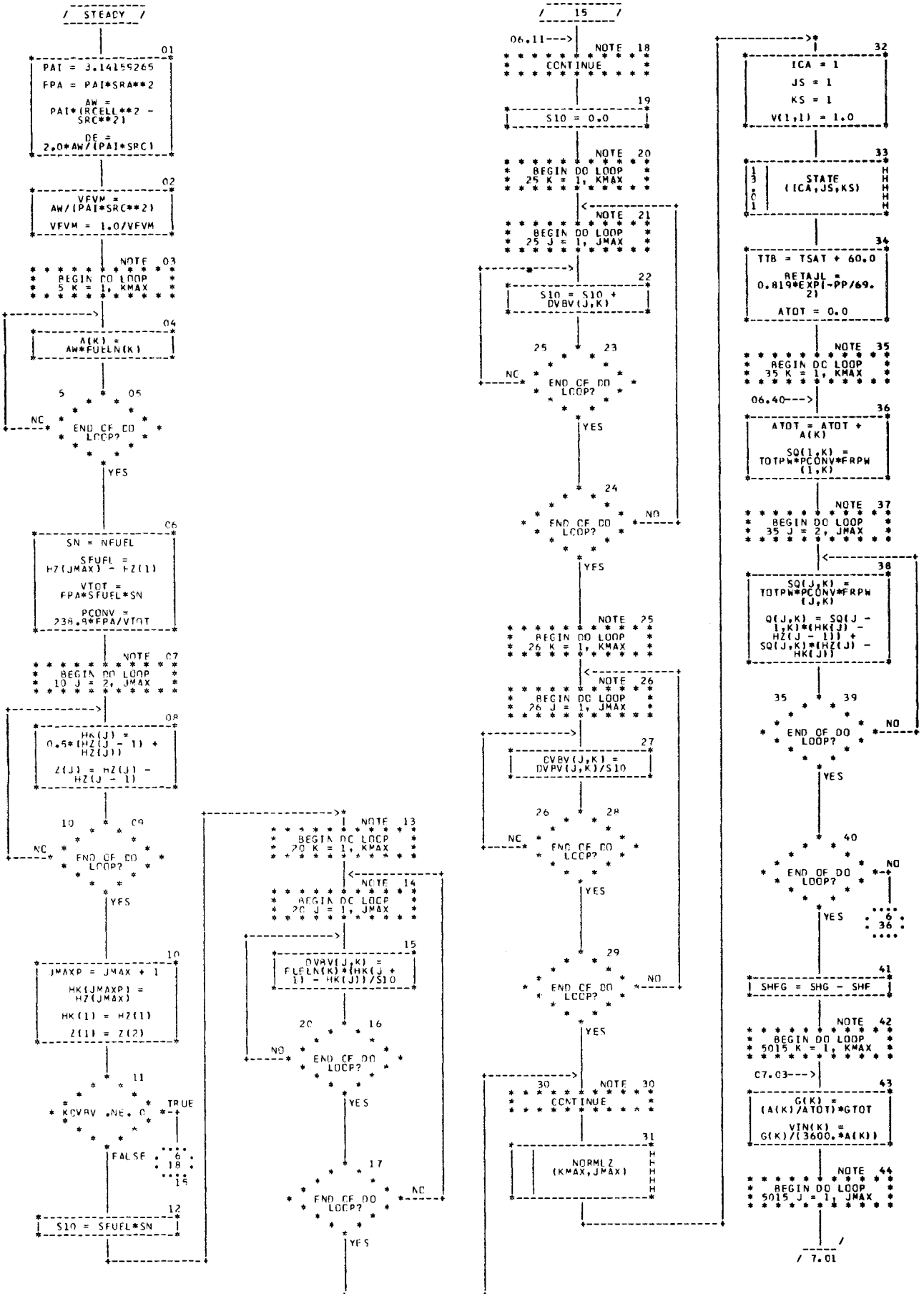

CHART TITLE - SUBROUTINE STEADY

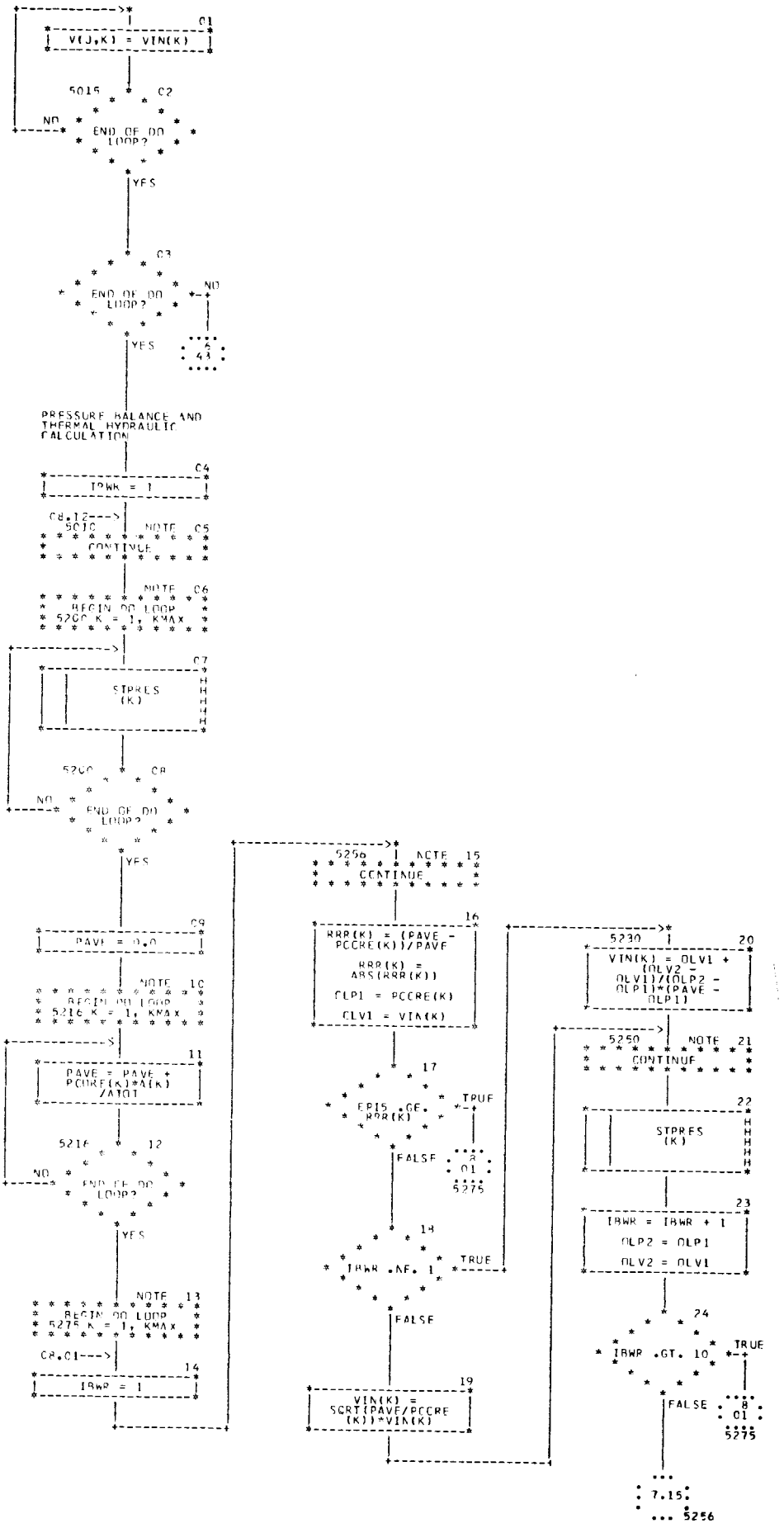

CHART TITLE - SUBROUTINE STEADY

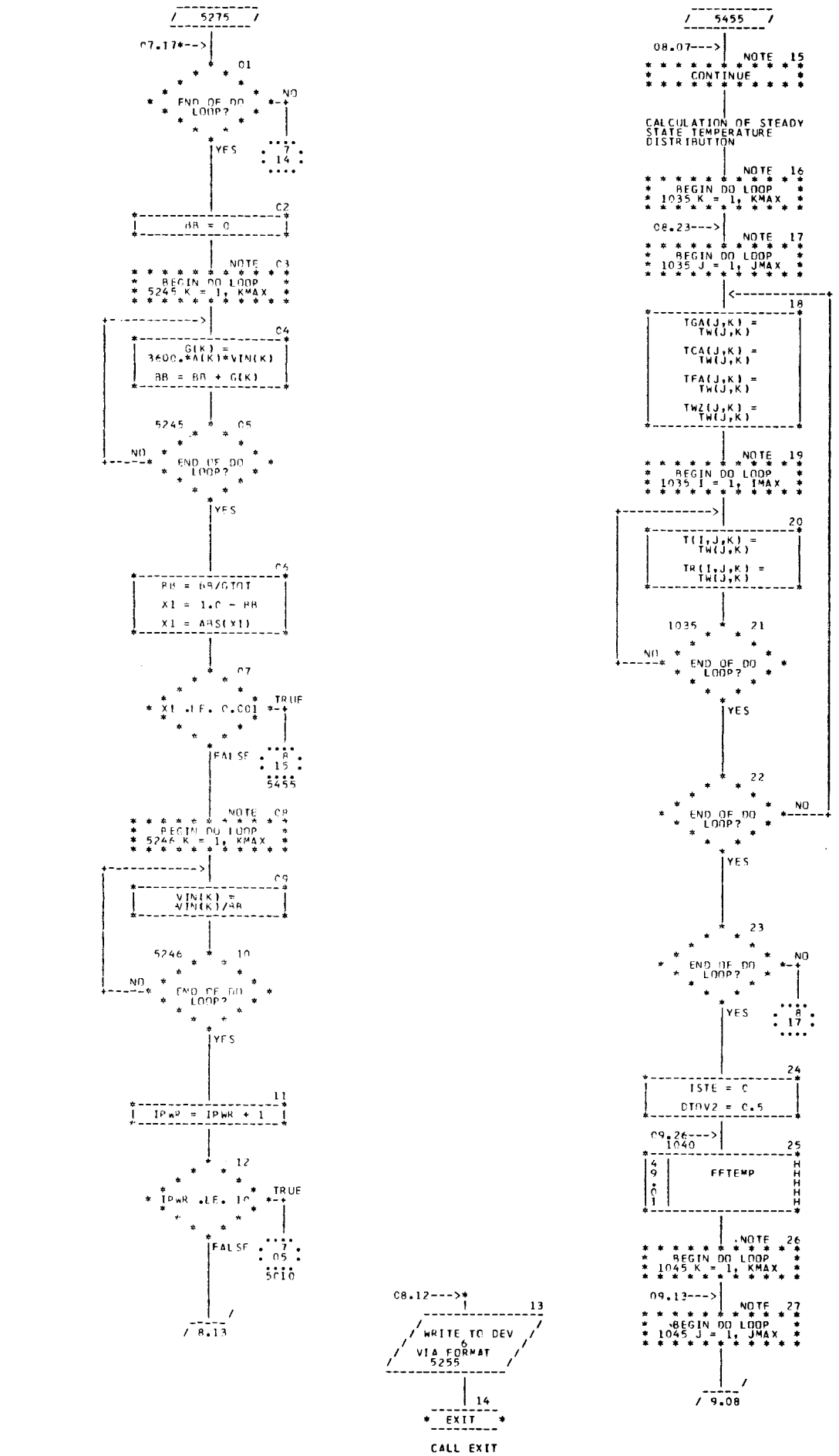

CHART TITLE - SUBROUTINE STEADY

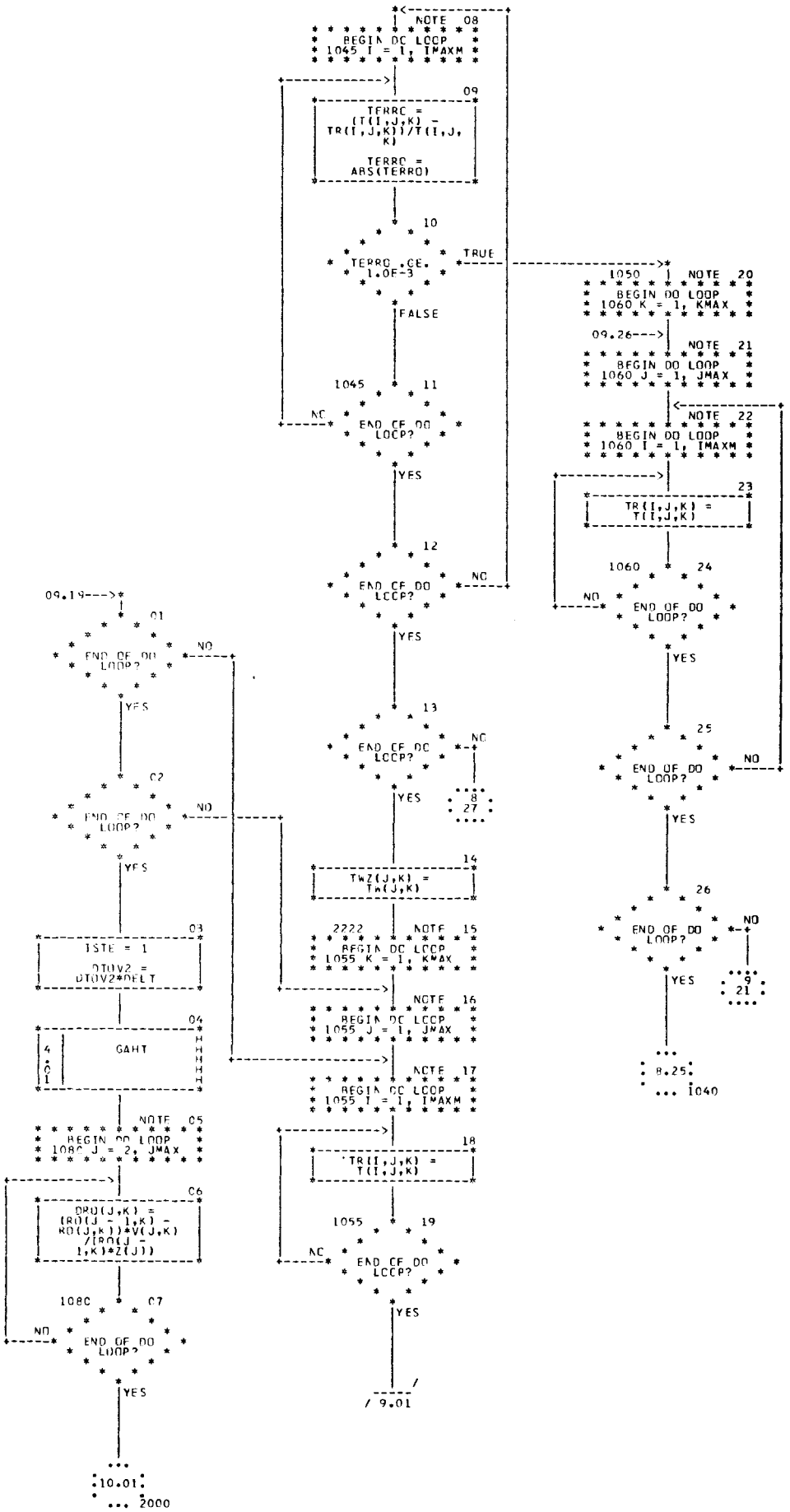

CHART TITLE - SUBROUTINE STEADY

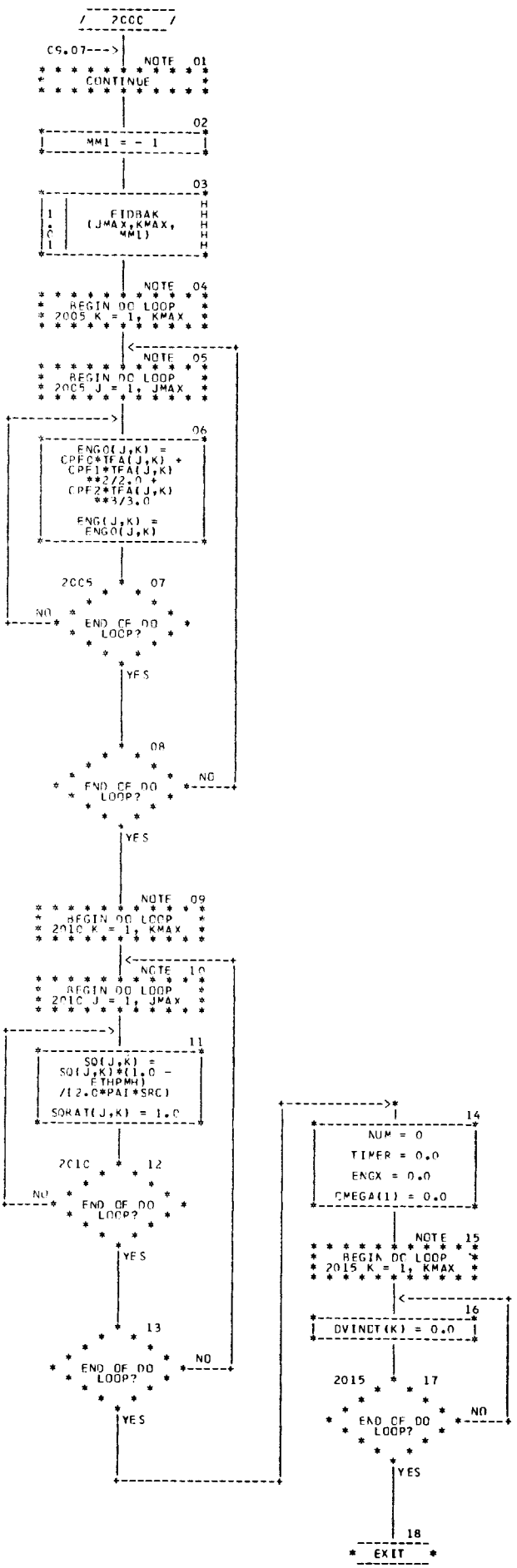

CHART TITLE - SUBROUTINE AIREKA

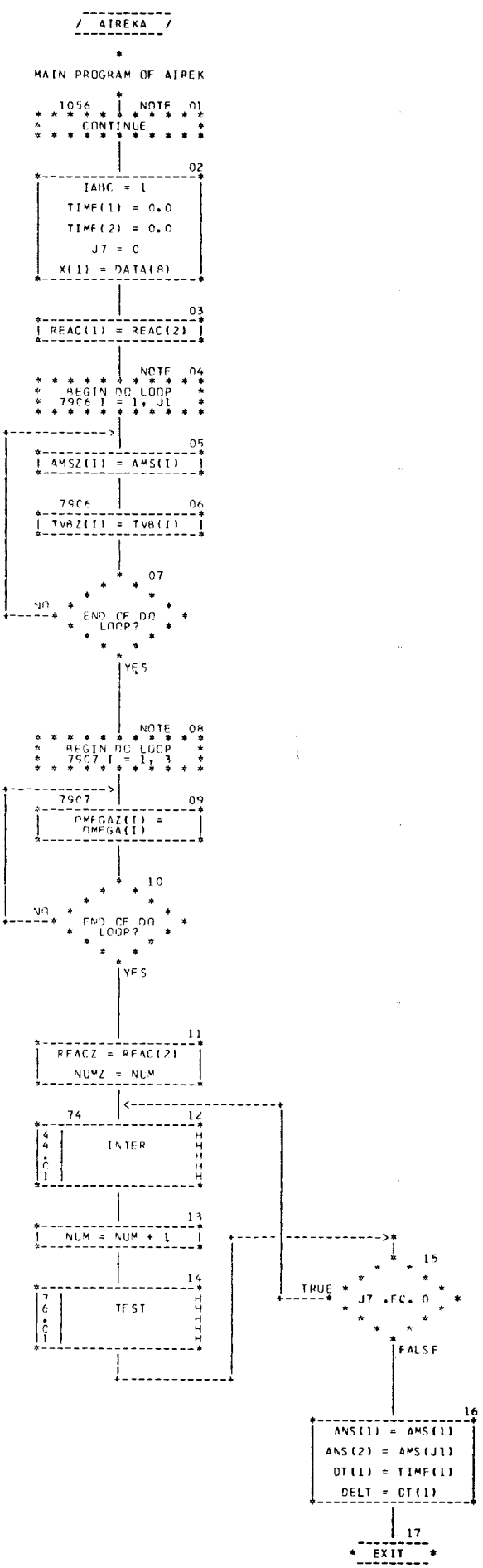

CHART TITLE - SUBROUTINE FIDBAK(IMAX,KMAX,KM1)

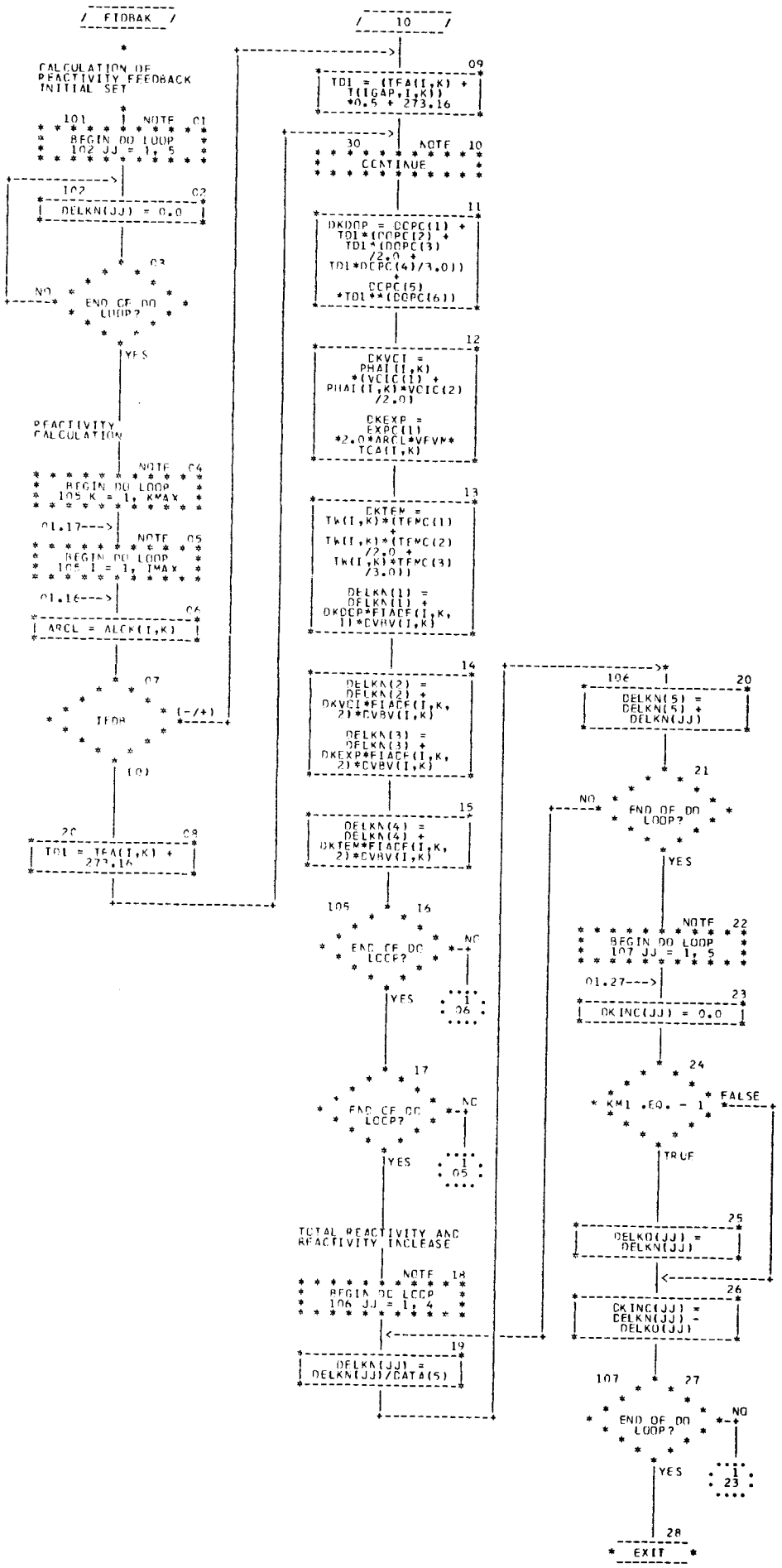

CHART TITLE - SUBROUTINE YKMAIN

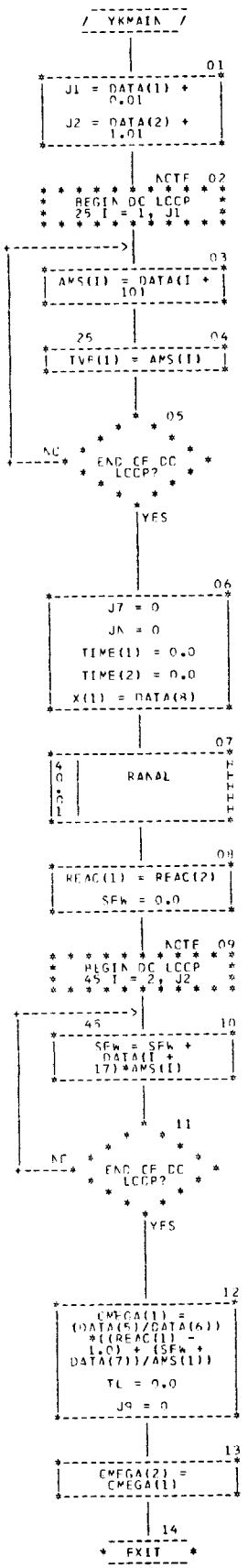

CHART TITLE - SUBROUTINE FFTEMP

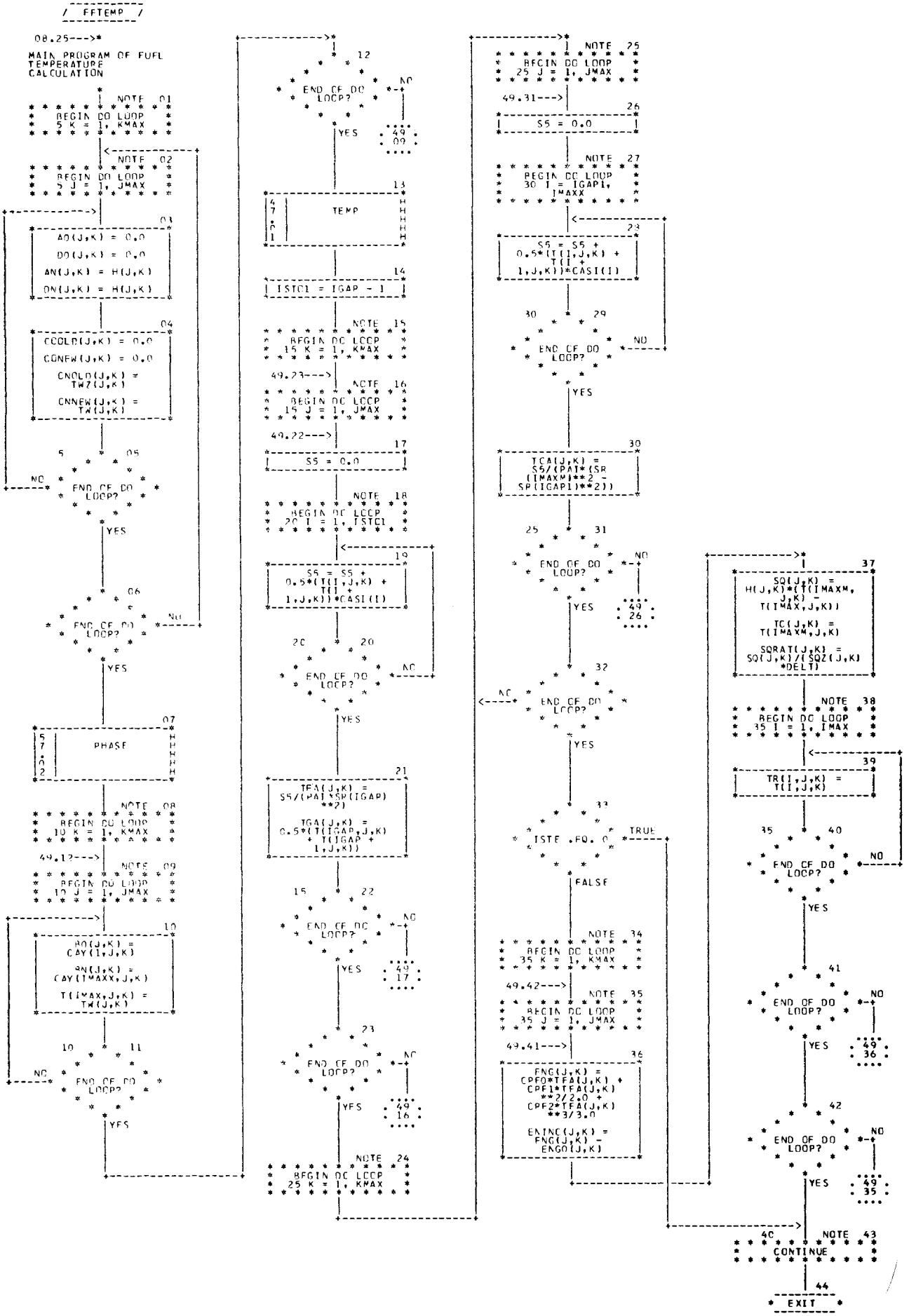

CHART TITLE - SUBROUTINE TEMP

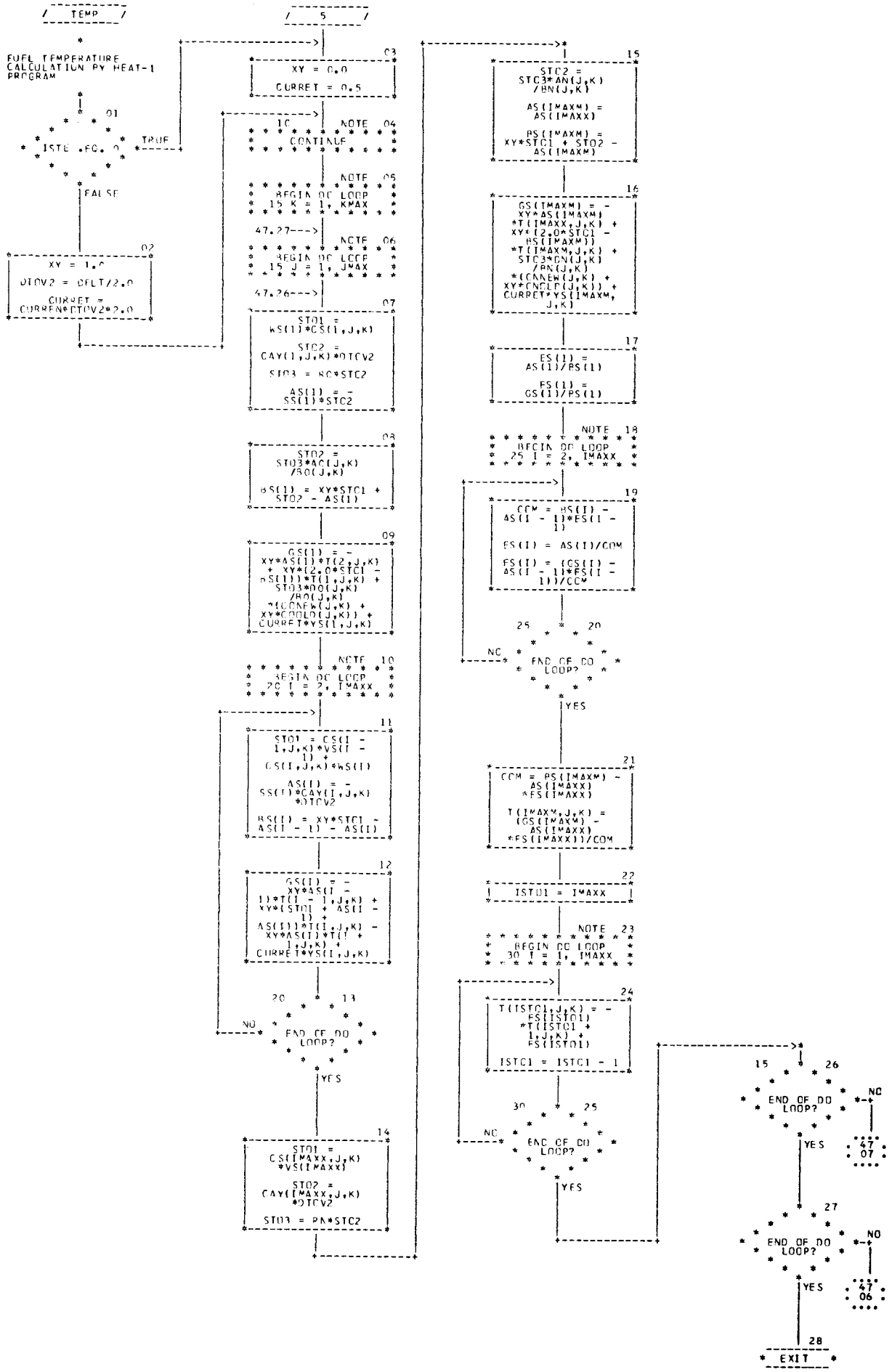

CHART TITLE - SUBROUTINE PHASE

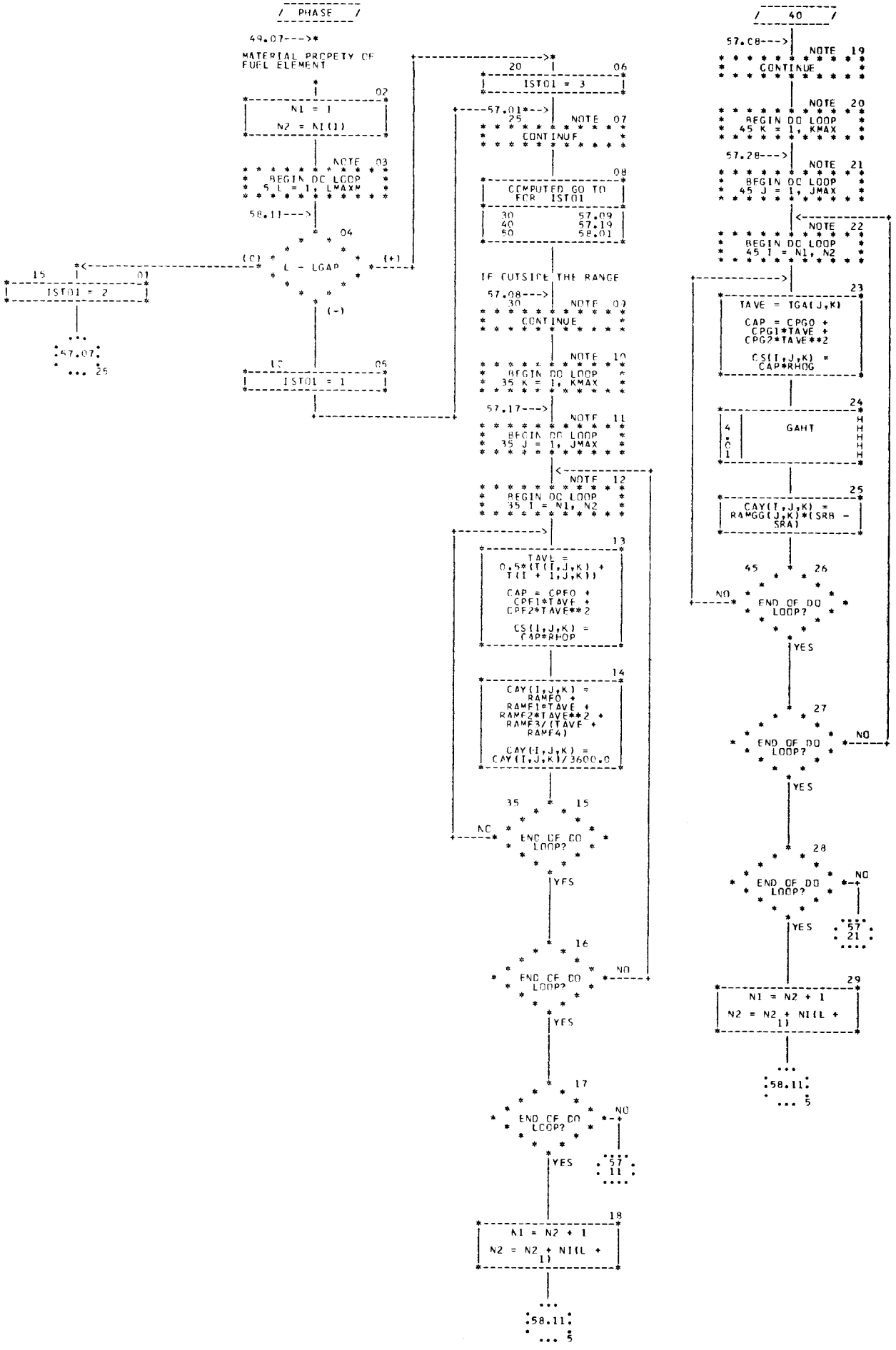

CHART TITLE - SUBROUTINE PHASE

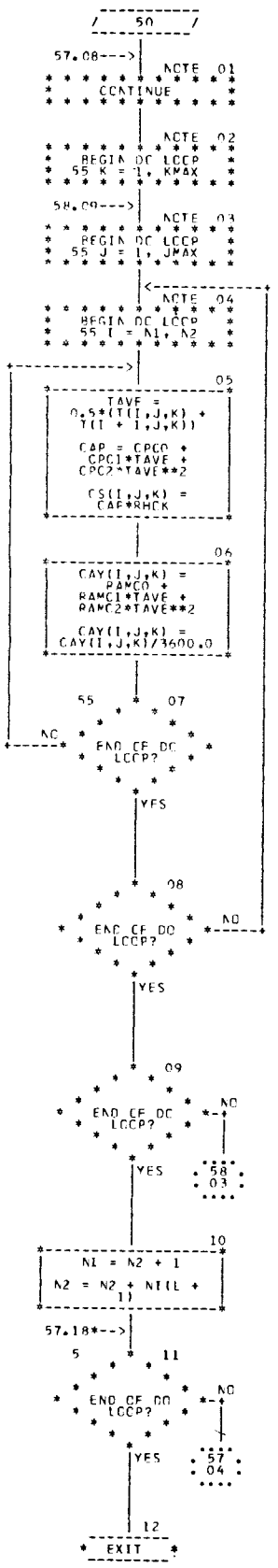

CHART TITLE - SUBROUTINE STATE(ICA,J,K)

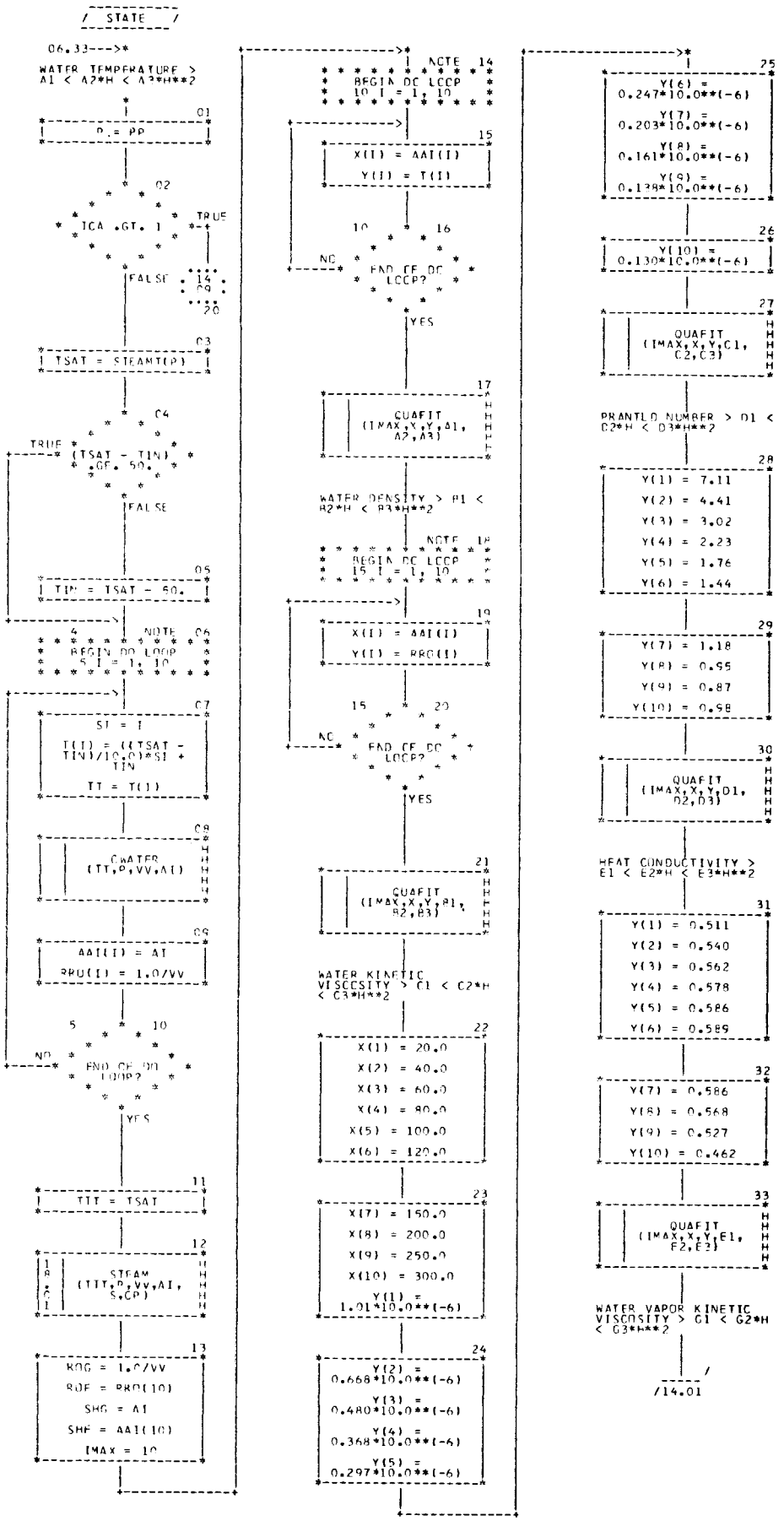

CHART TITLE - SUBROUTINE STATE(ICA,J,K)

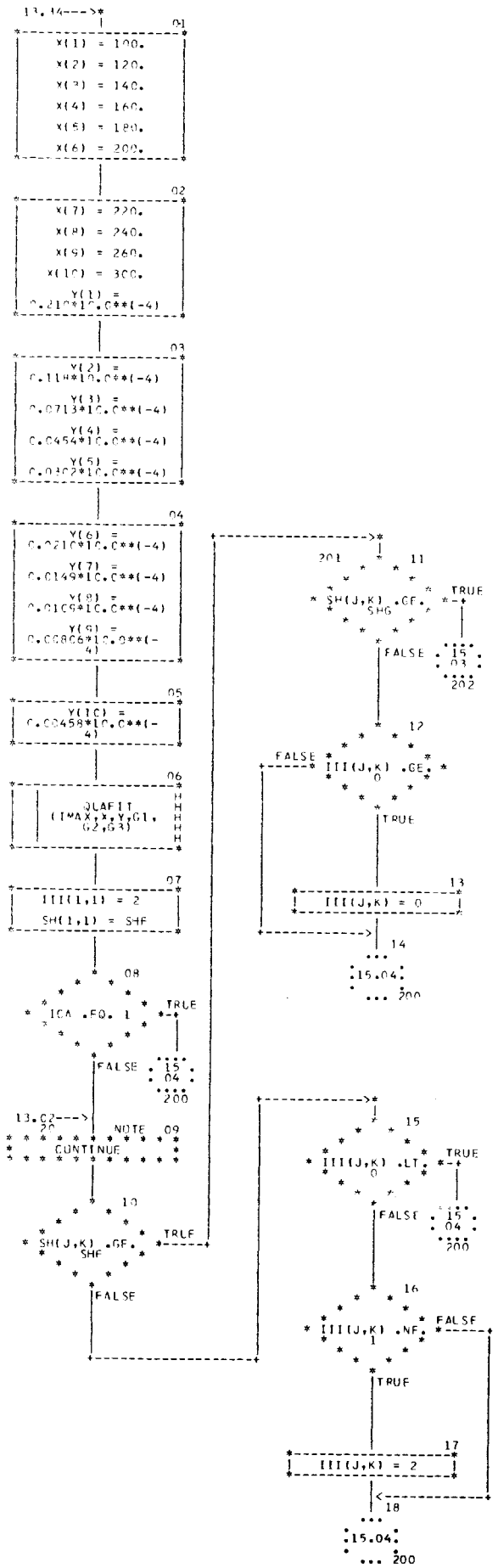

CHART TITLE - SUBROUTINE STATE(ICA,J,K)

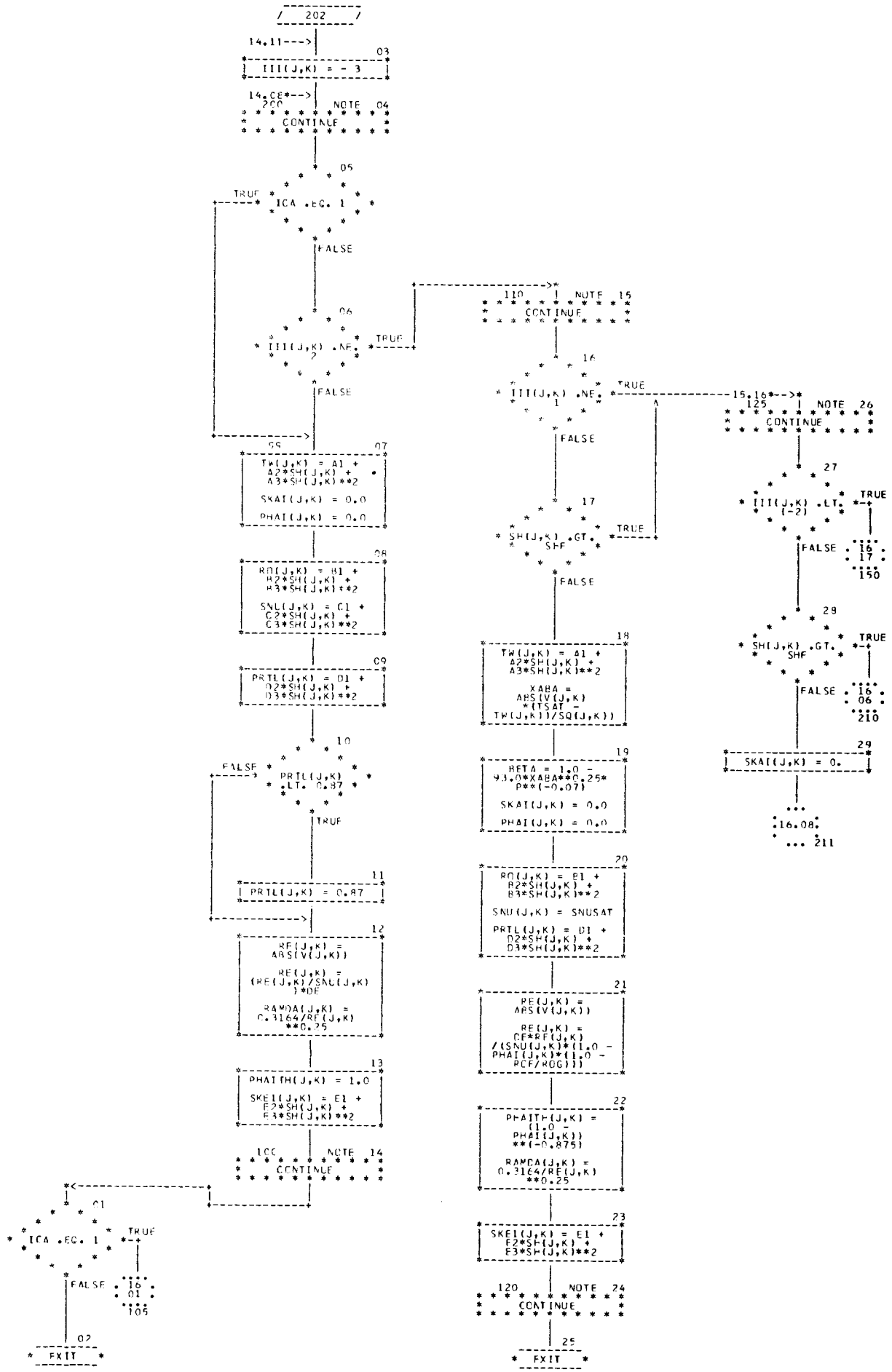

CHART TITLE - SUBROUTINE STATE(ICA,J,K)

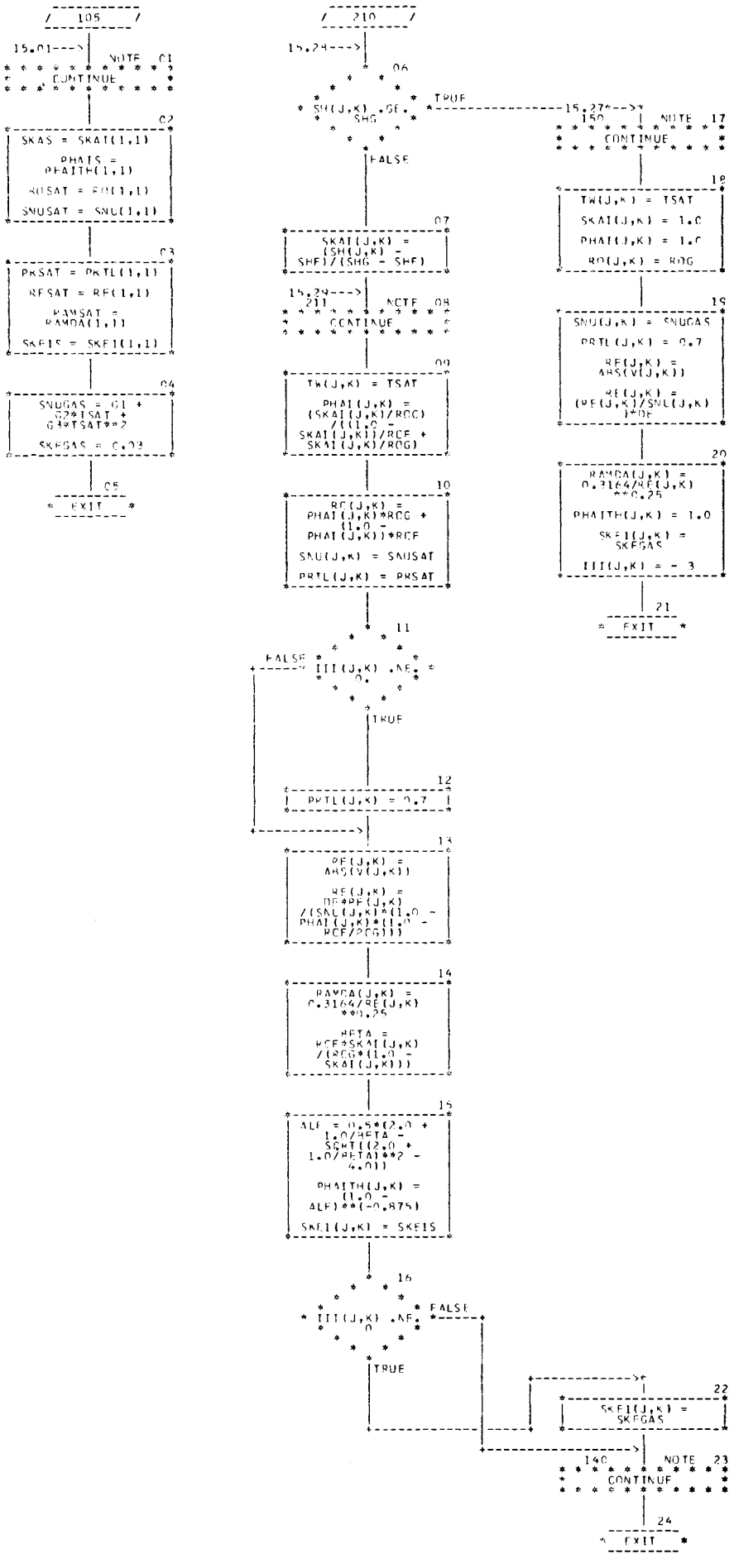

F U R E K A

A FORTRAN PROGRAM FOR REACTOR TRANSIENTS
IN A WATER MODERATED REACTOR

CASE NO. 106
DATE 44/7/23
NAME ISHIKAWA SPERT

INPUT DATA EDIT
1 GENERAL INFORMATION

FUEL RADIAL NODES	=	19	AXIAL NODES	=	10
NO. OF REG. IN FUEL	=	3	REG. NO. OF GAP	=	2
CHANNEL	=	4	NO. OF FUEL ELEMENT	=	1392
PELLET RADIUS	=	0.53900E-02 (M)	CLAD RADIUS (INNER)	=	0.54600E-02 (M)
CLAD RADIUS (OUTER)	=	0.59200E-02 (M)	EQ. CELL RADIUS	=	0.83844E-02 (M)
FUEL IN. DEAD LENGTH	=	0.11710E 00 (M)	FUEL OUT. DEAD LENGTH	=	0.64600E-01 (M)
FUEL DENSITY	=	0.10500E 05 (KG/M**3)	CLAD DENSITY	=	0.79100E 04 (KG/M**3)
REACTOR POWER	=	0.14000E 02 (MW)	OPERATING PRESSURE	=	0.10000E 03 (KG/CM**2)
COOLANT FLOW RATE	=	0.27688E 04 (M**3/HR)	COOLANT INLET TEMP.	=	0.26000E 03 (DEG. C)
PROMPT NEUT. TIME	=	0.16913E-04 (SEC)	EFF. DLYD. NEUT. FRACT.	=	0.72500E-02
NO. DLYD. NEUT. GROUP	=	0.60000E 01	WATER HEAT SOURCE	=	0.26000E-01
TIME INCREMENT (NUC)	=	0.50000E-03 (SEC)	TIME INCREMENT (HYD)	=	0.20000E-02 (SEC)
COMPUTING TIME	=	0.30000E 00 (SEC)	MAX. COMPUTING FREQUENCY	=	600
PRINT FREQUENCY	=	5	TEMP. PRINT FREQUENCY	=	50
NUC. BOIL. TEMP. ERROR (C)	=	0.10000E-01	HEAT FLUX TEST VALUE	=	0.10000E-02
PRESS. DROP TEST VALUE	=	0.50000E-02	CLAD TEMP. TEST VALUE	=	0.10000E 00
OPT. FOR DNB. FLUX	=	0.10000E 01	FORK. COMP. TEST VALUE	=	0.50000E-02
MIT. FOR POOL BOIL-2	=	0.33300E 00	MIT. FOR POOL BOIL-1	=	0.14900E 01
HEAT TRNS. CO. TEST VALUE	=	0.10000E-01			

TOTAL FUEL VOLUME	=	0.12335E 00 (M**3)	TOTAL FLOW AREA	=	0.15416E 00 (M**2)
CELL FLOW AREA	=	0.11075E-03 (M**2)	EQUI. DIA. OF CEL	=	0.11909E-01 (M)
EFFECTIVE FUEL LENGTH	=	0.97090E 00 (M)	REF. COOLANT VELOCITY	=	0.50378E 01 (M/SEC)
COOLANT INLET TEMP.	=	0.28000E 03 (DEG. C)	COOLANT INLET ENTHALPY	=	0.27070E 03 (KCAL/KG)
COOLANT SAT. TEMP.	=	0.30953E 03 (DEG. C)	COOLANT SAT. ENTHALPY	=	0.33388E 03 (KCAL/KG)
VAPOUR SAT. ENTHALPY	=	0.65132E 03 (KCAL/KG)	LIQUID SAT. DENSITY	=	0.69183E 03 (KG/M**3)
VAPOUR SAT. DENSITY	=	0.54215E 02 (KG/M**3)	POWER CONV. FACTOR	=	0.17669E 00 (KCAL/M)
FLOW TRANSIENT	=	0	INLET TEMP. TRANSIENT	=	0
NO FUEL RUPTURE	=	1	INTERVAL VOLUME CALC.	=	0

2 FUEL PIN INFORMATION

RADIAL NODE	RADIAL LENGTH (M)	INTERVAL LENGTH (M)	HEAT SOURCE	COMPOSITION
1	0.0		0.11456E 01	1
		0.38500E-03		
2	0.38500E-03		0.11465E 01	1
		0.38500E-03		
3	0.77000E-03		0.11482E 01	1
		0.38500E-03		
4	0.11550E-02		0.11502E 01	1
		0.38500E-03		
5	0.15400E-02		0.11528E 01	1
		0.38500E-03		
6	0.19250E-02		0.11562E 01	1
		0.38500E-03		
7	0.23100E-02		0.11623E 01	1
		0.38500E-03		
8	0.26950E-02		0.11693E 01	1
		0.38500E-03		
9	0.30800E-02		0.11774E 01	1
		0.38500E-03		
10	0.34650E-02		0.11916E 01	1
		0.38500E-03		
11	0.38500E-02		0.11998E 01	1
		0.38500E-03		
12	0.42350E-02		0.12191E 01	1
		0.38500E-03		
13	0.46200E-02		0.12307E 01	1
		0.38500E-03		
14	0.50050E-02		0.12554E 01	1
		0.38500E-03		
15	0.53900E-02		0.12855E 01	1
		0.0		
16	0.53900E-02		0.84951E-02	2
		0.26500E-03		
17	0.56550E-02		0.84951E-02	2
		0.26500E-03		
18	0.59200E-02		0.84951E-02	2
		0.24644E-02		
19	0.83844E-02		0.26000E-01	3

3 FUEL AXIAL INFORMATION

AXIAL NODE	AXIAL LENGTH (M)	INTERVAL LENGTH (M)	MESH CENTER HEIGHT (M)
1	0.0		0.0
		0.10000E 00	
2	0.10000E 00		0.50000E-01
		0.10000E 00	
3	0.20000E 00		0.15000E 00
		0.10000E 00	
4	0.30000E 00		0.25000E 00
		0.10000E 00	
5	0.40000E 00		0.35000E 00
		0.10000E 00	
6	0.50000E 00		0.45000E 00
		0.10000E 00	
7	0.60000E 00		0.55000E 00
		0.10000E 00	
8	0.70000E 00		0.65000E 00
		0.10000E 00	
9	0.80000E 00		0.75000E 00
		0.17090E 00	
10	0.97090E 00		0.88545E 00
			0.97090E 00

4 CHANNEL INFORMATION

CHANNEL 1

CHANNEL AREA = 0.55073E-01 (M**2) NO. OF FUEL IN CHANNEL = 500

INLET PRESS. COEFF. = 0.26100E 01 OUTLET PRESS. COEFF. = 0.20800E 01

AXIAL NODE	HEAT SOURCE	DOPPLER COEFF. IMPORTANCE	MODERATOR COEFF. IMPORTANCE	FRACTIONAL VOLUME
1	0.57191E 00	0.14593E-09	0.17262E 00	0.18498E-01
2	0.91526E 00	0.38086E-09	0.47455E 00	0.36996E-01
3	0.12481E 01	0.70165E-09	0.87141E 00	0.36996E-01
4	0.13794E 01	0.85444E-09	0.10611E 01	0.36996E-01
5	0.12846E 01	0.74270E-09	0.92236E 00	0.36996E-01
6	0.97950E 00	0.43663E-09	0.54231E 00	0.36996E-01
7	0.54008E 00	0.13871E-09	0.16996E 00	0.36996E-01
8	0.24501E 00	0.28736E-10	0.34863E-01	0.36996E-01
9	0.92153E-01	0.43545E-11	0.52821E-02	0.50111E-01
10	0.33333E-01	0.46154E-12	0.59128E-03	0.31613E-01

5 TEMPERATURE DEPENDENT MATERIAL CONSTANT

FUEL

THERMAL CONDUCTIVITY	(KCAL/M*HR*DC)	RAMF = 0.39265E 01 +-0.33520E-02 * T + 0.11355E-05 * T ** 2
HEAT CAPACITY	(KCAL/KG)	CAP = 0.65700E-01 +-0.95560E-06 * T + 0.81230E-08 * T ** 2
EXPANSION COEFFICIENT		ALF = 0.10000E-04 + 0.0 * T + 0.0 * T ** 2

GAP

TERMAL CONDUCTANCE	(KCAL/M**2*HR*DC)	RAMG = (0.63500E 01 + 0.34400E-01 * T +-0.79000E-05 * T ** 2)/ (0.22560E 02 + DELR*10E6)

CLAD

THERMAL CONDUCTIVITY	(KCAL/M*HR*DC)	RAMC = 0.12967E 02 + 0.39460E-02 * T + 0.0 * T ** 2
HEAT CAPACITY	(KCAL/KG)	CAP = 0.12068E 00 + 0.20053E-04 * T + 0.0 * T ** 2
EXPANSION COEFFICIENT		ALC = 0.18000E-04 + 0.0 * T + 0.0 * T ** 2

COOLANT

TEMPERATURE	(DEG.C)	TW =-0.65139E 02 + 0.15368E 01 * H +-0.12418E-02 * H ** 2
DENSITY	(KG/M**3)	RO = 0.83691E 03 + 0.94542E 00 * H +-0.41316E-02 * H ** 2
THERMAL CONDUCTIVITY	(KCAL/M*HR*DC)	SKE1 = 0.49088E 00 + 0.14291E-02 * H +-0.51164E-05 * H ** 2
KINETIC VISCOSITY	(M**2/SEC)	SNU = 0.10267E-05 +-0.88380E-08 * H + 0.20290E-10 * H ** 2
VAPOR KINETIC VISCOSITY	(M**2/SEC)	
PRANTLD NUMBER		PRTL = 0.71296E 01 +-0.65710E-01 * H + 0.15669E-03 * H ** 2

PARAMETER T IS COOLANT TEMPERATURE

PARAMETER H IS COOLANT ENTHALPY

6 KINETIC INFORMATION

GROUP NO.	DELAYED NEUTRON FRACTION	DECAY CONSTANT
1	0.35200E-01	0.12700E-01
2	0.20140E 00	0.31700E-01
3	0.18580E 00	0.11670E 00
4	0.40060E 00	0.31420E 00
5	0.14370E 00	0.14007E 01
6	0.33300E-01	0.38803E 01

DOPPLER COEFFICIENT

```
DKDOP  =-0.49300E 08 + 0.0          * TFA + 0.0          * TFA ** 2 + 0.0          * TFA ** 3/
        + 0.13600E 07 * TFA ** 0.50000E 00
```

VOID COEFFICIENT

```
DKVOID = 0.32000E 00 * PHAI + 0.0          * PHAI ** 2 / 2.0
```

TEMPERATURE COEFFICIENT

```
DKTEM  = 0.52070E-03 * TW  + 0.0          * TW ** 2 / 2.0 + 0.0          * TW ** 3 / 3.0
```

KINETIC PARAMETER

TIME (SEC)	REACTIVITY (DK/K)	TIME (SEC)	FLOW (M**3/HR)	TIME(SEC)	TEMPERATURE(DC)
0.0	0.0				
0.20000E-01	0.72500E-03				
0.40000E-01	0.21750E-02				
0.80000E-01	0.84825E-02				
0.10000E 02	0.84825E-02				
		* * * * *	* * * * *		

TRANSIENT OUTPUT

TIME STEP NUMBER 0

ELAPSED REACTOR TIME	(SEC)	1.0000	DOPPLER	(DOLLARS)	0.0
TIME INCREMENT	(SEC)	0.0020	CLAD EXPANSION	(DOLLARS)	0.0
REACTOR POWER	(MW)	0.19000E 02	TEMPERATURE	(DOLLARS)	0.0
EXCURSION POWER	(MW*SEC)	0.10000E 01	VOID	(DOLLARS)	0.0
INSERTED REACTIVITY	(DOLLARS)	0.39905E-58	AVERAGE FUEL TEMP.	(DEG. C)	552.8347
COMPENSATED REACTIVITY	(DOLLARS)	0.0	AVERAGE CLAD TEMP.	(DEG. C)	279.9771
INVERSE PERIOD	(1/SEC)	0.0	AVERAGE COOLANT TEMP.	(DEG. C)	264.0027

PRESSURE DROP INFORMATION

CHANNEL NO.		1	2	3	4
INLET VELOCITY	(M/SEC)	5.038	5.035	5.007	4.159
INLET VELOCITY CHANGE	(M/SEC**2)	0.0	0.0	0.0	0.0
CHAN. AVE. FUEL TEMP.	(DEG. C)	475.209	523.624	672.462	774.409
CHAN. AVE. COOLANT TEMP.	(DEG. C)	262.872	263.507	265.623	268.406
INTEGRATED TRANSFERED HEAT	(KCAL)	0.0	0.0	0.0	0.0
TOTAL PRESSURE DROP	(KG/CM**2)	0.69347E 00	0.69389E 00	0.69066E 00	0.69269E 00
INLET PRESSURE DROP	(KG/CM**2)	0.28826E 00	0.28797E 00	0.28488E 00	0.28491E 00
FRICTION DROP	(KG/CM**2)	0.10141E 00	0.10174E 00	0.10217E 00	0.75254E-01
ACCELERATION DROP	(KG/CM**2)	0.91777E-03	0.11328E-02	0.17937E-02	0.18938E-02
HEAD DROP	(KG/CM**2)	0.76303E-01	0.76215E-01	0.75914E-01	0.75505E-01
OUTLET PRESSURE DROP	(KG/CM**2)	0.22658E 00	0.22684E 00	0.22590E 00	0.25513E 00

CHANNEL 1

AXIAL NODE	COOLANT VELOCITY (M/SEC)	COOLANT TEMPERATURE (DEG. C)	COOLANT ENTHALPY (KCAL/KG)	COOLANT DENSITY (KG/M**3)	STEAM QUALITY	VOID FRACTION	COOLANT PATTERN
1	5.038	259.388	270.700	790.083	0.0	0.0	LIQID
2	5.042	260.377	271.266	789.350	0.0	0.0	LIQID
3	5.049	261.088	272.090	788.280	0.0	0.0	LIQID
4	5.058	261.948	273.091	786.972	0.0	0.0	LIQID
5	5.066	262.818	274.105	785.638	0.0	0.0	LIQID
6	5.074	263.555	274.967	784.497	0.0	0.0	LIQID
7	5.079	264.049	275.546	783.728	0.0	0.0	LIQID
8	5.081	264.303	275.845	783.330	0.0	0.0	LIQID
9	5.082	264.413	275.973	783.158	0.0	0.0	LIQID
10	5.083	264.482	276.055	783.049	0.0	0.0	LIQID

AXIAL NODE	PRESSURE DROP (KG/CM**2)	FUEL AVERAGE TEMPERATURE (DEG. C)	FUEL CENTR TEMPERATUR (DEG. C)	FUEL SURFACE TEMPERATURE (DEG. C)	CLAD SURFACE TEMPERATURE (DEG. C)	SURFACE HEAT FLUX (KCAL/M**2/HR)	ENERGY ACCUMULATED (CAL/GM-FUEL)
1	0.288	428.758	499.332	363.599	265.366	180993.145	0.0
2	0.307	528.565	655.984	414.864	269.163	289653.594	0.0
3	0.325	625.405	819.318	458.201	273.222	394975.258	0.0
4	0.343	664.474	888.015	474.329	275.568	436524.797	0.0
5	0.362	638.160	840.506	464.356	275.387	406554.953	0.0
6	0.380	550.859	690.734	426.869	273.346	309983.711	0.0
7	0.399	423.998	490.212	362.680	269.468	170919.863	0.0
8	0.417	337.596	364.441	312.031	266.767	77538.652	0.0
9	0.435	292.179	301.659	283.021	265.340	29163.788	0.0
10	0.467	274.556	277.899	271.309	264.818	10548.940	0.0

SELECTED NODES INFORMATIONS

CHANNEL	4	4	4	3	2
NODE	3	4	5	4	4
J.L.TEMP. (DEG.C)	315.58	315.73	315.63	315.41	314.85
DNB.HEAT.FLUX. (KC/HR*M**2)	0.54649E 07	0.53046E 07	0.51424E 07	0.59757E 07	0.61085E 07
HEAT.TRNS.COE. (KC/HR*M**2*C)	0.27262E 05	0.26736E 05	0.26198E 05	0.29985E 05	0.32324E 05
GAP.CONDUCTANCE (KC/HR*M**2*C)	0.38510E 04	0.41649E 04	0.39431E 04	0.35520E 04	0.28897E 04
GAP.DISTANCE. (MM)	0.0391	0.0351	0.0382	0.0435	0.0555
INTG.TRNSFD.HEAT. (CAL)	0.0	0.0	0.0	0.0	0.0

TEMPERATURE MAP IN FUEL

NODE	RADIUS (MM)					
1	0.0	1806.676	1977.940	1864.282	1616.483	1105.960
2	0.3850	1793.208	1963.903	1850.642	1604.195	1098.892
3	0.7700	1766.078	1935.470	1823.113	1579.602	1084.864
4	1.1550	1725.019	1892.060	1781.325	1542.734	1064.071
5	1.5400	1669.806	1832.974	1724.902	1493.763	1036.799
6	1.9250	1600.438	1757.591	1653.655	1433.101	1003.416
7	2.3100	1517.360	1665.693	1567.837	1361.500	964.366
8	2.6950	1421.703	1557.940	1468.458	1280.124	920.154
9	3.0800	1315.419	1436.326	1357.496	1190.551	871.345
10	3.4650	1201.094	1304.162	1237.753	1094.614	818.523
11	3.8500	1081.673	1165.635	1112.523	994.284	762.308
12	4.2350	959.967	1024.882	984.984	891.432	703.314
13	4.6200	838.358	885.318	857.814	787.709	642.142
14	5.0050	718.669	749.365	733.019	684.474	579.359
15	5.3900	602.143	618.509	611.924	582.747	515.457
16	5.3900	333.929	344.481	342.298	323.942	301.406
17	5.6560	315.553	324.220	323.424	307.553	290.326
18	5.9200	297.899	304.746	305.290	291.816	279.703
19	8.3844	263.341	265.801	268.274	263.856	262.253

TEMPERATURE DISTRIBUTION IN FUEL

CHANNEL 1

RADIAL NODE I	AXIAL NODE J 1	2	3	4	5	6	7	8	9	10
1	499.332	655.984	819.318	888.015	840.506	690.734	490.212	364.441	301.659	277.899
2	497.964	653.426	815.269	883.309	836.286	687.907	488.932	363.937	301.483	277.838
3	495.233	648.331	807.278	873.959	827.896	682.277	486.378	362.929	301.132	277.715
4	491.151	640.735	795.368	860.073	815.429	673.890	482.558	361.418	300.605	277.530
5	485.732	630.691	779.682	841.808	799.013	662.808	477.486	359.406	299.903	277.283
6	478.998	618.267	760.369	819.361	778.814	649.113	471.180	356.895	299.024	276.974
7	470.969	603.540	737.608	792.963	755.022	632.898	463.658	353.886	297.969	276.603
8	461.671	586.597	711.594	762.871	727.850	614.266	454.942	350.381	296.737	276.169
9	451.132	567.535	682.549	729.379	697.538	593.335	445.056	346.381	295.326	275.672
10	439.379	546.454	650.699	692.762	664.330	570.225	434.023	341.888	293.736	275.111
11	426.445	523.468	616.291	653.360	628.494	545.071	421.872	336.901	291.964	274.485
12	412.364	498.692	579.581	611.492	590.302	518.013	408.631	331.422	290.009	273.793
13	397.173	472.252	540.827	567.486	550.036	489.197	394.333	325.451	287.869	273.034
14	380.909	444.274	500.291	521.670	507.972	458.773	379.008	318.990	285.542	272.207
15	363.599	414.864	458.201	474.329	464.356	426.869	362.680	312.031	283.021	271.309
16	272.365	280.349	288.454	292.389	291.254	285.303	276.071	269.765	266.468	265.226
17	268.789	274.634	280.674	283.798	283.262	279.195	272.697	268.233	265.892	265.017
18	265.366	269.163	273.222	275.568	275.587	273.346	269.468	266.767	265.340	264.818
19	259.888	260.377	261.088	261.948	262.818	263.555	264.049	264.303	264.413	264.482

NO.	TIME (SEC)	POWER (MW)	ENERGY (MW*S)	PERIOD (1/SEC)	INSRT. REACT. (DOLLARS)	COMP. REACT. (DOLLARS)
1	0.50000E-03	0.19005E 02	0.95008E-02	0.99634E 00	0.25000E-02	0.78440E-03
2	0.10000E-02	0.19018E 02	0.19006E-01	0.17943E 01	0.50000E-02	0.78440E-03
3	0.15000E-02	0.19039E 02	0.28520E-01	0.24339E 01	0.75000E-02	0.78440E-03
4	0.20000E-02	0.19064E 02	0.38046E-01	0.29470E 01	0.10000E-01	0.78440E-03
5	0.25000E-02	0.19091E 02	0.47584E-01	0.30014E 01	0.11520E-01	0.18182E-02
6	0.30000E-02	0.19121E 02	0.57137E-01	0.33256E 01	0.13823E-01	0.18182E-02
7	0.35000E-02	0.19154E 02	0.66706E-01	0.35868E 01	0.16127E-01	0.18182E-02
8	0.40000E-02	0.19190E 02	0.76292E-01	0.37977E 01	0.18431E-01	0.18182E-02
9	0.45000E-02	0.19226E 02	0.85896E-01	0.38548E 01	0.20423E-01	0.29945E-02
10	0.50000E-02	0.19264E 02	0.95519E-01	0.39912E 01	0.22665E-01	0.29945E-02
11	0.55000E-02	0.19303E 02	0.10516E 00	0.41025E 01	0.24906E-01	0.29945E-02
12	0.60000E-02	0.19343E 02	0.11482E 00	0.41938E 01	0.27148E-01	0.29945E-02
13	0.65000E-02	0.19383E 02	0.12450E 00	0.42039E 01	0.29211E-01	0.39110E-02
14	0.70000E-02	0.19424E 02	0.13421E 00	0.42649E 01	0.31417E-01	0.39110E-02
15	0.75000E-02	0.19466E 02	0.14393E 00	0.43160E 01	0.33623E-01	0.39110E-02
16	0.80000E-02	0.19508E 02	0.15367E 00	0.43591E 01	0.35829E-01	0.39110E-02
17	0.85000E-02	0.19553E 02	0.16344E 00	0.45149E 01	0.38360E-01	0.48280E-02
18	0.90000E-02	0.19597E 02	0.17322E 00	0.45496E 01	0.40631E-01	0.48280E-02
19	0.95000E-02	0.19641E 02	0.18303E 00	0.45798E 01	0.42902E-01	0.48280E-02
20	0.10000E-01	0.19687E 02	0.19287E 00	0.46063E 01	0.45173E-01	0.48280E-02
21	0.10500E-01	0.19732E 02	0.20272E 00	0.46298E 01	0.47443E-01	0.57273E-02
22	0.11000E-01	0.19778E 02	0.21260E 00	0.46512E 01	0.49714E-01	0.57273E-02
23	0.11500E-01	0.19824E 02	0.22250E 00	0.46707E 01	0.51984E-01	0.57273E-02
24	0.12000E-01	0.19871E 02	0.23242E 00	0.46888E 01	0.54255E-01	0.57273E-02
25	0.12500E-01	0.19917E 02	0.24237E 00	0.47139E 01	0.56548E-01	0.66071E-02
26	0.13000E-01	0.19964E 02	0.25234E 00	0.47302E 01	0.58823E-01	0.66071E-02
27	0.13500E-01	0.20012E 02	0.26233E 00	0.47456E 01	0.61098E-01	0.66071E-02
28	0.14000E-01	0.20059E 02	0.27235E 00	0.47605E 01	0.63373E-01	0.66071E-02
29	0.14500E-01	0.20107E 02	0.28239E 00	0.47840E 01	0.65673E-01	0.74720E-02
30	0.15000E-01	0.20156E 02	0.29246E 00	0.47983E 01	0.67953E-01	0.74720E-02
31	0.15500E-01	0.20204E 02	0.30255E 00	0.48123E 01	0.70233E-01	0.74720E-02
32	0.16000E-01	0.20253E 02	0.31266E 00	0.48260E 01	0.72513E-01	0.74720E-02
33	0.16500E-01	0.20302E 02	0.32280E 00	0.48464E 01	0.74812E-01	0.83208E-02
34	0.17000E-01	0.20351E 02	0.33296E 00	0.48600E 01	0.77095E-01	0.83208E-02
35	0.17500E-01	0.20401E 02	0.34315E 00	0.48734E 01	0.79379E-01	0.83208E-02
36	0.18000E-01	0.20451E 02	0.35337E 00	0.48868E 01	0.81663E-01	0.83208E-02
37	0.18500E-01	0.20501E 02	0.36360E 00	0.49076E 01	0.83967E-01	0.91577E-02
38	0.19000E-01	0.20551E 02	0.37387E 00	0.49211E 01	0.86255E-01	0.91577E-02
39	0.19500E-01	0.20602E 02	0.38415E 00	0.49345E 01	0.88543E-01	0.91577E-02
40	0.20000E-01	0.20653E 02	0.39447E 00	0.49479E 01	0.90830E-01	0.91577E-02
41	0.20500E-01	0.20710E 02	0.40481E 00	0.59720E 01	0.95633E-01	0.99821E-02
42	0.21000E-01	0.20776E 02	0.41518E 00	0.68063E 01	0.10042E 00	0.99821E-02
43	0.21500E-01	0.20851E 02	0.42559E 00	0.74916E 01	0.10521E 00	0.99821E-02
44	0.22000E-01	0.20932E 02	0.43603E 00	0.80568E 01	0.11001E 00	0.99821E-02
45	0.22500E-01	0.21019E 02	0.44652E 00	0.85306E 01	0.11481E 00	0.10799E-01
46	0.23000E-01	0.21111E 02	0.45705E 00	0.89206E 01	0.11961E 00	0.10799E-01
47	0.23500E-01	0.21207E 02	0.46763E 00	0.92475E 01	0.12440E 00	0.10799E-01
48	0.24000E-01	0.21307E 02	0.47826E 00	0.95234E 01	0.12919E 00	0.10799E-01
49	0.24500E-01	0.21410E 02	0.48894E 00	0.97617E 01	0.13400E 00	0.11611E-01
50	0.25000E-01	0.21516E 02	0.49967E 00	0.99634E 01	0.13879E 00	0.11611E-01
51	0.25500E-01	0.21624E 02	0.51045E 00	0.10138E 02	0.14359E 00	0.11611E-01
52	0.26000E-01	0.21735E 02	0.52129E 00	0.10292E 02	0.14838E 00	0.11611E-01